Fuel-Optimal Space-Flight Transfer Solutions

Through a Redundant Adjoint Variable Transformation

by

John Arthur Lawton

Dissertation submitted to the Faculty of the

Virginia Polytechnic Institute and State University

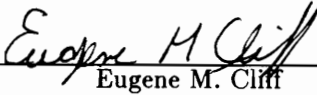in partial fulfillment of the Requirements for the degree of

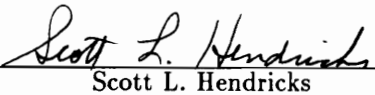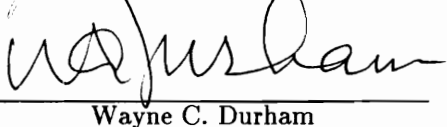DOCTOR OF PHILOSOPHY

in

Aerospace Engineering

APPROVED:

Frederick H. Lutze, Chairman

Eugene M. Cliff

John A. Burns

Scott L. Hendricks

Wayne C. Durham

April 1991

Blacksburg, Virginia

Fuel-Optimal Space-Flight Transfer Solutions

Through a Redundant Adjoint Variable Transformation

by

John Arthur Lawton

Dr. Frederick H. Lutze, Chairman

Aerospace Engineering

(ABSTRACT)

A transformation between minimum dimension adjoint variables and redundant adjoint variables is derived in this dissertation. The transformation is then applied between the adjoint variables associated with Cartesian position and velocity vectors and a set of redundant adjoint variables associated with certain regularized variables (Schumacher variables). This transformation proves to be very beneficial when it is applied to minimum-fuel space rendezvous and intercept problems. It facilitates using attributes from the two systems simultaneously; a new necessary condition in Schumacher adjoints is derived in this dissertation, and this together with classical necessary conditions for fuel-optimal transfer (existing in the position and velocity space) leads to a numerical algorithm which seems to be quite robust in finding candidate optimal control solutions for space transfer problems.

ACKNOWLEDGEMENTS

It is definitely true that a man is not an island, and a project such as this one would not be in the least bit possible if it were not for the aid of many people. First, and foremost, I would like to thank my family for the tremendous support I have received during this endeavor; they have put up with moving thrice, with at times uncertain means of support, and with a sometimes grumpy (especially during preliminary exams) and often missing husband/father. My wife, Debbie, has been the most ideal wife one could possibly dream of; her love, prodding, patience, perseverance, all without ever complaining, has meant more to me than words can quite grasp. My children, the delights of my eyes, Becca, Tommy, and Sammy, also were very understanding of their Daddy's need to "get that dissertation finished." The twins to be born just days after this project draws to a close provided the final impetus to finish this dissertation without further delay. My family's prayers, which provided the required breakthroughs, wisdom, and strength from God, were invaluable. This truly was a family project.

In terms of technical and professional help, my greatest debt and utmost thanks are due to Dr. Lutze, who had the idea for this approach to optimal space transfer in the first place, who provided much technical advice and direction, and who was always willing to spend countless hours discussing the project. Thank are due to Dr. Cliff and Dr. Burns, for teaching me much about Engineering and Mathematics, especially optimization and optimal control, and for generously providing technical counsel. Thanks are similarly due to Dr. Hendricks and Dr. Durham, for their valuable time put into this project, and for their sincere support.

Without the help of Dr. Jeff Blanton and Ted Sims, who provided various means of leave from work and financial support, who were willing to go along with my unorthodox means

TABLE OF CONTENTS

1.0 INTRODUCTION

The problem of finding the sequence of propulsive burns of a space vehicle in order to transfer it from one orbit to another with the minimum amount of fuel expended, to either intercept the second orbit or to rendezvous with it, has been investigated for some time. In fact, Hohmann, after whom the so-called Hohmann transfer is named, published his results on optimum time-open circular orbit to circular orbit transfer in 1925[22]. Much of the pioneering work in the search for optimal transfers between more general orbital configurations and related theory was accomplished by Lawden beginning in the 1950's[28,29,30].

Several authors have presented excellent histories of this endeavor to find minimum fuel trajectories. Edelbaum[11], for example, provides an interesting and very thorough review of the early history of fuel-optimal trajectory analysis. Many of the classical and interesting traits of fuel optimal rendezvous problems, especially for the open time case (no final time specified for the maneuvers), are found in papers by Edelbaum[11] and by Gobetz and Doll[17]. While not specifically a historical treatise, Marec[35] presents a broad treatment of optimal space flight transfer, with historical references interwoven with the technical derivations. Vasudevan[51] also presents a broad, as well as more recent, review of fuel-optimal space trajectory theory. Most relevant to the approach of this current dissertation are the works in the genre of Lawden[28,29,30], Lion and Handelsmann[33], Glandorf[14,15], Prussing and colleagues,[7,41,42,43,54] Jezewski,[23,24] and Vasudevan and Lutze.[50,51,52]

The main feature these works have in common with the current research is the use of primer vector theory (the primer vector is the vector adjoint to velocity) and related notions for an impulsive approximation to the thrusting arcs environment. As far as the impulsive thrust

approximation, Robbins[44] discusses in depth the accuracy of such an approximation. In a simplified summary, as long as the thrusting arcs are short in duration as compared with the coasting arcs, then the approximation is good. As far as primer vector theory is concerned, the interesting feature of the papers listed above which are most related to this current work is that they use the primer vector from optimal control theory (associated with finite burn time thrusting histories) in an impulsive approximation environment. Essentially, the optimal control theory is applied to the finite burn case, then taken to the limit as the thrust magnitude becomes infinite over a zero time span while holding the total impulse fixed.

The works of Prussing, Chiu, and Wellnitz use the theory of Lion and Handelsmann directly in order to update the coasting and thrusting histories of the transfer trajectory in an iterative process. That is, Lion and Handelsmann extended the primer vector theory of Lawden to be defined on non-optimal trajectories (as well as on optimal trajectories as Lawden defined it), then show, when the trajectory is non-optimal (based on necessary conditions on the primer vector), how the trajectories can be modified to reduce the amount of fuel required to do the transfer.

Vasudevan and Lutze[50,51,52] take a different approach to the same problem. They solve for candidate optimal solutions using a Quasi-Newton parameter optimization routine with projected constraints in order to find the lowest characteristic velocity (the total sum of the incremental velocities). The number of burns to use in order to accomplish the transfer is assumed a priori in this approach. Then, after the fact, primer vector theory is invoked to check that the correct number of burns was used. If the primer vector magnitude is ever greater than one on the transfer trajectory history, then an additional burn is assumed and the solution process is repeated. This process is continued until all necessary conditions, those of constrained parameter optimization theory and those of optimal control theory, are satisfied.

This current research project similarly investigates the application of optimal control theory on trajectories taken in the limit as the finite burn rocket thrusts approach instantaneous velocity changes, for both intercept and rendezvous problems. These instantaneous impulse trajectories are then converted to corresponding finite thrust trajectories. The solution process itself, however, is completely different from those mentioned above. The chief thing that is new in this project is that the adjoint variables corresponding to position and velocity elements of the space vehicle(s) are transformed to a redundant set of adjoint variables, in order to check necessary conditions of optimal control theory. These variables are adjoint to a set of regularized state variables whose general class is due to Burdet[6], and whose specific definition/derivation is due to Schumacher[46,47,48] (for convenience, these coordinates will be called "Schumacher coordinates" or "Schumacher variables" in this dissertation).

This transformation of the adjoint variables to a set of redundant adjoint variables is the essential feature of the new algorithm proposed in this research. Just as certain problems in linear algebra and in calculus can be solved more readily in some transformed space (for example, integrating some function over the volume of a sphere in spherical coordinates versus in Cartesian coordinates), while being difficult at best in the original space, so also certain problems associated with the adjoint variables can be solved more readily in a transformed space. In particular, the adjoint variables associated with Schumacher coordinates have many nice features not found in those associated with $\bar{r}$ and $\bar{v}$.

One such feature is the fact that the Schumacher adjoint variables for the time open transfer problem are all simple harmonic oscillators in the change-in-true-anomaly independent variable, η. Thus, calculating primer vector histories in order to check the classical necessary conditions is a very simple task in the transformed adjoint space. Indeed, they can be calculated readily on a hand-held calculator. Another important feature, to be brought out in chapter 4, is

that a new necessary condition for the time open case is derived from the Schumacher adjoint variables. This feature does not exist, at least not in recognizable form, in the adjoint variables of $\bar{r}$ and $\bar{v}$.

It is important to point out, in this context of transformed adjoint variables, that this transformation, at least in some sense, is not directly tied to the transformation of the state variables. That is, for many purposes, the two sets of variables can be treated as independent. It is true that the state variables can be transformed first, then the adjoint variables can be computed through the derivatives of the Hamiltonian directly in the usual manner. However, nothing prevents the state calculations from being done in one set of variables (say, Cartesian position and velocity, or classical orbital elements, or canonical variables, or whatever variables happen to be convenient for the problem at hand), while the adjoint variables are transformed to another set (again convenient for the problem at hand). As one example, alluded to in the preceding paragraph, the state of the space vehicle could be handled in $\bar{r}$ and $\bar{v}$ space, while the adjoint variables are transformed to those associated with Schumacher coordinates for propagation along the coasting arc, then transformed back so that the primer vector (the adjoint vector associated with velocity, $\bar{v}$) can be aligned with the velocity vector change ($\Delta\bar{v}$).

This idea of independently transforming state and adjoint variables is actually a natural one, in light of the canonical transformation theory of classical mechanics.[18,27] In that theory, as well as in Hamiltonian theory, the generalized coordinates and the generalized momenta are treated as independent quantities. Then, lumping the concepts of various theories under one simplified idea, a transformation is sought which facilitates the solution process of the particular problem. Indeed, the problem becomes one of solving for a transformation! The extension of this to the theory of optimal control is natural because optimal control theory, and its notation, stem from Hamiltonian theory in classical mechanics. The state variables of the optimal control

problem are analogous to generalized coordinates of classical mechanics (indeed, they are often, though not always, generalized coordinates). Similarly, the adjoint variables are analogous to the generalized momenta. The integrand of an integral cost function corresponds to the Lagrangian. Finally, the Hamiltonian (sometimes called the pseudo-Hamiltonian) of optimal control theory is analogous to the Hamiltonian of classical mechanics. Marec[35] and Komatsuzaki[27] discuss some applications of canonical transformation theory as applied to optimal control problems.

This current project concentrates this idea of independent transformations of the state and adjoint variables on one particular transformation, that between Cartesian position and velocity and the redundant Schumacher coordinates. The equations for transformations between sets of adjoint variables will be developed more generally, then will be specifically applied to that one transformation. The relationship between the Schumacher adjoint variables and the primer vector will be derived. Then, from this applied theory, an algorithm for finding solutions to various instantaneous impulse intercept and rendezvous problems will be proposed. These will be supplemented with a conversion from instantaneous impulse burn solutions to finite thrust burn solutions, again with the adjoint transformation being an integral part of the conversion.

This algorithm, as mentioned previously, is quite different in nature from previously existing algorithms. While all of the algorithms due to other researchers mentioned above in some form or another seek to minimize the characteristic velocity of the interceptor trajectory, the algorithm proposed in this work does not use the characteristic velocity at all. At the various burns, the change in velocity is used, with the aid of classical primer vector theory, to determine the adjoint variables on the impulsive burn trajectory. Then, these adjoint variables along with the state variables are used to check various necessary conditions (some old and some

new) of optimal control theory. The resulting iteration process terminates when all the necessary conditions are satisfied. The characteristic velocity is never used.

In this sense, the current algorithm for solving impulsive burn trajectories is more like the common numerical boundary value solution methods used for various optimal control problems than it is to the other impulsive burn solution algorithms mentioned above. In these boundary value solution methods, the boundary value problem in the state and adjoint differential equations resulting from the application of the Maximum Principle (and the associated transversality conditions on the adjoint variables) is solved by a shooting method. The initial and/or final state and adjoint variables are iterated upon until a trajectory is obtained which satisfies all the necessary conditions (namely, maximization of the Hamiltonian, transversality of the adjoint variables, and state boundary conditions) are satisfied. The resulting trajectory is termed an extremal (i.e., candidate optimum solution), since the necessary conditions are not sufficient conditions. If it is known that an optimal control exists, and if all the extremals can be determined, then the extremal control yielding the lowest cost is indeed the optimal control. More commonly, it cannot be determined for a certainty that all extremals are found, but the best extremals are considered optimal for engineering purposes until evidence to the contrary arises.

The point is that the boundary value solution process does not directly seek to minimize the cost, but merely to satisfy the optimal control necessary conditions as applied to cost function and differential equations of the problem. As was just mentioned, this is also what is done for impulsive trajectories in this dissertation. It is of interest to note that optimal control numerical methods do exist which seek to directly minimize the cost through gradient descent methods in function spaces (see for example Kelley[26], and Chapter 7 of Bryson and Ho[4]). These methods are called direct methods, while those which seek to satisfy the necessary conditions

without direct use of the cost function in the numerical process are called indirect methods. The boundary value shooting method variety of indirect methods, however, has attained much success in solving many optimal control problems. It is believed that the loosely analogous indirect techniques used in this research are similarly very competitive for finding impulsive thrust space transfer extremals.

Furthermore, since the adjoint variables along the extremal are determined as an integral part of the solution process, the converged impulsive burn extremal, together with the state variables, can be fed as initial conditions into a finite burn multiple shooting algorithm of the genré just mentioned. This has proven to be very successful, with the resulting shooting method algorithm typically converging in just a few steps using these initial conditions.

2.0 ADJOINT VARIABLE TRANSFORMATIONS

2.1 Introduction

The heart of the findings of this project is the use of adjoint variable transformations to obtain some new information, some supplementary information, and some workload-reducing information about the optimal control problem at hand in order to facilitate finding solutions. More specifically, the transformations are from the adjoint variables associated with Cartesian position and velocity state variables ($\bar{r}$ and $\bar{v}$) to a set of redundant adjoint variables associated with redundant, regularized Schumacher variables.

As a first step toward developing the redundant adjoint variable transformation, the adjoint variable transformation to a non-redundant system will be derived. That is what is done in this chapter.

2.2 General Square Adjoint Variable Transformations

In what follows, it is tacitly assumed throughout that the form of the optimal control cost function is in the Mayer form; that is, the cost is merely a function of the state at the end time, so there is no integral cost functional. The reason for this assumption is that the definitions for the variational differential equations and the adjoint differential equations will be taken directly from the theory of differential equations; an integral cost requires a slight modification of the definition of the adjoint variables. (Indeed, the transformations described

are not limited to optimal trajectories, nor even to an optimal control problem statement; they are true for any set of differential equations that are in the class described.) At the end of the derivation of the transformation, it will then be shown how to modify the results when an integral cost occurs in a problem.

Define two systems of equations, each with a different independent variable (t and s):

$$\dot{x}_1(t) \;=\; f_1(\, x_1(t),\, u_1(t)\,) \qquad\qquad 2.2.1$$

and

$$x_2{}'(s) \;=\; f_2(\, x_2(s),\, u_2(s)\,)\,. \qquad\qquad 2.2.2$$

The derivatives above are defined as $(\dot{\,})\; \triangleq\; \frac{d}{dt}(\,)$ and $(\,)'\; \triangleq\; \frac{d}{ds}(\,)$. Also, $x_1 \in \Re^n$, $x_2 \in \Re^n$, $u_1 \in \Re^m$, and $u_2 \in \Re^m$, so that $f_1 : \Re^n \times \Re^m \to \Re^n$ and $f_2 : \Re^n \times \Re^m \to \Re^n$. It is assumed that

$$(h,y) : \Re^n \times \Re \;\to\; \Re^n \times \Re \qquad\qquad 2.2.3$$

is a unique transformation from (x_1, t) to (x_2, s), with

$$\det(\, \frac{\partial h}{\partial x_1}\,) \;\neq\; 0 \qquad\qquad 2.2.4$$

(at least not at any point of interest). In this, and in all that follows in this section, it is tacitly assumed that if t and s appear in related equations (as Eqs. 2.2.1 and 2.2.2), or in the same equation, then they are just transformed variations of one another at the same instant in time (or whatever the independent variable may be), unless stated otherwise. Next, consider a point $\tilde{x}_1(t)$ arbitrarily close to $x_1(t)$; that is, it is on a neighboring trajectory at the same time. Then,

$$\tilde{x}_2(s) \; = \; x_2(s) \; + \; \frac{\partial h}{\partial x_1}(\tilde{x}_1(t) - x_1(t)) \; + \; \mathcal{O}(\parallel \tilde{x}_1(t) - x_1(t) \parallel) \qquad 2.2.5$$

(with $s = y(x_1(t), t)$), where $\mathcal{O}(\epsilon)$ (read "order of ϵ" -- i.e., a function of higher order terms) is such that

$$\lim_{\epsilon \to 0} \frac{\mathcal{O}(\epsilon)}{\epsilon} \; = \; 0. \qquad 2.2.6$$

(Note that in the term $\frac{\partial h}{\partial x_1}$ above, and throughout this dissertation, the convention used for partial derivatives with respect to vectors is to expand the gradient row-wise; that is, for example, $\frac{\partial h}{\partial x_1} = \left[\frac{\partial h}{\partial x_1^1} \; \frac{\partial h}{\partial x_1^2} \; \cdots \; \frac{\partial h}{\partial x_1^n} \right].$) The difference between the point and its neighbor (for both the x_1 space and the x_2 space) can also be written with the common δ difference operator, so that Eq. 2.2.5 looks like

$$\delta x_2(s) \; = \; \frac{\partial h}{\partial x_1} \delta x_1(t) \; + \; \mathcal{O}(\parallel \delta x_1(t) \parallel). \qquad 2.2.7$$

Next, in order to see how the adjoint variables of one system are transformed to those of the other system, the variational equations of differential equations theory[31] are needed. The variational differential equations for the two spaces, x_1 and x_2, are

$$\dot{\eta}_1(t) \; = \; \frac{\partial f_1}{\partial x_1} \, \eta_1(t), \qquad 2.2.8$$

and

$$\eta_2'(s) \; = \; \frac{\partial f_2}{\partial x_2} \, \eta_2(s). \qquad 2.2.9$$

The variational equations are linearized versions of the original state variable differential equations. Their solutions, viz. the fundamental solution matrices, transfer hyperplanes tangent to the trajectory from time (or whatever the independent variable may be) t_1 to another time t_2 (see Pontryagin[37] and Leitmann[32] for detailed descriptions of the variational equations). The solutions for these variational differential equations can be written

$$\eta_1(t) = \Phi_1(t, t_0)\, \eta_1(t_0) \qquad\qquad 2.2.10$$

and

$$\eta_2(s) = \Phi_2(s, s_0)\, \eta_2(s_0). \qquad\qquad 2.2.11$$

Now, Pontryagin[37] shows that, using the variational equation solutions,

$$\tilde{x}_1(t) = x_1(t) + \epsilon \eta_1(t) + \mathcal{O}_1(t, \epsilon) \qquad\qquad 2.2.12$$

and

$$\tilde{x}_2(s) = x_2(s) + \epsilon \eta_2(s) + \mathcal{O}_2(s, \epsilon). \qquad\qquad 2.2.13$$

That is, the variational equations are basically derivatives of the state with respect to a change in initial conditions. Here, $\mathcal{O}_1(t, \epsilon)$ is a uniform function of t which is of order ϵ, and analogously for $\mathcal{O}_2(s, \epsilon)$. Subtracting $x_1(t)$ from both sides of Eq. 2.2.12, it can be written

$$\delta x_1(t) = \epsilon \eta_1(t) + \mathcal{O}_1(t, \epsilon). \qquad\qquad 2.2.14$$

Similarly, from Eq. 2.2.13,

$$\delta x_2(s) = \epsilon \eta_2(s) + \mathcal{O}_2(s, \epsilon). \qquad 2.2.15$$

But, $\delta x_2(s)$ is also equal to the right hand side of Eq. 2.2.7. Substituting the right hand side of Eq. 2.2.14 into 2.2.7,

$$\delta x_2(s) = \frac{\partial h}{\partial x_1}[\epsilon \eta_1(t) + \mathcal{O}_1(t, \epsilon)] + \mathcal{O}(\epsilon \eta_1 + \mathcal{O}_1(t, \epsilon)). \qquad 2.2.16$$

Equating the right hand sides of Eqs. 2.2.15 and 2.2.16,

$$\epsilon \eta_2(s) + \mathcal{O}_2(s, \epsilon) = \frac{\partial h}{\partial x_1}[\epsilon \eta_1(t) + \mathcal{O}_1(t, \epsilon)] + \mathcal{O}(\epsilon \eta_1 + \mathcal{O}_1(t, \epsilon)). \qquad 2.2.17$$

There are three distinct "order of" functions in this equation, all of which have the property described in Eq. 2.2.6. That is, they are higher order terms in ϵ, so that dividing through by ϵ and letting $\epsilon \to 0$ will rid the equation of these terms. $\mathcal{O}_1(t,\epsilon)$ and $\mathcal{O}_2(t,\epsilon)$ have this property by construction. It must yet be shown that $\dfrac{\mathcal{O}(\epsilon\eta_1 + \mathcal{O}_1(t,\epsilon))}{\epsilon} \to 0$ as $\epsilon \to 0$. To this end, note that

$$\frac{\|\mathcal{O}(\epsilon\eta_1 + \mathcal{O}_1(t,\epsilon))\|}{\epsilon} = \frac{\|\mathcal{O}(\epsilon\eta_1 + \mathcal{O}_1(t,\epsilon))\|}{\|\epsilon\eta_1 + \mathcal{O}_1(t,\epsilon)\|} \frac{\|\epsilon\eta_1 + \mathcal{O}_1(t,\epsilon))\|}{\epsilon} \qquad 2.2.18$$

$$\leq \frac{\|\mathcal{O}(\epsilon\eta_1 + \mathcal{O}_1(t,\epsilon))\|}{\|\epsilon\eta_1 + \mathcal{O}_1(t,\epsilon)\|} \frac{\epsilon\|\eta_1\| + \|\mathcal{O}_1(t,\epsilon))\|}{\epsilon}, \qquad 2.2.19$$

where the inequality holds through the triangle inequality of norms. Now, the limit of the product of two terms is the product of the limits of those terms. The left term on the right side of the inequality $\to 0$, and the right term approaches $\|\eta_1\|$. Hence, the limit of the right side of the inequality is zero as $\epsilon \to 0$, so that by the sandwich theorem $\dfrac{\mathcal{O}(\epsilon\eta_1 + \mathcal{O}_1(t,\epsilon))}{\epsilon} \to 0$ as $\epsilon \to 0$.

Consequently, dividing both sides of Eq. 2.2.17 by ϵ, and taking the limit as $\epsilon \to 0$,

$$\eta_2(s) = \frac{\partial h}{\partial x_1} \eta_1(t).$$
2.2.20

Or, if it is understood that the notation $\dfrac{\partial x_2}{\partial x_1}$ more rigorously means $\dfrac{\partial h(x_1(t))}{\partial x_1(t)}$, then this equation can be written

$$\boxed{\eta_2(s) = \frac{\partial x_2}{\partial x_1} \eta_1(t).}$$
2.2.21

Thus, the transformation between the two sets of variational equations is effected by the pre-multiplication by the Jacobian of the transformation of the state variables.

Substituting Eqs. 2.2.10 and 2.2.11 (the solutions of $\eta_1(t)$ and $\eta_2(s)$ in terms of transition matrices) into the previous equation will yield the transformation between the transition matrices of these variational equations. That is,

$$\Phi_2(s, s_0) \, \eta_2(s_0) = \frac{\partial x_2}{\partial x_1} \Phi_1(t, t_0) \, \eta_1(t_0).$$
2.2.22

But, evaluating the variational transformation at t_0 gives

$$\eta_1(t_0) = \left(\frac{\partial x_2(s_0)}{\partial x_1(t_0)} \right)^{-1} \eta_2(s_0),$$
2.2.23

so that substituting the right hand side of this for $\eta_1(t_0)$ where it occurs on the right side of the equals sign in the previous equation,

$$\Phi_2(s, s_0)\, \eta_2(s_0) = \left(\frac{\partial x_2(s)}{\partial x_1(t)}\right) \Phi_1(t, t_0) \left(\frac{\partial x_2(s_0)}{\partial x_1(t_0)}\right)^{-1} \eta_2(s_0).$$ 2.2.24

Since $\eta_2(s_0)$ is arbitrary in this equation (i.e., it must hold for all $\eta_2(s_0) \in \Re^n$), then

$$\boxed{\Phi_2(s, s_0) = \left(\frac{\partial x_2(s)}{\partial x_1(t)}\right) \Phi_1(t, t_0) \left(\frac{\partial x_2(s_0)}{\partial x_1(t_0)}\right)^{-1}}$$ 2.2.25

is the transformation from the first to the second transition matrix. This has the appearance of a similarity transformation, except that since the transformation matrix is time varying, the pre-multiplication matrix is evaluated at t (thinking of "s" as "s(t)"), while the post-multiplication matrix is evaluated at t_0.

Next, turning to a discussion of how this transformation affects the adjoint variables, the adjoint differential equations for the two systems are

$$\dot{\lambda}_1(t) = -\left(\frac{\partial f_1}{\partial x_1}\right)^T \lambda_1(t)$$ 2.2.26

and

$$\lambda_2'(s) = -\left(\frac{\partial f_2}{\partial x_2}\right)^T \lambda_2(s),$$ 2.2.27

with solutions

$$\lambda_1(t) = \Psi_1(t, t_0)\, \lambda_1(t_0)$$ 2.2.28

and

$$\lambda_2(s) = \Psi_2(s, s_0)\, \lambda_2(s_0).$$ 2.2.29

$\Psi_1(t, t_0)$ and $\Psi_2(s, s_0)$ are transition matrices for the adjoint variables. Now, a fact to be used subsequently is that any adjoint transition matrix Ψ is related to the associated variational transition matrix Φ by

$$\Psi = \Phi^{-T}, \qquad\qquad 2.2.30$$

(where Φ^{-T} means $(\Phi^{-1})^T \equiv (\Phi^T)^{-1}$). To see this, note that

$$\lambda^T(t)\, \eta(t) = \Big(\Psi(t, t_0)\, \lambda(t_0)\Big)^T \Phi(t, t_0)\, \eta(t_0) \qquad\qquad 2.2.31$$

$$= \lambda^T(t_0)\, \Psi^T(t, t_0)\, \Phi(t, t_0)\, \eta(t_0). \qquad\qquad 2.2.32$$

But,

$$\lambda^T(t)\, \eta(t) = \lambda(t_0)\, \eta(t_0) \qquad\qquad 2.2.33$$

because

$$\frac{d}{dt}\Big(\lambda^T \eta\Big) = \dot{\lambda}^T \eta + \lambda^T \dot{\eta} = -\lambda^T A\, \eta + \lambda^T A\, \eta = 0 \qquad\qquad 2.2.34$$

(where "A" is shorthand for $\left[\frac{\partial f}{\partial x}\right]$). So

$$\lambda^T(t_0)\, \eta(t_0) = \lambda^T(t_0)\, \Psi^T(t, t_0)\, \Phi(t, t_0)\, \eta(t_0). \qquad\qquad 2.2.35$$

Since this equation must hold for all $\lambda(t_0)$ and $\eta(t_0)$, a set of n independent λ vectors and a another set of n independent η vectors can be used to build nonsingular matrices Λ and Y, respectively, so that applying this previous equation to the whole set yields

$$\Lambda^T(t_0) \ Y(t_0) \ = \ \Lambda^T(t_0) \ \Psi^T(t,t_0) \ \Phi(t,t_0) \ Y(t_0) . \qquad 2.2.36$$

Pre-multiplying both sides by Λ^{-T} and post-multiplying by Y^{-T} gives

$$\Psi^T(t,t_0) \ \Phi(t,t_0) \ = \ I \qquad 2.2.37$$

for all t. Or,

$$\Psi(t,t_0) \ = \ \Phi^{-T}. \qquad 2.2.38$$

Now, using this fact, first define

$$A \ \triangleq \ \left(\frac{\partial x_2(s)}{\partial x_1(t)} \right) \qquad 2.2.39$$

and

$$A_0 \ \triangleq \ \left(\frac{\partial x_2(s_0)}{\partial x_1(t_0)} \right) \qquad 2.2.40$$

for simplicity of notation. Also, let Φ_1 mean $\Phi_1(t,t_0)$, and similarly for Φ_2. So applying fundamental linear algebra rules of multiplication, transposition, and inversion, the following steps result:

$$\Phi_2 = A\,\Phi_1 A_0^{-1} \tag{2.2.41}$$

$$\Phi_2^T = A_0^{-T} \Phi_1^T A^T \tag{2.2.42}$$

$$\Phi_2^{-T} = A^{-T} \Phi_1^{-T} A_0^T \tag{2.2.43}$$

Using Eq. 2.2.30 to relate the previous equation to the adjoint transition matrices,

$$\Psi_2 = A^{-T} \Psi_1 \, A_0^T. \tag{2.2.44}$$

For clarity, once again explicitly denoting the independent variables in each matrix gives

$$\boxed{\Psi_2(s, s_0) = \left(\frac{\partial x_2(s)}{\partial x_1(t)}\right)^{-T} \Psi_1(t, t_0) \left(\frac{\partial x_2(s_0)}{\partial x_1(t_0)}\right)^{T}.} \tag{2.2.45}$$

Pre-multiplying both sides by $\left(\dfrac{\partial x_2(s)}{\partial x_1(t)}\right)^{T}$ and post-multiplying both sides by $\lambda_2(t_0)$ gives

$$\left(\frac{\partial x_2(s)}{\partial x_1(t)}\right)^{T} \Psi_2(s, s_0)\, \lambda_2(s_0) = \Psi_1(t, t_0) \left(\frac{\partial x_2(s_0)}{\partial x_1(t_0)}\right)^{T} \lambda_2(s_0). \tag{2.2.46}$$

Or,

$$\left(\frac{\partial x_2(s)}{\partial x_1(t)}\right)^{T} \lambda_2(s) = \Psi_1(t, t_0) \left(\frac{\partial x_2(s_0)}{\partial x_1(t_0)}\right)^{T} \lambda_2(s_0). \tag{2.2.47}$$

Defining a new variable

$$q(t) \triangleq \left(\frac{\partial x_2(s)}{\partial x_1(t)}\right)^T \lambda_2(s), \qquad\qquad 2.2.48$$

the previous equation can be written

$$q(t) = \Psi_1(t, t_0) \, q(t_0). \qquad\qquad 2.2.49$$

So, $\Psi_1(t, t_0)$ maps all $q(t_0)$ to $q(t)$, so it is a transition matrix for the function $q(t)$. That is, $q(t)$ has the same transition matrix as $\lambda_1(t)$; so, $q(t)$ is clearly adjoint to $\eta_1(t)$, and thus is adjoint to $x_1(t)$.

But, is $q(t) = \lambda_1(t)$? This, of course, depends what is meant by $\lambda_1(t)$. It is clear by the development above that the variational variables $\eta_2(s)$ transform to $\eta_1(t)$; what is required is that the transformed adjoint vector $q(t)$ have the same exact relationship to $\eta_1(t)$ as $\lambda_2(s)$ has to $\eta_2(s)$. Recall from Eq. 2.2.33 that

$$\lambda_2^T(s)\eta_2(s) = c \qquad \text{(a constant for all s).} \qquad\qquad 2.2.50$$

This is used, for example, in the development of the Maximum Principle as done by Leitmann[32]; since a set of n independent η vectors in the hyperplane tangent to the limiting surface of the optimal trajectory will remain in the tangent hyperplane at a later point in time as propagated by Eq. 2.2.10 or 2.2.11, a set of adjoint vectors orthogonal to the hyperplane will remain orthogonal to the hyperplane as propagated in time (i.e., $\lambda^T \eta = 0$ in that case). In

general, the transfer matrix of the variational equations transforms tangent hyperplanes to a given surface of motion (for whatever type of motion is desired, whether for optimal control, or whether considering some other variation in initial conditions of the state) to tangent hyperplanes at another time, since the variational equations are derivatives of the state with respect to changes in initial conditions[37]. This means that the desire to have adjoint and variational equations in each space to have the same relationship to each other requires that if $\lambda_2^T(s)\eta_2(s) = c$, then in the transformed space $\lambda_1^T(t)\eta_1(t) = c$ (i.e., they have the same value of the constant value c).

In this vein, consider a matrix $\Lambda_2(s)$ of n independent adjoint vectors, where these vectors are the columns of the matrix. Similarly, in the other system, denote the analogous matrix $\Lambda_1(t)$. Let matrices of n independent variational vectors in each system similarly be denoted $H_2(s)$ and $H_1(t)$. Finally, let the transformed set of vectors, $q(t)$, be denoted $Q(t)$. Then consider

$$\Lambda_2^T H_2 = C. \qquad 2.2.51$$

C is a matrix of constant values resulting from the inner product of every adjoint vector with every variational vector; it is the matrix of "c" values of Eq. 2.2.50. Then, of course,

$$\Lambda_2^T \left[\left(\frac{\partial x_2}{\partial x_1} \right) \left(\frac{\partial x_2}{\partial x_1} \right)^{-1} \right] H_2 = C, \qquad 2.2.52$$

since the term in brackets is equal to the identity matrix. Rearranging, this becomes

$$\left[\left(\frac{\partial x_2}{\partial x_1} \right)^T \Lambda_2 \right]^T \left(\frac{\partial x_2}{\partial x_1} \right)^{-1} H_2 = C. \qquad 2.2.53$$

But, by Eqs. 2.2.21 and 2.2.49 this is

$$Q^T H_1 \;\; = \;\; C. \hspace{4cm} 2.2.54$$

So, this says that the transformed quantities, Q, indeed hold the unique relationship to H_1 as Λ_2 does to H_2. Hence,

$$Q(t) \;\; = \;\; \Lambda_1(t) \hspace{4cm} 2.2.55$$

as desired. So the transformation of the adjoint variables can be written without qualification as

$$\boxed{\lambda_1(t) \;\; = \;\; \left(\frac{\partial x_2(s)}{\partial x_1(t)}\right)^T \lambda_2(s) \; .} \hspace{3cm} 2.2.56$$

As a result of the fact that this transformation uniquely preserves the orientation of the adjoint vectors to the variational vectors for the two spaces, any optimal control satisfying the the Maximum Principle necessary condition in one space (along with the appropriate optimal state and adjoint values), will satisfy it with respect to the transformed state and adjoint values. In the same way, if the transversality conditions are satisfied in one space, they will be satisfied in the other space (again, because the adjoint and variational vectors in one space maintain the same orientation to each other in the other space -- the matrix of constants C is the same in both systems). Not only that, but preservation of C in the transformation means that the

specific orientation of the adjoint vectors within the subspace of vectors which satisfy transversality will be the same in both systems. This means that a control and adjoint response synthesized from the Maximum Principle in one system will have the exact same behavior in the transformed system. For example, if only one choice of adjoint vectors, within the subspace of all vectors which satisfy transversality, will hit the desired final state in one class of optimal control problem, then the transformed adjoint vector will do the same.

To confirm the specific property that transversality is maintained, consider the specific case where either the initial or final points (either of which is being considered) of the x_1 trajectory must lie on the intersection of p smooth surfaces, $\sigma_1(x_1) = 0$; that is, $\sigma_1 : \Re^n \to \Re^p$ are C^1 functions (see Leitmann[32] pages 115 and 140). Then, the surfaces in x_2 space can be determined by $\sigma_2(x_2) = \sigma_1(x_1(x_2))$. Transversality requirements in either system consist of the requirement that η at that endpoint (either initial or final, whichever is being considered) must satisfy

$$\frac{\partial \sigma}{\partial x} \eta = 0, \qquad\qquad 2.2.57$$

and the requirement that λ there must be orthogonal to η. (That is, λ must be orthogonal to the $(n-p)$-dimension hyperplane that is tangent the the $(n-p)$-dimensional manifold defined by σ -- see pp. 118-119 of Leitmann[32] and p. 310 of Lee and Markus[31].) λ orthogonal to η, $\lambda^T \eta = 0$, means that λ must lie in the span of the rows of $\frac{\partial \sigma}{\partial x}$; i.e.,

$$\lambda = \left(\frac{\partial \sigma}{\partial x}\right)^T \alpha, \quad \text{for some } \alpha \in \Re^p. \qquad\qquad 2.2.58$$

To evaluate these conditions, the following partial derivative is needed:

$$\frac{\partial \sigma_2}{\partial x_2} = \frac{\partial \sigma_1}{\partial x_1} \frac{\partial x_1}{\partial x_2} \qquad\qquad\qquad 2.2.59$$

$$= \frac{\partial \sigma_1}{\partial x_1} \left[\frac{\partial x_2}{\partial x_1}\right]^{-1}. \qquad\qquad 2.2.60$$

Hence, the condition

$$\frac{\partial \sigma_2}{\partial x_2} \eta_2 = 0 \qquad\qquad\qquad 2.2.61$$

becomes

$$\frac{\partial \sigma_1}{\partial x_1} \left[\frac{\partial x_2}{\partial x_1}\right]^{-1} \eta_2 = 0. \qquad\qquad 2.2.62$$

But, the multiplication of the last two terms in this equation is just η_1 by Eq. 2.2.21. This then implies that

$$\frac{\partial \sigma_1}{\partial x_1} \eta_1 = 0. \qquad\qquad\qquad 2.2.63$$

That is,

$$\frac{\partial \sigma_2}{\partial x_2} \eta_2 = 0 \quad \Rightarrow \quad \frac{\partial \sigma_1}{\partial x_1} \eta_1 = 0. \qquad 2.2.64$$

The next question to be answered concerning transversality is, if λ_2 is orthogonal to η_2, will the transformed $\lambda_1(t)$ be orthogonal to η_1? To this end, consider

$$\lambda_1{}^T \eta_1 = \left[\left[\frac{\partial x_2}{\partial x_1} \right]^T \lambda_2 \right]^T \eta_1 \qquad\qquad 2.2.65$$

$$= \lambda_2^T \, \frac{\partial x_2}{\partial x_1} \, \eta_1 \qquad\qquad 2.2.66$$

$$= \lambda_2^T \, \eta_2. \qquad\qquad 2.2.67$$

So, λ_1 will be orthogonal to η_1 if λ_2 is orthogonal to η_2. This fact together with Eq. 2.2.64 show that the adjoint variable transformation does indeed preserve transversality.

So far, as was mentioned at the beginning of this section, it has been assumed that the cost function was only in Mayer form. Now consider the addition of a Lagrange form integral cost functional, $\int_{t_0}^{t_f} L(x_1(t), \, u(t)) \, dt$. If this is the case, augment the state to include one new variable x_1^0, which is defined by

$$\dot{x}_1^0 = L(x_1(t), \, u(t)), \qquad\qquad 2.2.68$$

and

$$x_1^0(0) = 0, \qquad\qquad 2.2.69$$

so that

$$\tilde{f}(\tilde{x}_1, \, u) = \begin{bmatrix} L(x_1(t), \, u(t)) \\ f(x_1(t), \, u(t)) \end{bmatrix} \qquad\qquad 2.2.70$$

is the augmented state velocity. The cost is now just $x_1^0(t_f)$, so the problem is converted to Mayer form, meaning that the previous theory holds. The adjoint differential equation is now

$$\dot{\lambda}_1(t) \;=\; -\left[\frac{\partial \tilde{f}(\tilde{x}_1, u)}{\partial \tilde{x}_1}\right]^T \tilde{\lambda}_1(t) \;=\; -\left[\frac{\partial f(x_1, u)}{\partial x_1}\right]^T \lambda_1(t) \;-\; \lambda_1^0\left[\frac{\partial L(x_1, u)}{\partial x_1}\right]^T. \qquad 2.2.71$$

This is the standard form of the adjoint differential equations for optimal control problems with integral cost terms. The transformation equation $h(x_1)$ needs to be augmented also. x_2 needs to modified in the same manner, so let $x_2^0(s) = x_1^0(t)$ (which in turn will mean that

$$\frac{d}{ds}x_2^0 \;=\; \frac{1}{\dot{y}}L(x_2(x_1), u), \qquad 2.2.72$$

where $\dot{y}$ comes from Eq. 2.2.4, and

$$x_2^0(0) \;=\; 0). \qquad 2.2.73$$

Therefore,

$$\tilde{h}(\tilde{x}_1) \;=\; \begin{bmatrix} x_1^0 \\ h(x_1) \end{bmatrix}. \qquad 2.2.74$$

Using this in the transformation equation, Eq. 2.2.56, yields

$$\lambda_1^0 \;=\; \lambda_2^0 \qquad 2.2.75$$

and

$$\lambda_1(t) \;=\; \left(\frac{\partial h}{\partial x_1}\right)^T \lambda_2(s). \qquad 2.2.76$$

The Maximum Principle states that λ_1^0 is a constant such that $\lambda_1^0 \leq 0$, and similarly for λ_2^0.

Eq. 2.2.76 shows that the transformation for the adjoint variables is not affected in form by the addition of the integral cost term (though the adjoint variables are affected, since λ_1^0 times $\frac{\partial L}{\partial x_1}$ is added to the differential equation for the adjoint variables -- see Eq. 2.2.71).

2.3   *Example 1 — Linear Transformations*

As a simple example illustrating the adjoint variable transformation, consider the following linear transformation of the state:

$$x_2(t) \; = \; M \, x_1(t).$$

<div align="right">2.3.1</div>

Then, of course,

$$\frac{\partial x_2}{\partial x_1} \; = \; M$$

<div align="right">2.3.2</div>

so that

$$\lambda_2(t) \; = \; M^{-T} \lambda_1(t).$$

<div align="right">2.3.3</div>

If M is orthogonal (i.e., $M^{-1} = M^T$), then

$$\lambda_2(t) \; = \; M \, \lambda_1(t).$$

<div align="right">2.3.4</div>

A special case of an linear orthogonal transformation is a simple change of Cartesian

coordinate systems. E.g., when the state $x_1(t) = \begin{bmatrix} \bar{r}_1(t) \\ \bar{v}_1(t) \end{bmatrix}$ is the three components of position and and three components of velocity in an orbital mechanics problem, and the rotation from the original system to a new system is effected by the orthogonal cosine matrix A, then

$$M = \begin{bmatrix} A & 0 \\ 0 & A \end{bmatrix}. \tag{2.3.5}$$

Eq. 2.3.4 then gives that

$$\lambda_{\bar{r}_2} = A \lambda_{\bar{r}_1} \tag{2.3.6}$$

and

$$\lambda_{\bar{v}_2} = A \lambda_{\bar{v}_1}. \tag{2.3.7}$$

That is, the adjoint variables just undergo the same vector rotation. $\lambda_{\bar{v}}$ is the primer vector of fuel optimal trajectory analysis in either system. It is a necessary condition for optimality that the thrust vector must point in the direction of the primer vector (with maximum thrust magnitude) whenever the magnitude of the primer vector is greater than one; whenever it is less than one, the rocket engine should have zero thrust. Since the thrust vector would also be rotated by the same A, $\bar{T}_2 = A\bar{T}_1$, the transformed thrust vector still points in the direction of the transformed primer vector on an optimal trajectory; that is, the optimal thrust is still pointing in the same physical direction, as it of course must.

2.4 Example 2 – Transformation to Polar Coordinates

Vasudevan[45] investigated, in his Masters thesis, fuel-optimal rendezvous transfers in the

plane using polar coordinates. He developed an analog of the primer vector in those coordinates. The transformation equations from polar coordinates, $[\ r\ \ \theta\ \ \nu\ \ h\ ]^T$, to Cartesian coordinates, $[\ x\ \ y\ \ \dot{x}\ \ \dot{y}\ ]^T$, are

$$
\begin{aligned}
x &= r\cos\theta \\
y &= r\sin\theta \\
\dot{x} &= \nu\cos\theta\ -\ \frac{h}{r}\sin\theta \\
\dot{y} &= \nu\sin\theta\ +\ \frac{h}{r}\cos\theta.
\end{aligned}
$$

2.4.1

ν is the radial velocity and h is the angular momentum per unit mass. Consider x_2 to be the Cartesian system and x_1 to be the polar system. Then

$$
\frac{\partial x_2}{\partial x_1} = \begin{bmatrix} \cos\theta & -r\sin\theta & 0 & 0 \\[2ex] \sin\theta & r\cos\theta & 0 & 0 \\[2ex] \frac{h}{r^2}\sin\theta & A_{32} & \cos\theta & -\frac{\sin\theta}{r} \\[2ex] -\frac{h}{r^2}\cos\theta & A_{42} & \sin\theta & \frac{\cos\theta}{r} \end{bmatrix}
$$

2.4.2

where

$$
A_{32} = -(\frac{h}{r}\cos\theta + \nu\sin\theta)
$$

2.4.3

and

$$
A_{42} = (-\frac{h}{r}\sin\theta + \nu\cos\theta).
$$

2.4.4

Then, using Eq. 2.2.56,

$$\lambda_r = \lambda_x \cos\theta + \lambda_y \sin\theta + \lambda_{\dot{x}} \frac{h}{r^2} \sin\theta - \lambda_{\dot{y}} \frac{h}{r^2} \cos\theta$$

$$\lambda_\theta = -\lambda_x\, r \sin\theta + \lambda_y\, r \cos\theta + \lambda_{\dot{x}} A_{32} + \lambda_{\dot{y}} A_{42}$$

2.4.5

$$\lambda_\nu = \lambda_{\dot{x}} \cos\theta + \lambda_{\dot{y}} \sin\theta$$

$$\lambda_h = -\lambda_{\dot{x}} \frac{\sin\theta}{r} + \lambda_{\dot{y}} \frac{\cos\theta}{r}\,.$$

The λ_h equation can also be written

$$r\lambda_h = -\lambda_{\dot{x}} \sin\theta + \lambda_{\dot{y}} \cos\theta\,. \qquad 2.4.6$$

The vector $\begin{bmatrix} \lambda_\nu \\ r\lambda_h \end{bmatrix}$ is the primer vector analog used by Vasudevan.[50] (Actually, his is the negative of this vector since he used a minimum principle in deriving the optimal control necessary conditions, and a maximum principle is used in this dissertation.) It is equivalent to rotating a coordinate system from the (x, y) system to the local (radial, transverse) system in order to obtain the primer vector in that local system.

2.5 *Example 3 — Transformation to Classical Orbital Coordinates*

Consider next a transformation between Cartesian position and velocity vectors as the orbital state to a slight variation of the classical orbital elements: a (semi-major axis of the orbit), e (eccentricity), i (inclination), Ω (right ascension of the ascending node), ω (argument of

peri-apsis), and M (mean anomaly at the current time). As developed here, the equations would only be valid for elliptical orbits. The transformation between the adjoint variables of these two systems will not be developed in detail, but will be briefly sketched. The main details will be shown, as well as the form of the solution. Specifically, it will be shown how the primer vector can be transformed into the classical element adjoint variables, and how the transformed primer vector could potentially be used in practice.

The transformation from the classical elements to $\bar{r}$ and $\bar{v}$ is

$$\bar{r} \;=\; \frac{a(1-e^2)}{1+e\cos\nu}\; T(\Omega,\, i,\, \omega) \begin{bmatrix} \cos\nu \\ \sin\nu \\ 0 \end{bmatrix}$$

$$\text{2.5.1}$$

$$\bar{v} \;=\; \sqrt{\frac{\mu(1+e^2+2e\cos\nu)}{a(1-e^2)}}\; T(\Omega,\, i,\, \omega) \begin{bmatrix} -\sin\nu \\ \cos\nu \\ 0 \end{bmatrix}.$$

Here, $T(\Omega,\, i,\, \omega)$ is transpose of the 3-1-3 rotation matrix from inertial coordinates to the local peri-focal coordinate system. Also, ν is the true anomaly. It is a function of e and M through the well-known transformation to eccentric anomaly and thence to Kepler's equation; so, $\nu = \nu(e,\, M)$. Calculating the partial derivatives of $\bar{r}$ and $\bar{v}$ is a straightforward task. The derivatives with respect to 'a' are immediate:

$$\frac{\partial \bar{r}}{\partial a} \;=\; \frac{\bar{r}}{a}$$

$$\text{2.5.2}$$

and

$$\frac{\partial \bar{v}}{\partial a} \;=\; -\frac{\bar{v}}{2a}.$$

$$\text{2.5.3}$$

Those derivatives with respect to e and M will have to take into account the places where these variables appear explicitly, plus through $\nu(e, M)$. E.g., $\bar{r} = \bar{r}(e, \nu(e, M))$, so

$$\frac{\partial \bar{r}}{\partial e} = \frac{\partial \bar{r}}{\partial e}\bigg|_{\nu} + \frac{\partial \bar{r}}{\partial \nu}\frac{\partial \nu}{\partial e}, \qquad 2.5.4$$

where $\frac{\partial \bar{r}}{\partial e}\big|_{\nu}$ means the derivative while holding ν constant. Notice also that $\frac{d}{d\theta}\cos\theta = \cos(\theta + \frac{\pi}{2})$, and that $\frac{d}{d\theta}\sin\theta = \sin(\theta + \frac{\pi}{2})$, so that

$$\frac{\partial}{\partial\Omega}T(\Omega, i, \omega) = T(\Omega + \tfrac{\pi}{2}, i, \omega), \qquad 2.5.5$$

and similarly for the other two derivatives.

Denote the representation of $\bar{r}$ and $\bar{v}$ in Cartesian coordinates by x_2, and the classical elements by x_1. For convenience, define

$$A(t) = \left(\frac{\partial x_2(t)}{\partial x_1(t)}\right)^T \qquad 2.5.6$$

and

$$B(t) = \left(\frac{\partial x_2(t)}{\partial x_1(t)}\right)^{-T}. \qquad 2.5.7$$

So, $A(t)$ is the transpose of the matrix of partials described immediately above, and $B(t)$ is the inverse of $A(t)$. So,

$$
\lambda_1 \;=\; \begin{bmatrix} \lambda_a \\ \lambda_e \\ \lambda_i \\ \lambda_\Omega \\ \lambda_\omega \\ \lambda_M \end{bmatrix} \;=\; A(t) \begin{bmatrix} \lambda_{\overline{r}} \\ \lambda_{\overline{v}} \end{bmatrix} \;=\; A(t)\,\lambda_2 \,. \qquad\qquad 2.5.8
$$

Since $A(t)$ is a full matrix, the primer vector, $\lambda_{\overline{v}}$, does not transform to a simple subset of the λ_1 adjoint variables (such as was the case in the transformation between Cartesian and polar coordinates).

In order to make use of this transformation as relates to the primer vector, the dynamics of the λ_1 must be determined. So, the dynamics of a, e, i, Ω, ω, and M must be determined. The derivatives of these elements in an inverse square gravity field subject to another force (such as rocket thrust in this case) can be written in Gauss' form of Lagrange's planetary equations as shown by Geyling and Westerman[12] (p. 182). That is,

$$
\dot{a} \;=\; 2\sqrt{\frac{a^3}{\mu(1-e^2)}}\left[T_R\, e\sin\nu + \frac{a(1-e^2)}{r}T_T\right] \qquad\qquad 2.5.9
$$

$$
\dot{e} \;=\; \sqrt{\frac{a(1-e^2)}{\mu}}\left[T_R\sin\nu + T_T(\cos E + \cos\nu)\right] \qquad\qquad 2.5.10
$$

$$
\frac{di}{dt} \;=\; \frac{1}{\sqrt{\mu a(1-e^2)}}\,T_N\, r\cos(\omega+\nu) \qquad\qquad 2.5.11
$$

$$\dot{\Omega} = \frac{1}{\sin i \sqrt{\mu a(1-e^2)}} T_N \, r \sin(\omega + \nu) \qquad \qquad 2.5.12$$

$$\dot{\omega} = -\dot{\Omega} \cos i - \sqrt{\frac{a(1-e^2)}{\mu e^2}} \left\{ T_R \cos \nu - T_T \left[1 + \frac{r}{a(1-e^2)}\right] \sin \nu \right\} \qquad 2.5.13$$

and

$$\dot{M} = n - \frac{2}{\sqrt{\mu \alpha}} T_R \, r - \dot{\omega}\sqrt{1-e^2} - \dot{\Omega}\sqrt{1-e^2} \cos i \; . \qquad \qquad 2.5.14$$

T_R, T_T, and T_N are the components of thrust in the radial, transverse, and normal directions, respectively. They are rotated from inertial space in a 3-1-3 rotation with Euler angles of Ω, i, and $(\omega + \nu)$, so they also are dependent on the orbital elements. Since the adjoint variable differential equations (cf. Eqs. 2.2.26 and 2.2.27) involve the partial derivatives of the right hand sides of Eqs. 2.5.9 − 2.5.14 with respect to a, e, ... , M, the adjoint variable differential equations on thrusting arcs of the trajectory would be very messy, to say the least. It is doubtless that they would be of much use on thrusting arcs. On, coasting arcs, however, where the thrust is zero,

$$\dot{a} = 0 \qquad \qquad 2.5.15$$

$$\dot{e} = 0 \qquad \qquad 2.5.16$$

$$\frac{di}{dt} = 0 \qquad \qquad 2.5.17$$

$$\dot{\Omega} = 0 \qquad\qquad\qquad\qquad 2.5.18$$

$$\dot{\omega} = 0 \qquad\qquad\qquad\qquad 2.5.19$$

$$\dot{M} = \sqrt{\frac{\mu}{a^3}} \cdot \qquad\qquad\qquad\qquad 2.5.20$$

The resulting adjoint differential equations for coasting arcs are

$$\dot{\lambda_a} = \frac{3}{2} \sqrt{\frac{\mu}{a^5}} \, \lambda_M \qquad\qquad\qquad\qquad 2.5.21$$

$$\dot{\lambda_e} = 0 \qquad\qquad\qquad\qquad 2.5.22$$

$$\dot{\lambda_i} = 0 \qquad\qquad\qquad\qquad 2.5.23$$

$$\dot{\lambda_\Omega} = 0 \qquad\qquad\qquad\qquad 2.5.24$$

$$\dot{\lambda_\omega} = 0 \qquad\qquad\qquad\qquad 2.5.25$$

$$\dot{\lambda_M} = 0 \, . \qquad\qquad\qquad\qquad 2.5.26$$

Solving these,

$$\lambda_a = \frac{3}{2} \sqrt{\frac{\mu}{a^5}} \, \lambda_M \, t \, + \, \lambda_{a0} \qquad\qquad\qquad\qquad 2.5.27$$

$$\lambda_e = \text{constant} \qquad\qquad 2.5.28$$

$$\lambda_i = \text{constant} \qquad\qquad 2.5.29$$

$$\lambda_\Omega = \text{constant} \qquad\qquad 2.5.30$$

$$\lambda_\omega = \text{constant} \qquad\qquad 2.5.31$$

$$\lambda_M = \text{constant}. \qquad\qquad 2.5.32$$

$\lambda_a(t)$ is a linear function of time and the last five adjoint variables are constants. Since these expressions are so simple, they are ideal for propagating the adjoint variables along coasting arcs of transfer trajectories between burns. So, on coasting arcs between burns, the primer vector in Cartesian coordinates can be aligned with the $\Delta \bar{v}^l$ with magnitude of one at each end of the coasting arc; then, the primer vector can be transformed to $\lambda_a, \ldots, \lambda_M$ in order to propagate the primer vector along the trajectory through these simple equations to test the necessary conditions required of the primer vector.

In order to facilitate doing this, partition the matrix of Eq. 2.5.7 as

$$B = \begin{bmatrix} B_{11} & B_{12} \\ B_{21} & B_{22} \end{bmatrix} = \begin{bmatrix} B_1 \\ B_2 \end{bmatrix}, \qquad\qquad 2.5.33$$

where B_{11}, etc., are all 3×3 submatrices, and B_1 and B_2 are 3×6 submatrices. Furthermore, let subscript "0" refer to the initial time on this coasting arc (t_0), and let subscript "f" refer to the final time on this coasting arc (t_f). Then,

$$\lambda_{\overline{V}0} = B_{20} \begin{bmatrix} \lambda_{a0} \\ \lambda_e \\ \lambda_i \\ \lambda_\Omega \\ \lambda_\omega \\ \lambda_M \end{bmatrix} \qquad\qquad 2.5.34$$

and

$$\lambda_{\overline{V}f} = B_{2f} \begin{bmatrix} \alpha\lambda_M t + \lambda_{a0} \\ \lambda_e \\ \lambda_i \\ \lambda_\Omega \\ \lambda_\omega \\ \lambda_M \end{bmatrix}, \qquad\qquad 2.5.35$$

where $\alpha = \frac{3}{2}\sqrt{\frac{\mu}{a^5}}$. These two equations can be rearranged to solve for the adjoints associated with the classical elements from the two primer vectors at the ends of the coasting arcs. Defining the 3×6 matrix

$$\tilde{B}_{2f} \triangleq \begin{bmatrix} B_{21f} & \begin{bmatrix} B_{22f} + B_{21f} \begin{bmatrix} 0 & 0 & \alpha t_f \\ 0 & 0 & 0 \\ 0 & 0 & 0 \end{bmatrix} \end{bmatrix} \end{bmatrix}, \qquad\qquad 2.5.36$$

$$\begin{bmatrix} \lambda_{a0} \\ \lambda_e \\ \lambda_i \\ \lambda_\Omega \\ \lambda_\omega \\ \lambda_M \end{bmatrix} = \begin{bmatrix} B_{20} \\ \tilde{B}_{2f} \end{bmatrix}^{-1} \begin{bmatrix} \lambda_{\overline{V}0} \\ \lambda_{\overline{V}f} \end{bmatrix}. \qquad\qquad 2.5.37$$

Then, as a function of time,

$$\lambda_1(t) = \begin{bmatrix} \lambda_{a0} + \alpha\,\lambda_M t \\ \lambda_e \\ \lambda_i \\ \lambda_\Omega \\ \lambda_\omega \\ \lambda_M \end{bmatrix}, \qquad \qquad \text{2.5.38}$$

and

$$\lambda_{\bar{v}}(t) = B_2(t)\,\lambda_1(t) \qquad \qquad \text{2.5.39}$$

will propagate the primer vector along the coasting arc.

It is not certain that this method of propagating the primer vector would gain any advantage over current methods. It is shown as an example merely to demonstrate one type of analysis which can be done using the transformations of adjoint variables. In the next chapter it will be shown that when the primer vector is transformed into redundant Schumacher adjoint variables, the propagation of the primer vector is greatly simplified; also, the form of the equations leads to a new check for optimality not found in the variables adjoint to $\bar{r}$ and $\bar{v}$.

There is, however, another possible application of the transformation to the adjoint variables associated with classical elements which may be worth pursuing. The form of the elements themselves, a, e, ... , M, lends itself naturally to a boundary condition for a class of orbital transfers which yield simple transversality conditions in λ_a, ... , λ_M. Suppose it is desired to transfer from one elliptical orbit to another, but it is irrelevant both at what point in

the original orbit the maneuver commences, and at what point in the final orbit the injection occurs. That is, the problem is not one of rendezvous, but one of injecting into an orbit at whatever point requires the least amount of fuel. The resulting boundary conditions are that a, e, i, Ω, and ω are specified for both trajectories, but M is free for both trajectories. The resulting transversality conditions require that $\lambda_M = 0$ at the beginning and at the end of the maneuver (while the other adjoint variables are free). Thus, the state boundary conditions and adjoint transversality requirements are very simple in this system. This is in contrast with terminal constraints which are moving boundaries in $\bar{r}$, $\bar{v}$ space, and with their resulting messy transversality conditions for $\lambda_{\bar{r}}$ and $\lambda_{\bar{v}}$.

When considering numerically solving state and adjoint differential equations for finite thrust optimal control problems, however, the simple form of the $\bar{r}$, $\bar{v}$ differential equations on thrusting arcs (as contrasted with Lagrange's planetary equations, Eqs. 2.5.9 - 2.5.14) makes that system more desirable. So, the transversality conditions can be specified in the classical adjoint variables, then transformed to $\lambda_{\bar{r}}$ and $\lambda_{\bar{v}}$ to be propagated along the trajectory through a numerical differential equations solver. As stated above, this is the whole reason for using adjoint transformations: to take advantage of salient features in any given system, and transform to another system when solutions or parts of solutions are easier in that other system.

The basic form for the resulting numerical problem is:

1)   set a, e, i, Ω, and ω to the desired values, and $\lambda_M = 0$, at the beginning of the trajectory;

2)   guess values for $\lambda_a, \ldots, \lambda_\omega$, M, at the beginning of the trajectory, and for t_f (unless t_f, the total time of flight, is already specified);

3)   transform the state and adjoint variables to $\bar{r}$, $\bar{v}$ space at the starting point;

4)   numerically solve the state and adjoint differential equations propagating them to time t_f (using the thrust control mandated by the Maximum Principle);

5) at the endpoint, transform back to classical element space to check that the differences between a, ..., ω, and λ_M and their requisite values are zero (and that the Hamiltonian is zero -- unless t_f is specified, in which case the Hamiltonian is free);

6) if they are not close enough to zero, update the guessed values in step two (typically using a quasi-Newton method and/or a multiple shooting method), and repeat steps three through six until convergence is reached.

3.0 REDUNDANT ADJOINT VARIABLE TRANSFORMATIONS

3.1 Introduction

The previous chapter contains the derivation of the transformation between two sets of adjoint variables associated with two sets of state variables which share a common dimension (i.e., a "square" transformation). In this chapter, the transformation of adjoint variables associated with a transformation from one state, usually of minimum dimension, to another of higher dimension, called a redundant state, will be derived. A common example of a redundant state is the set of Euler parameters used in rotational dynamics of a solid body[25]. In orbital mechanics, several authors have studied the theory of redundant orbital elements[3,6,49]. Stiefel and Scheifele[49] have even shown the theoretical and practical relationships between Euler parameters and redundant orbital variables. These redundant variables are usually developed from the context of regularizing the variables; that is, regularized variables are those where singularities of the variables have been eliminated ("regular" is another word for "analytic" used in complex analysis to mean the derivative of the function contains no singularities in the domain). This, of course, is also why Euler parameters are so frequently used; they rid the singularities inherent in the calculations of the Euler angle rates (e.g., the 3-1-3 Euler angles mentioned above have a singularity when $i = 0$).

The regularized variables concentrated on in this dissertation are of a class of variables which are attributed to Burdet[6]; the derivation of the specific variables is due to Schumacher[46,47]. These variables have various nice features, and many of them, particularly those associated with derivatives with respect to the elements, have been used already in the homotopy approach to optimal space transfer developed by Vasudevan[52] and by Vasudevan and

Lutze. The adjoint variables associated with these Schumacher variables also have some attributes not found in other adjoint variables, which also benefit the optimal control solution process. So, it is desirable to be able to transform between Cartesian position and velocity adjoint variables and the adjoint Schumacher variables. This chapter develops the theory of such redundant adjoint transformations.

3.2 *Redundancy and Constants of the Motion*

Whenever a minimum dimension state is transformed to a redundant one, additional constants of the motion arise, which are equal in number to the difference between the dimension of the redundant set and the dimension of the minimal set. For example, with the four Euler parameters $(\beta_0, \beta_1, \beta_2, \beta_3)$, which replace three Euler angles (e.g., ψ, θ, and ϕ of the 3-2-1 transformation from inertial to body fixed coordinates), the additional constant is

$$\beta_0^2 + \beta_1^2 + \beta_2^2 + \beta_3^2 = 1. \qquad 3.2.1$$

That is, the trajectory lies on a three dimensional manifold (a hyper-sphere) in the four dimensional space, $\Re^4$ (see Stiefel and Scheifele[49]). To visualize this, consider that one angle θ can be replaced by the redundant pair $\gamma_1 = \cos\theta$ and $\gamma_2 = \sin\theta$, with $\gamma_1^2 + \gamma_2^2 = 1$; the resulting trajectory lies on a one-dimensional curve, commonly called a circle, in a two dimensional space (the $\gamma_1 - \gamma_2$ plane). Similarly, two angles can be replaced with three functions of sines and cosines of the angles; the resulting trajectories will lie on a two-dimensional surface (a sphere) in the three dimensional space.

In some sense this Eq. 3.2.1 can be thought of as a constraint, since initial values of the

β_i can be given which do not satisfy Eq. 3.2.1; then this equation will remain not satisfied as a function of time, and the dynamics of the motion will be incorrect. However, once Eq. 3.2.1 is satisfied, it will automatically remain satisfied without having to try to keep it on the constraint. In fact, the transformation from Euler Angles to Euler Parameters automatically satisfies the constraint. If one is to call it a constraint, it should be thought of as an autonomous constraint, since no external effort is required to keep the values of the variables on the constraint. It is probably more proper to consider this equation as a constant of the motion.

If the state of a system is redundant, then the resulting adjoint variables will also be redundant. They also will have constants of the motion (as will be shown in the next section). Pontryagin, et al[36], and also Bryson, Denham and Dreyfus[4] have shown that when the motion in an optimal control problem is constrained to lie on a subspace of the full dimension of the state, a redundancy exists in the adjoint variables. That is, there is some arbitrariness in the choice of the adjoint variables. They use this fact to develop conventions for values of the adjoint variables upon entering and leaving the constraints -- each set of authors has different, equivalent conventions. For the purposes of autonomous constraints associated with redundant coordinates, the mathematical theory still applies to help understand the redundancy inherent in the adjoint variables.

The arbitrariness of the adjoint variables, when the motion of the state lies on a vector of constraint equations $g(x) = $ const., $g(x):\Re^n \rightarrow \Re^m$ and $\lambda \in \Re^n$, can be described by the fact that if λ satisfies the adjoint equation, transversality, and is such that the Hamiltonian is maximized, etc., then so does $\tilde{\lambda}$ described by the following for any vector $\nu \in \Re^m$:

$$\tilde{\lambda} = \lambda + \left(\frac{\partial g}{\partial x}\right)^T \nu. \qquad 3.2.2$$

This is the case because $\left(\dfrac{\partial g}{\partial x}\right)^T$ is normal to the hyperplane tangent to the surface described by

$g(x)$, and the derivative of x, $\dot{x} = f(x, u)$, must lie in the hyperplane tangent to that surface.

Hence, $\dfrac{\partial g}{\partial x} f(x, u) = 0$ so that $\lambda^T f(x, u) = \tilde{\lambda}^T f(x, u)$; in other words, the maximum principle is the

same for either adjoint vector. If $\dot{x}$ had some component in the span of $\left(\dfrac{\partial g}{\partial x}\right)^T$ (i.e., it did

not lie entirely in the hyperplane), then the trajectory would immediately depart from the

constraint. In the case of constrained optimization, a control $u(t)$ must be chosen which forces $\dot{x}$

to remain in the hyperplane tangent to $g(x)$; in the case of redundant variables, $\dot{x} = f(x, u)$

automatically remains in the hyperplane tangent to $g(x)$ _for_ _all_ controls $u(t)$.

A test for true redundancy can be obtained by taking the derivative of $g(x)$ with respect

to time:

$$\dot{g}(x(t)) \;=\; \frac{\partial g(x(t))}{\partial x}\,\dot{x}(t) \;=\; \frac{\partial g(x(t))}{\partial x}\,f(x(t), u(t)) \,. \qquad\qquad 3.2.3$$

If it is identically zero, $\dot{g}(x(t)) \equiv 0$, then the constraint is truly autonomous; i.e., $g(x)$ is a set of

m constants of the motion. Except for the trivial case, Eq. 3.2.3 is identically zero if and only if

$f(x, u)$ is orthogonal to all vectors in the span of $\dfrac{\partial g}{\partial x}$; i.e., it lies in the hyperplane tangent to

$g(x)$.

If it is desired, for whatever reason, to bring any redundant adjoint variable $\bar{\lambda}(t)$, at

some time t, into the hyperplane tangent to $g(x)$, this can be accomplished through

$$\lambda \;=\; \left[I - \left(\frac{\partial g}{\partial x}\right)^T \left(\frac{\partial g}{\partial x}\right) \right] \bar{\lambda}, \qquad\qquad 3.2.4$$

if the rows are orthonormal. (This is just the matrix form of

$$\lambda \;=\; \bar{\lambda} \;-\; \sum_{i=1}^{m} \left[\bar{\lambda}^T \left(\frac{\partial g_i}{\partial x} \right)^T \right] \left(\frac{\partial g_i}{\partial x} \right)^T .)$$ 3.2.5

If the rows are not orthonormal, then replace $\frac{\partial g}{\partial x}$ in the above by a $m \times n$ orthonormal matrix whose rows are a basis for the span of the rows of $\frac{\partial g}{\partial x}$ (obtained through the Gramm–Schmidt orthogonalization procedure, or, more practically numerically, through the QR factorization of the transpose of $\frac{\partial g}{\partial x}$). These facts will be used in the subsequent section to help build a transformation to redundant adjoint variables from a minimum dimensional set.

3.3 The Transformation of Redundant Adjoint Vectors

Consider a state transformation to a minimum dimension state $x_1(t) \in \Re^n$ from a redundant state $x_2(s) \in \Re^r$ (with the possibility of change of independent variables $s \rightarrow t$); $r > n$ and $m \overset{\triangle}{=} r - n$. Let $x_1(t) = h(x_2(t))$, $h(x_2): \Re^r \rightarrow \Re^n$, effect the transformation, and let $\frac{\partial h}{\partial x_2}$ have maximal rank. Furthermore, let $g(x_2): \Re^n \rightarrow \Re^m$ be a set of m independent functions of x_2 defining the redundancy of the $x_2(t)$ equations, with the columns of $\left[\frac{\partial g}{\partial x_2} \right]^T$ not in the span $\left[\frac{\partial h}{\partial x_2} \right]^T$; also, they are constants of the motion, or autonomous constraints, so that $\dot{g}(x_2(t)) \equiv 0$.

Now, augment the state $x_1(t)$ to one of dimension r,

$$\tilde{x}_1(t) \;\overset{\triangle}{=}\; \left[\begin{array}{c} x_1(t) \\ \hline g \end{array} \right].$$ 3.3.1

The trajectory of the augmented state, then, lies on an n-dimensional manifold of the r-dimensional space, just as the redundant state x_2; the difference is that g = constant in this

space is just a hyperplane since it is a linear variety. This augmentation of the state requires $h(x_2)$ to be augmented also:

$$\tilde{h}(x_2) \triangleq \begin{bmatrix} h(x_2) \\ ---- \\ g(x_2) \end{bmatrix}. \qquad 3.3.2$$

The adjoint variables associated with the augmented state are now

$$\tilde{\lambda}_1(t) = \begin{bmatrix} \lambda_{x_1}(t) \\ ---- \\ \lambda_g \end{bmatrix}. \qquad 3.3.3$$

Before proceeding with the definition of the transformation between the adjoint variables of $\tilde{\lambda}_1(t)$ and $\lambda_2(s)$, it must be made clear that augmenting the state and adjoint variables in the "1" system in this manner in no way changes the optimal control solution in that system. The new Hamiltonian in that system is

$$\tilde{H}(\tilde{\lambda}_1, \tilde{x}_1, u) = \lambda_1^T f_1(x_1, u) + \lambda_g^T \dot{g} \qquad 3.3.4$$

Since $\dot{g} \equiv 0$ when the constraints are properly satisfied, the value of the Hamiltonian is unchanged as long as $\lambda_1(t)$ behaves the same in the augmented system. To guarantee that the autonomous constraints are properly satisfied, augment the initial and/or terminal constraints:

$$\tilde{\phi} = \begin{bmatrix} \phi \\ ---- \\ g - g^* \end{bmatrix}, \qquad 3.3.5$$

where g^* is the requisite constant value. This, of course, only needs to be done in theory, because in practice this would automatically take place. Next, notice that

$$\dot{\lambda}_1 \;=\; -\left[\frac{\partial \tilde{H}}{\partial x_1}\right]^T \;=\; -\left[\frac{\partial f_1(x_1, u)}{\partial x_1}\right]^T \lambda_1 \;-\; \left[\frac{\partial \dot{g}}{\partial x_1}\right]^T \lambda_g\,. \qquad 3.3.6$$

But,

$$\frac{\partial \dot{g}}{\partial x_1} = 0 \qquad 3.3.7$$

when $g = g^*$, so $\lambda_1(t)$ is unchanged in the augmented space. These facts say that the same optimal control $u^*(t)$ will satisfy the maximum principle in both systems -- the optimal control solution is unchanged.

Now, the transformation of the adjoint variables of the previous section applies directly because $\tilde{\lambda}_1(t)$ and $\lambda_2(s)$ both are of dimension "r". So,

$$\lambda_2(s) \;=\; \left(\frac{\partial \tilde{h}}{\partial x_2}\right)^T \tilde{\lambda}_1(t)\,. \qquad 3.3.8$$

But this is also

$$\lambda_2(s) \;=\; \left[\left[\frac{\partial h}{\partial x_2}\right]^T \quad \left[\frac{\partial g}{\partial x_2}\right]^T\right] \tilde{\lambda}_1(t)\,. \qquad 3.3.9$$

Or,

$$\boxed{\lambda_2(s) \;=\; \left[\frac{\partial h}{\partial x_2}\right]^T \lambda_1(t) \;+\; \left[\frac{\partial g}{\partial x_2}\right]^T \lambda_g\,.} \qquad 3.3.10$$

The second term of the sum on the right hand side of this equation is a vector orthogonal to the

tangent hyperplane of $g(x_2)$. It is comparable to the second term in the sum on the right hand side of Eq. 3.2.2, the equation defining the arbitrariness of the redundant adjoint vector. Recall, in conjunction with this, that λ_g is the m–vector adjoint to the constraints g.

Inverting the matrix in Eq. 3.3.8 effects the transformation in the other direction:

$$\tilde{\lambda}_1(t) = \left(\frac{\partial \tilde{h}}{\partial x_2}\right)^{-T} \lambda_2(s),$$ 3.3.11

or,

$$\boxed{\left[\begin{array}{c} \lambda_1(t) \\ \hline \lambda_g \end{array}\right] = \left(\frac{\partial \tilde{h}}{\partial x_2}\right)^{-T} \lambda_2(s).}$$ 3.3.12

Thus, the transformation not only gives the desired unique $\lambda_1(t)$, but also what the particular λ_g is for the given redundant $\lambda_2(s)$. As stated in Section 3.2, it does not matter what the value of λ_g is in Eqs. 3.3.10 and 3.3.12 as regards the Maximum Principle, since the inner product of the state velocity vector, $f_2(x_2(s), u(s))$ with $\frac{\partial g}{\partial x_2}$ is zero for all controls u(s).

3.4 Transformation to Schumacher Variables

In this section, the redundant adjoint transformation equations developed above will be applied to the Schumacher variables. The Schumacher variables are

$$x_2(\eta) = \left[\begin{array}{c} \hat{r} \\ u \\ \hat{r}' \\ u' \\ h \end{array}\right],$$ 3.4.1

and they are defined to be:

$$u = \frac{1}{|\bar{r}|};$$

3.4.2

$$\hat{r} = u\,\bar{r};$$

3.4.3

$$u' \triangleq \frac{du(\eta)}{d\eta} = -\frac{\dot{r}}{h} = -\frac{\bar{r}\cdot\bar{v}}{h\,|\bar{r}|};$$

3.4.4

$$\hat{r}' \triangleq \frac{d\hat{r}}{d\eta} = \hat{h} \times \hat{r};$$

3.4.5

$$h = |\bar{h}|;$$

3.4.6

where,

$$\bar{h} = \bar{r} \times \bar{v};$$

3.4.7

$$\hat{h} = \frac{\bar{h}}{h};$$

3.4.8

and η, the new independent variable, is the change in true anomaly from the current true anomaly ($\eta = \nu - \nu_0$, and $\dot{\eta} = \dot{\nu} = \frac{h}{r^2}$). These are solutions to the following linear and regular differential equations under spherical gravity and no thrust or perturbing functions:

$$\hat{r}'' + \hat{r} = 0 \qquad\qquad 3.4.9$$

and

$$u'' + u = \frac{\mu}{h^2} . \qquad\qquad 3.4.10$$

(They are obviously linear, and they are regular because the variable "r" no longer occurs in the denominator of the differential equation as it does in

$$\ddot{\bar{r}} + \frac{\mu}{r^3}\bar{r} = 0, \qquad\qquad 3.4.11$$

the governing differential equation in Cartesian coordinates.)

The transformation to $x_1(t)$ is through the following equations (which define $h(x_2)$):

$$\bar{r} = \frac{\hat{r}}{u}; \qquad\qquad 3.4.12$$

$$\bar{v} = h(u\hat{r}' - u'\hat{r}). \qquad\qquad 3.4.13$$

The constants of the motion for the Schumacher variables are also needed to make up the rest of the transformation equation $\tilde{h}(x_2)$. As constructed, $\hat{r}$ is always a unit vector, so that one constant is

$$g_1(x_2) = \tfrac{1}{2}\hat{r}^T\hat{r} = \tfrac{1}{2} . \qquad\qquad 3.4.14$$

Similarly, $\hat{r}'$ is also a unit vector, since $\hat{h}$ is a unit vector, and $\hat{h}$ and $\hat{r}$ are orthogonal, so the cross product of them results is a unit vector. So, another constant of Schumacher variables is

$$g_2(x_2) \;=\; \tfrac{1}{2}\,\hat{r}'^T\hat{r}' \;=\; \tfrac{1}{2}\,. \qquad\qquad\qquad 3.4.15$$

Finally, $\hat{r}$ and $\hat{r}'$ are orthogonal by construction, so the final constant of Schumacher variables is

$$g_3(x_2) \;=\; \hat{r}^T\hat{r}' \;=\; 0\,. \qquad\qquad\qquad 3.4.16$$

Putting it all together,

$$g(x_2) \;=\; \begin{bmatrix} \tfrac{1}{2}\,\hat{r}^T\hat{r} \\[6pt] \tfrac{1}{2}\,\hat{r}'^T\hat{r}' \\[6pt] \hat{r}^T\hat{r}' \end{bmatrix}. \qquad\qquad\qquad 3.4.17$$

It will be shown in the next chapter, when the differential equation for $x_2(\eta)$ is given for all trajectories (including thrusting trajectories), that $\dot{g}(x_2) \equiv 0$ for all thrust vectors (and, for that matter, for all forces of any type).

Next, adjoining $h(x_2)$ and $g(x_2)$ to make $\tilde{h}(x_2)$,

$$\tilde{h}(x_2) \;=\; \begin{bmatrix} \dfrac{\hat{r}}{u} \\[8pt] h(\,u\,\hat{r}' - u'\,\hat{r}\,) \\[8pt] \tfrac{1}{2}\hat{r}^T\hat{r} \\[6pt] \tfrac{1}{2}\hat{r}'^T\hat{r}' \\[6pt] \hat{r}^T\hat{r}' \end{bmatrix}. \qquad\qquad\qquad 3.4.18$$

Now, the partial $\dfrac{\partial \tilde{h}(x_2)}{\partial x_2}$ is straightforward, so, using the transformation Eq. 3.3.8,

$$\lambda_2(\eta) = A \tilde{\lambda}_1(t),$$

where

$$A = \begin{bmatrix} \frac{1}{u}I & -hu'I & \hat{r} & 0 & \hat{r}' \\[2ex] -\frac{\hat{r}^T}{u^2} & h\hat{r}'^T & 0 & 0 & 0 \\[2ex] 0 & huI & 0 & \hat{r}' & \hat{r} \\[2ex] 0 & -h\hat{r}^T & 0 & 0 & 0 \\[2ex] 0 & (u\hat{r}'-u'\hat{r})^T & 0 & 0 & 0 \end{bmatrix}.$$

"I" in this matrix denotes the 3×3 identity matrix. Recall that

$$\lambda_2 \triangleq \begin{bmatrix} \lambda_{\hat{r}} \\ \lambda_u \\ \lambda_{\hat{r}'} \\ \lambda_{u'} \\ \lambda_h \end{bmatrix}$$

and

$$\tilde{\lambda}_1 \triangleq \begin{bmatrix} \lambda_{\bar{r}} \\ \lambda_{\bar{v}} \\ \lambda_g \end{bmatrix}.$$

The determinant of the matrix A is

$$\det(A) \;=\; -\frac{h^2}{u^2}, \qquad\qquad 3.4.22$$

which means that A is not singular except when $r = \frac{1}{u} = 0$ (i.e., trajectories through the center of attraction), or when $h = 0$ (rectilinear motion, for which the Shumacher variables do not exist). Notice that the last three rows times λ_2 is indeed $\left[\dfrac{\partial g}{\partial x_2}\right]^T \lambda_2$.

For effecting transformations the other direction, the inverse of A is needed. Using straightforward Gaussian elimination yields

$$
A^{-1} \;=\;
\begin{bmatrix}
u(I-\hat{r}\hat{r}^T) & -u^2\hat{r} & B_{13} & B_{14} & h(u\,\hat{r}+u'\hat{r}') \\[2ex]
0 & 0 & B_{23} & B_{24} & \dfrac{\hat{r}'}{u} \\[2ex]
\hat{r}^T & u & 0 & 0 & -h \\[2ex]
0 & 0 & \hat{r}'^T & u' & -h \\[2ex]
0 & 0 & \hat{r}^T & u & 0
\end{bmatrix}
\qquad 3.4.23
$$

where

$$B_{13} \;=\; u'(I - \hat{r}\hat{r}^T - \hat{r}'\hat{r}'^T) - u\,\hat{r}'\hat{r}^T, \qquad\qquad 3.4.24$$

$$B_{14} \;=\; -u\,u'\hat{r} - (u^2+u'^2)\hat{r}', \qquad\qquad 3.4.25$$

$$B_{23} \;=\; \frac{1}{h\,u}(I-\hat{r}\hat{r}^T-\hat{r}'\hat{r}'^T), \qquad\qquad 3.4.26$$

and

$$B_{24} = -\frac{1}{hu}(u\hat{r} + u'\hat{r}').$$

<div align="right">3.4.27</div>

Since λ_g is the last three rows of A^{-1} times $\lambda_2(\eta)$,

$$\lambda_g = \begin{bmatrix} \hat{r}^T\lambda_{\hat{r}} + u\lambda_u - h\lambda_h \\\\ \hat{r}'^T\lambda_{\hat{r}'} + u'\lambda_{u'} - h\lambda_h \\\\ \hat{r}^T\lambda_{\hat{r}'} + u\lambda_{u'} \end{bmatrix}.$$

<div align="right">3.4.28</div>

In order to make this transformation useful in terms of necessary conditions for fuel-optimal transfer, the primer vector is needed in the Schumacher adjoint variables. It is important to be able to transform both directions. Consider first, however, the transformation from Schumacher variables to Cartesian variables. This way, it can be seen which of the Schumacher variables correspond to the primer vector; that is, it will be seen what variables are mapped into the primer vector. Considering A^{-1} of Eq. 3.4.23, by inspection of the second row, whose product by λ_2 is the primer vector, $\lambda_{\overline{v}}$, it is evident that the primer vector is a function only of $\lambda_{\hat{r}'}$, $\lambda_{u'}$, and λ_h, since the other terms are multiplied by zero. Similarly, by inspection of A, Eq. 3.4.19, it is clear that these three are functions only of $\lambda_{\overline{v}}$ (and the portion that lies orthogonal to the surface $g(x_2)$). Hence, in some sense at least, $\lambda_{\hat{r}'}$, $\lambda_{u'}$, and λ_h correspond to the primer vector in Schumacher coordinates.

To make this concrete, multiply the third row of A by λ_1 to obtain

$$\lambda_{\hat{r}'} = hu\lambda_{\overline{v}} + \hat{r}'\lambda_{g1} + \hat{r}\lambda_{g2}.$$

<div align="right">3.4.29</div>

Of course, if $\lambda_g = 0$, this reduces to

$$\lambda_{\hat{r}'} = h \, u \, \lambda_{\overline{v}};$$

3.4.30

or, since $h \, u = v_T$, the transverse component of velocity, this is

$$\lambda_{\hat{r}'} = v_T \, \lambda_{\overline{v}}.$$

3.4.31

Similarly, multiplying the fourth row of A by λ_1 ,

$$\lambda_{u'} = -h \, \hat{r}^T \, \lambda_{\overline{v}}.$$

3.4.32

The fifth row times λ_1 is

$$\lambda_h = (u \, \hat{r}' - u' \, \hat{r})^T \, \lambda_{\overline{v}}.$$

3.4.33

Transforming the other direction, using A^{-1}, returns that

$$\lambda_{\overline{v}} = \frac{1}{h \, u}(I - \hat{r} \, \hat{r}^T - \hat{r}' \, \hat{r}'^T)\lambda_{\hat{r}'} - \frac{1}{h \, u}(u \, \hat{r} + u' \hat{r}')\lambda_{u'} + \frac{\hat{r}'}{u}\lambda_h.$$

3.4.34

The term in parenthesis of the first term on the right hand side of this equation is a matrix which rids the vector it multiplies of its components in the $\hat{r}$ and in the $\hat{r}'$ directions, leaving only the projection of the vector in the $\hat{h}$ direction. Hence, the equation can be rewritten

$$\lambda_{\overline{v}} = \frac{(\hat{h}^T \lambda_{\hat{r}'})\hat{h}}{hu} - \frac{1}{hu}(u\hat{r} + u'\hat{r}')\lambda_{u'} + \frac{\hat{r}'}{u}\lambda_h. \qquad 3.4.35$$

Noting that $\hat{r}$, $\hat{r}'$, and $\hat{h}$ form a local orthogonal basis (describing a radial, transverse, out-of-plane coordinate system), rewrite this equation as

$$\lambda_{\overline{v}} = -\frac{\lambda_{u'}}{h}\hat{r} + \frac{(h\lambda_h - u'\lambda_{u'})}{hu}\hat{r}' + \frac{\hat{h}^T \lambda_{\hat{r}'}}{hu}\hat{h}. \qquad 3.4.36$$

For convenience, denote the specific representation of the primer vector in this local basis using Schumacher adjoints by $\overline{S}$. That is,

$$\overline{S} = \begin{bmatrix} -\dfrac{\lambda_{u'}}{h} \\ \text{-----------} \\ \dfrac{(h\lambda_h - u'\lambda_{u'})}{hu} \\ \text{-----------} \\ \dfrac{\hat{h}^T \lambda_{\hat{r}'}}{hu} \end{bmatrix}. \qquad 3.4.37$$

And,

$$\lambda_{\overline{v}} = T\,\overline{S}(\eta)\,, \qquad 3.4.38$$

for

$$T \triangleq \begin{bmatrix} \hat{r} & \hat{r}' & \hat{h} \end{bmatrix}, \qquad 3.4.39$$

where $\hat{r}$, $\hat{r}'$, and $\hat{h}$ are represented in any desired coordinates.

In the next chapter, it will be shown that this local primer vector, $\bar{S}$, indeed satisfies the Maximum Principle in the x_2, λ_2 system. Then, the simple solutions of the Schumacher adjoint differential equations on coasting arcs will be given, so that these adjoint variables can be manipulated in this space. The functional form of the differential equation in this transformed space will be shown to give a new necessary condition for time open transfer problems. Also, other tests of optimality related to the derivative of the primer vector will be given in terms of the transformed adjoint space.

When finite thrust trajectories are computed using the methods to be derived in Chapter 10, the transformation from Schumacher adjoints to $\lambda_{\bar{r}}$ will also be needed. Multiplying the first row of A^{-1} by λ_2 gives, after simplifications analogous to those done above for $\lambda_{\bar{v}}$,

$$
\begin{aligned}
\lambda_{\bar{r}} \;=\; & u(h\lambda_h - u'\lambda_{u'} - u\,\lambda_u)\,\hat{r} \;+\; [u(\lambda_{\hat{r}}^T \hat{r}' - \lambda_{\hat{r}'}^T \hat{r}) + h\,u'\lambda_h - (u^2 + u'^2)\lambda_{u'}]\,\hat{r}' \\
& +\; (u\lambda_{\hat{r}}^T \hat{h} + u'\lambda_{\hat{r}'}^T \hat{h})\,\hat{h}.
\end{aligned}
\tag{3.4.40}
$$

Before proceeding to the next chapter, to discuss the optimal control problem in Schumacher space, one last detail must be taken care of. In that chapter time, t, will be appended to the state in both Cartesian coordinates and in Schumacher coordinates. This way, the class of transfer problems where maximum time is specified can be handled in the Schumacher coordinates, for otherwise time is not in the problem at all since the independent variable is the change in true anomaly, η. Therefore, it must be shown what happens to the transformation when t is appended to both systems. Let

$$x_1^\# = \begin{bmatrix} \tilde{x}_1 \\ t \end{bmatrix} \qquad\qquad 3.4.41$$

and

$$x_2^\# = \begin{bmatrix} x_2 \\ t \end{bmatrix} \qquad\qquad 3.4.42$$

and

$$h^\#(x_2^\#) = \begin{bmatrix} \tilde{h}(x_2) \\ t \end{bmatrix}. \qquad\qquad 3.4.43$$

Then,

$$\frac{\partial h^\#(x_2^\#)}{\partial x_2^\#} = \begin{bmatrix} \dfrac{\partial \tilde{h}(x_2)}{\partial x_2} & 0 \\ 0 & 1 \end{bmatrix}. \qquad\qquad 3.4.44$$

In view of adjoint transformation equation, Eq. 3.3.8, the off-diagonal zero vectors of this matrix makes the transformation of the adjoint to time, λ_t , separable from the rest of the adjoint variables. So, the λ_t is the same in both spaces (due to the "1" in the lower right diagonal), and the transformation of the rest of the adjoint variables is unchanged. Thus, this addition of t and λ_t to the problem can be ignored except where needed, and then these variables are the same in both systems. Thus, in the next chapter and following, when t and λ_t are discussed, specific reference to whether these are in Cartesian or in Schumacher coordinates will not in general be made.

As was just mentioned, λ_t was added to the problem because it is needed for the Schumacher adjoints for the time specified problem, so it is not really required in the Cartesian

adjoints except as it relates to the transformation. What, then, is λ_t in Cartesian adjoints? Consider the usual Hamiltonian in Cartesian space

$$H = \lambda_{\bar{r}}^T \bar{v} + \lambda_{\bar{v}}^T \left(-\frac{\mu}{r^3}\bar{r} + \bar{t} \right). \qquad 3.4.45$$

Now, since time does not explicitly appear in H, H is a constant whose value is zero for time open problems, or a nonzero constant otherwise. Next, consider the augmented Hamiltonian

$$H^{\#} = H + \dot{t}\lambda_t = H + \lambda_t. \qquad 3.4.46$$

In the augmented space the seventh variable is $x_7 = t$, so that now the time specified problem becomes a problem of specifying x_7 (i.e., $x_7(t_f) = t_f$), and the independent variable time is always free. Hence, $H^{\#} = 0$ always. In turn, this says that

$$\lambda_t = -H \qquad 3.4.47$$

from Eq. 3.4.45. That is, λ_t is just the negative of the usual Hamiltonian. This is why it is often loosely said that the Hamiltonian is adjoint to the independent variable. This relationship between λ_t and the Hamiltonian will be exploited to help understand the numerical solutions of finite thrust trajectories in Chapters 9 and 10.

4.0 THE OPTIMAL CONTROL PROBLEM IN SCHUMACHER COORDINATES

4.1 Introduction

Once the adjoint variables $\lambda_{\bar{r}}$ and $\lambda_{\bar{v}}$ are transformed to Schumacher adjoint variables, the dynamics of these variables is needed in order to propagate them in time (or in η). In this chapter, the differential equations for the Schumacher adjoint variables are given for any general thrusting or coasting arc (analytic solutions for coasting arcs will be derived in the next chapter). Then, the Maximum Principle is investigated in this space in order to verify that the transformed primer vector, $\bar{S}(\eta)$, derived in the previous chapter, does indeed satisfy the Maximum Principle in Schumacher variables (as the primer vector does in Cartesian position and velocity space). Finally, it will be shown how transversality requirements on the adjoint variables affect the Schumacher adjoint variables.

4.2 The Optimal Control Problem Statement

The state for the Schumacher coordinates, with time, t, appended to the basic set of nine redundant variables for the case when maximum time for the orbital transfer is specified, is:

$$x_2 = \begin{bmatrix} \hat{r} \\ u \\ \hat{r}' \\ u' \\ h \\ t \end{bmatrix}. \qquad 4.2.1$$

Schumacher derived the equations of motion in these coordinates in his doctoral dissertation[46]. These equations can be used directly, with the specific thrust vector (thrust per unit mass) in local coordinates (i.e., with the basis vectors $\hat{r}$, $\hat{r}'$, and $\hat{h} = \hat{r} \times \hat{r}'$),

$$\bar{T}^l = \begin{bmatrix} T_1 \\ T_2 \\ T_3 \end{bmatrix},$$ 4.2.2

taking the place of the perturbing force. Also, the derivative of time with respect to η is: $\frac{dt}{d\eta} = \frac{1}{h\,u^2}$. Thus, the equations of motion under spherical gravity and thrust only are:

$$\frac{dx_2}{d\eta} = \begin{bmatrix} \hat{r}' \\[2mm] u' \\[2mm] -\hat{r} + \dfrac{T_3}{h^2 u^3}\hat{h} \\[2mm] -u + \dfrac{\mu}{h^2} - \dfrac{T_1 u + T_2 u'}{h^2 u^3} \\[2mm] \dfrac{T_2}{h u^3} \\[2mm] \dfrac{1}{h u^2} \end{bmatrix}.$$ 4.2.3

The optimal control problem to be addressed here is to minimize the integral of the Euclidean norm of the thrust over the time of flight:

$$\min \int_0^{t_f} |\,\overline{T}\,|\ dt, \qquad\qquad 4.2.4$$

with the restriction $|\,\overline{T}\,| \leq T_{max}$. Since $dt = \dfrac{dt}{d\eta} d\eta = \dfrac{1}{hu^2} d\eta$, this integral is, in the new independent variable η,

$$\min \int_0^{\eta_f} \frac{|\,\overline{T}\,|}{hu^2}\ d\eta. \qquad\qquad 4.2.5$$

So, $\dfrac{|\,\overline{T}\,|}{hu^2}$ is the transformed Lagrange-form cost function.

The Hamiltonian for this system is

$$H = \langle \lambda_{\hat{r}}\,,\ \hat{r}'\rangle\ +\ \lambda_u\, u'\ +\ \langle \lambda_{\hat{r}'}\,,\ (-\hat{r} + \frac{T_3}{h^2 u^3}\hat{h})\rangle\ +\ \lambda_{u'}\,(-u + \frac{\mu}{h^2} - \frac{T_1 u + T_2 u'}{h^2 u^3})$$

$$+\ \lambda_h\, \frac{T_2}{hu^3}\ +\ \frac{(\lambda_t + \lambda_0\,|\,\overline{T}\,|)}{hu^2}. \qquad\qquad 4.2.6$$

The adjoint variables $\lambda_{\hat{r}}$ and $\lambda_{\hat{r}'}$ are vectors having three elements each, while the rest of the adjoint variables are scalars. The scalar constant $\lambda_0 \leq 0$ according to the Maximum Principle; for normal problems ($\lambda_0 \neq 0$), λ_0 can be taken to equal -1, since the set of adjoint variables can be scaled accordingly. $\lambda_0 = -1$ will be assumed in what follows. The differential equations for the adjoint variables are, for a general state x, $\dfrac{d\lambda_x}{d\eta} = -\left(\dfrac{\partial H}{\partial x}\right)^T$. Hence,

$$\frac{d}{d\eta}\lambda_{\hat{r}}\ =\ \lambda_{\hat{r}'} + \frac{T_3}{h^2 u^3}\,(\lambda_{\hat{r}'} \times \hat{r}')$$

$$\frac{d}{d\eta}\lambda_u = \lambda_{u'} - \frac{2uT_1 + 3u'T_2}{h^2u^4}\lambda_{u'} + \frac{3T_3}{h^2u^4}\langle\lambda_{\hat{r}'}, \hat{h}\rangle + \frac{3T_2}{hu^4}\lambda_h + \frac{2}{hu^3}(\lambda_t + \lambda_0|\overline{T}|)$$

$$\frac{d}{d\eta}\lambda_{\hat{r}'} = -\lambda_{\hat{r}} - \frac{T_3}{h^2u^3}(\lambda_{\hat{r}'} \times \hat{r})$$

<div style="text-align:right">4.2.7</div>

$$\frac{d}{d\eta}\lambda_{u'} = -\lambda_u + \frac{T_2}{h^2u^3}\lambda_{u'}$$

$$\frac{d}{d\eta}\lambda_h = \frac{2\mu}{h^3}\lambda_{u'} - \frac{2(uT_1 + u'T_2)}{h^3u^3}\lambda_{u'} + \frac{2T_3}{h^3u^3}\langle\lambda_{\hat{r}'}, \hat{h}\rangle + \frac{T_2}{h^2u^3}\lambda_h + \frac{1}{h^2u^2}(\lambda_t + \lambda_0|\overline{T}|)$$

$$\frac{d}{d\eta}\lambda_t = 0$$

The ten state differential equations together with the ten adjoint differential equations form a total system of twenty differential equations. When solving for finite thrust burn solutions, this system must be solved as a boundary value problem with the boundary conditions consisting of state boundary conditions and transversality requirements on the adjoint variables. The thrust control vector history is determined by the Maximum Principle. When the upper bound on the thrust, T_{max}, is relaxed in order to allow instantaneous impulse thrust, the solutions of Eqs. 4.2.7 for the case when $T_1 = T_2 = T_3 = 0$ are needed, in order to propagate the adjoint variables on the coasting arcs. They are very simple differential equations in that case: simple harmonic oscillators. So the solutions are simple functions of sines and cosines of the independent variable η.

4.3 The Maximum Principle

A necessary condition for a given thrust history and resultant trajectory to be optimal is

the Maximum Principle, namely, on the optimal trajectory the Hamiltonian must be maximized almost everywhere on $\eta \in [0, \eta_f]$ by the optimal thrust (where "almost everywhere" means except on a set of measure zero[44] -- see p. 310 of Lee and Markus[31] for a description of the Maximum Principle). Furthermore, λ_0 is a non-positive constant; assuming the particular problem at hand is a normal problem (i.e., $\lambda_0 \neq 0$), the adjoint variables can be scaled such that $\lambda_0 = -1$. In order to analyze this Maximum Principle for these coordinates, recall that the primer vector in the local system, transformed from the Cartesian $\bar{r}$ and $\bar{v}$ adjoint variables, is

$$\overline{S} = \begin{bmatrix} \dfrac{-\lambda_{u'}}{h} \\[2ex] \dfrac{h\lambda_h - u'\lambda_{u'}}{hu} \\[2ex] \dfrac{\langle \lambda_{\hat{r}'}, \hat{h} \rangle}{hu} \end{bmatrix}. \qquad\qquad 4.3.1$$

Notice that in the Hamiltonian, Eq. 4.2.6, the three elements of this vector are factors of the three elements of $\overline{T}^l$ in the Hamiltonian, so that

$$H_0 = \frac{1}{hu^2}\langle \overline{S}, \overline{T}^l \rangle - \frac{|\overline{T}|}{hu^2} \qquad\qquad 4.3.2$$

is the Hamiltonian less the parts which contain no thrust terms (with $\lambda_0 = -1$). Hence, finding the thrust which maximizes H_0 at any point on the optimal trajectory will yield the same thrust as maximizing H. Furthermore, the divisor, hu^2, common to both terms of H_0, is always non-negative, so that, with $H_1 = hu^2 H_0$,

$$\max_{\| \overline{T} \| \in [0, T_{max}]} H_1 \qquad\qquad 4.3.3$$

is the same condition as maximizing the Hamiltonian. H_1 can also be written

$$H_1 = ((\overline{S}, \hat{e}) - 1) |\overline{T}|, \qquad\qquad 4.3.4$$

where $\hat{e}$ is the direction of thrust. If $S < 1$ at any point on the trajectory, where $S \equiv |\overline{S}|$, then the factor in parentheses will be negative for all $\hat{e}$ directions of thrust, making $H_1 \leq 0$. In that case $\overline{T}^l = 0$, yielding $H_1 = 0$, is the optimal thrust for this point on the trajectory. On the other hand, if $S > 1$ the optimal thrust is $\overline{T}^l = T_{max} \frac{\overline{S}}{S}$, because $\hat{e} = \frac{\overline{S}}{S}$ will maximize the factor in parentheses and T_{max} is the maximum value of $|\overline{T}|$. If $S \equiv 0$ on any finite duration of of the independent variable η, the thrust control is singular; singular trajectories will not be discussed here. Recapitulating, the optimal thrust is

$$\overline{T}^l = \begin{cases} T_{max} \dfrac{\overline{S}}{S}, & S > 1 \\[2mm] 0, & S < 1 \end{cases}. \qquad\qquad 4.3.5$$

Since S is the primer vector magnitude, this is the same necessary condition as when the optimal control necessary condition is investigated in $\overline{r}$, $\overline{v}$ coordinates.

4.4 Transversality

For rendezvous problems, where the position and velocity vectors are defined at the beginning and the end of the transfer orbit, the transversality requirements on the corresponding adjoint variables do not give any specific information on the initial and final values of these

adjoint variables. These values must be determined by the requirement of making the trajectory meet the proper endpoint values.

If an intercept is desired instead of a rendezvous, then only the position vector, $\bar{r}$, is specified at both endpoints. The velocity vector, $\bar{v}$, is unspecified at the terminal point, so transversality dictates that the corresponding adjoint vector, the primer vector, must be zero there. In this case, the boundary conditions corresponding to the final value of $\bar{v}$ is replaced by the boundary condition $\lambda_{\bar{v}} = 0$. Since $\bar{S} = T^T \lambda_{\bar{v}}$ from Eq. 3.4.36, this means that $\bar{S} = 0$. Inspecting the components of $\bar{S}$, Eq. 4.3.1, this in turn means that $\lambda_{\hat{r}'} = \lambda_{u'} = \lambda_h = 0$ at the termination of the transfer trajectory. Furthermore, in view of the requirement that $\bar{S} = 0$, the condition on the thrust control, Eq. 4.3.5, implies that a fuel optimal intercept will _never_ thrust at the endpoint of the trajectory.

For problems where final time is not specified, the transversality condition on λ_t requires it to be zero at both ends of the trajectory. Since its derivative with respect to η is zero, it is constant along the whole trajectory, namely, $\lambda_t \equiv 0$. In this case, t and λ_t can be dropped from the problem (with, of course, factors of λ_t being dropped), since they have no affect on the other state and adjoint variables. On the other hand, if final time is specified, then the proper constant value of λ_t must be determined along with the other initial adjoint variables to make the trajectory match the endpoints _in the prescribed time._

One final note is in order concerning transversality requirements. Since η is the independent variable for Shumacher coordinates, if η_f is not specified, then the constant value of the Hamiltonian must be zero, $H \equiv 0$. Hence, the proper value of η_f must be determined in order to make H=0.

5.0 VERIFICATION OF IMPULSIVE THRUST TRAJECTORIES – TIME OPEN

5.1 Introduction

One way to obtain approximate solutions to the optimal control problems defined previously is to use an impulsive approximation to each thrusting arc, allowing a change in velocity over zero time at each "burn", then solve a parameter optimization problem yielding optimal velocity changes and coasting angles. The primer vector theory derived by Lawden, and also by Lion and Handelsmann, can be used to verify if impulsive burn trajectories found by this scheme, or by any other scheme, actually satisfy the necessary conditions obtained from the Maximum Principle. The main two conditions are: $|\lambda_{\bar{v}}| \leq 1$, which in turn implies that $|\bar{S}| \leq 1$, on an optimal trajectory; and, $\frac{dp}{dt} = 0$ (where $p \equiv |\lambda_{\bar{v}}|$) at times of interior burns, or immediately after the first burn following an initial coast, or immediately before the last burn preceding a final coast.

The second condition is the same as $S' = 0$, where $S \triangleq |\bar{S}|$. This can be proven by the following arguments. First, let $R \triangleq T^T$ (where T , from Eq. 3.4.39, transforms vectors in the local radial, transverse, normal coordinate system to the inertial coordinate system in which $\bar{r}$ and $\bar{v}$ are defined). Then

$$\bar{S} = R\,\lambda_{\bar{v}} \qquad\qquad 5.1.1$$

and

$$\bar{S}' = R'\lambda_{\bar{v}} + R\lambda_{\bar{v}}' . \qquad\qquad 5.1.2$$

Now,

$$R' = \begin{bmatrix} \hat{r}'^T \\ -\hat{r}^T \\ 0 \end{bmatrix}, \tag{5.1.3}$$

so that

$$\bar{S}' = R' R^T \bar{S} + R \lambda'_{\bar{v}} \tag{5.1.4}$$

$$= \begin{bmatrix} 0 & 1 & 0 \\ -1 & 0 & 0 \\ 0 & 0 & 0 \end{bmatrix} \bar{S} + R \lambda'_{\bar{v}} \tag{5.1.5}$$

$$= \begin{pmatrix} S_2 \\ -S_1 \\ 0 \end{pmatrix} + \frac{1}{h u^2} R \dot{\lambda}_{\bar{v}}. \tag{5.1.6}$$

Then solving this for $\dot{\lambda}_{\bar{v}}$ gives

$$\dot{\lambda}_{\bar{v}} = h u^2 R^T \left[\bar{S}' - \begin{pmatrix} S_2 \\ -S_1 \\ 0 \end{pmatrix} \right]. \tag{5.1.7}$$

Using these equations in the equation for $\dot{p}$ gives rise to the following sequence of equalities whenever $p \neq 0$:

$$\dot{p} \;=\; \frac{\lambda_{\overline{v}} \cdot \dot{\lambda}_{\overline{v}}}{p} \tag{5.1.8}$$

$$=\; \frac{1}{S} \, \lambda_{\overline{v}}^T \, \dot{\lambda}_{\overline{v}} \tag{5.1.9}$$

$$=\; \frac{h \, u^2}{S} \, (R^T \overline{S})^T \, R^T \left[\overline{S}' \;-\; \begin{pmatrix} S_2 \\ -S_1 \\ 0 \end{pmatrix} \right] \tag{5.1.10}$$

$$=\; \frac{h \, u^2}{S} \, \overline{S}^T R \, R^T \left[\overline{S}' \;-\; \begin{pmatrix} S_2 \\ -S_1 \\ 0 \end{pmatrix} \right] \tag{5.1.11}$$

$$=\; \frac{h \, u^2}{S} \, \overline{S}^T \left[\overline{S}' \;-\; \begin{pmatrix} S_2 \\ -S_1 \\ 0 \end{pmatrix} \right] \tag{5.1.12}$$

$$=\; \frac{h \, u^2}{S} \left[\overline{S}^T \overline{S}' \;-\; 0 \right] \tag{5.1.13}$$

$$=\; h \, u^2 \, \frac{\overline{S}^T \overline{S}'}{S} \tag{5.1.14}$$

$$=\; h \, u^2 \, S' \, . \tag{5.1.15}$$

Hence, if $\dot{p} = 0$ and $p \neq 0$, then $S' = 0$.

These conditions will be used in this chapter in the transformed Shumacher adjoint

space, for the time open transfer problem, to see what advantage is gained with those variables. The first advantage has already been stated in the previous chapter: propagating the primer vector on coasting arcs in Schumacher adjoint variables is much simpler than in Cartesian adjoint variables. The second advantage is that, due to the interrelationship of the adjoint variables comprising the transformed primer vector, $\bar{S}$, a new necessary condition for the time open problem results. The "time specified" problem will be addressed in the next chapter.

5.2 *State and Adjoint Variable Solutions on Coasting Arcs*

On coasting arcs, i.e. portions of the trajectory where thrust is zero, the differential equations for the Schumacher coordinates become

$$\hat{r}'' + \hat{r} = 0$$

$$u'' + u = \frac{\mu}{h^2} \qquad\qquad 5.2.1$$

$$h' = 0 \ .$$

Hence, $\hat{r}$, $\hat{r}'$, u, and u$'$ are simple harmonic oscillators, and h is a constant. Therefore,

$$\hat{r}(\eta) = \hat{r}_0 \cos\eta + \hat{r}_0' \ \sin\eta$$

$$\hat{r}'(\eta) = -\hat{r}_0 \sin\eta + \hat{r}_0' \ \cos\eta$$

$$u(\eta) = \frac{\mu}{h^2} + (u_0 - \frac{\mu}{h^2})\cos\eta + u_0' \sin\eta \qquad 5.2.2$$

$$u'(\eta) = -(u_0 - \frac{\mu}{h^2})\sin\eta + u_0' \cos\eta$$

$$h = \text{constant} .$$

Similarly, the adjoint variables corresponding to $\hat{r}$, $\hat{r}'$, u, u', as well as h, are also simple harmonic oscillators on coasting arcs when $\lambda_t = 0$ (i.e., when final time is not specified). The differential equations, in this case, are

$$\frac{d^2}{d\eta^2}\lambda_{\hat{r}} = \frac{d}{d\eta}\lambda_{\hat{r}'} = -\lambda_{\hat{r}} \quad \Rightarrow \quad \frac{d^2}{d\eta^2}\lambda_{\hat{r}} + \lambda_{\hat{r}} = 0$$

$$\frac{d^2}{d\eta^2}\lambda_u = \frac{d}{d\eta}\lambda_{u'} = -\lambda_u \quad \Rightarrow \quad \frac{d^2}{d\eta^2}\lambda_u + \lambda_u = 0$$

$$\frac{d^2}{d\eta^2}\lambda_{\hat{r}'} = -\frac{d}{d\eta}\lambda_{\hat{r}} = -\lambda_{\hat{r}'} \quad \Rightarrow \quad \frac{d^2}{d\eta^2}\lambda_{\hat{r}'} + \lambda_{\hat{r}'} = 0 \qquad 5.2.3$$

$$\frac{d^2}{d\eta^2}\lambda_{u'} = -\frac{d}{d\eta}\lambda_u = -\lambda_{u'} \quad \Rightarrow \quad \frac{d^2}{d\eta^2}\lambda_{u'} + \lambda_{u'} = 0$$

$$\frac{d}{d\eta}\lambda_h = \frac{2\mu}{h^3}\lambda_{u'} \quad \Rightarrow \quad \frac{d^2}{d\eta^2}\lambda_h + \lambda_h = \lambda_{ho} .$$

These have solution

$$\lambda_{\hat{r}}(\eta) = \lambda_{\hat{r}0}\cos\eta + \lambda_{\hat{r}'_0}\sin\eta$$

$$\lambda_{\hat{r}'}(\eta) = -\lambda_{\hat{r}0}\sin\eta + \lambda_{\hat{r}'_0}\cos\eta$$

$$\lambda_{u}(\eta) = \lambda_{u0}\cos\eta + \lambda_{u'_0}\sin\eta \qquad\qquad 5.2.4$$

$$\lambda_{u'}(\eta) = -\lambda_{u0}\sin\eta + \lambda_{u'_0}\cos\eta$$

$$\lambda_{h}(\eta) = \frac{2\mu}{h^3}\lambda_{u0}\left(\cos\eta - 1\right) + \frac{2\mu}{h^3}\lambda_{u'_0}\sin\eta + \lambda_{h0}\,.$$

The simple form of these equations facilitate computing the local primer vector, $\overline{S}(\eta)$, on coasting arcs between impulsive burns, in order to check if the trajectory satisfies the Maximum Principle necessary condition.

5.3 Computation of the Local Primer Vector Between Burns

Since the limiting thrust becomes just a change in vector velocity, $\Delta\overline{v}^l$, the Maximum Principle states that the local primer vector, $\overline{S}(\eta)$, must be collinear and co-directional with this $\Delta\overline{v}^l$ at each burn. Furthermore, the primer magnitude must equal one $(S = 1)$ at each $\Delta\overline{v}^l$ as shown by Lawden, and by Lion and Handelsmann. Hence, $\overline{S} = \frac{\Delta\overline{v}^l}{\Delta v}$, with $\Delta v \triangleq |\Delta\overline{v}^l|$. In Schumacher coordinates,

$$\Delta \bar{v}^l \;=\; T\,\Delta \bar{v} \;=\; \begin{bmatrix} h^- u'^- - h^+ u'^+ \\[4pt] u^-(h^+ \cos\phi - h^-) \\[4pt] h^+ u^- \sin\phi \end{bmatrix}, \qquad 5.3.1$$

in the local basis $(\hat{r},\ \hat{r}',\ \hat{h})$. A minus sign indicates immediately before the burn, and a plus sign indicates immediately after the burn. Also, $\sin\phi = \langle \hat{r}'^+, \hat{h}^- \rangle$, and $\cos\phi = \langle \hat{r}'^+, \hat{r}'^- \rangle$.

From the $\overline{S} = \dfrac{\Delta \bar{v}^l}{\Delta v}$ relationship, therefore,

$$\begin{bmatrix} \dfrac{-\lambda_{u'}}{h} \\[10pt] \dfrac{h\lambda_h - u'\lambda_{u'}}{hu} \\[10pt] \dfrac{\langle \lambda_{\hat{r}'},\ \hat{h} \rangle}{hu} \end{bmatrix} \;=\; \begin{bmatrix} h^- u'^- - h^+ u'^+ \\[10pt] u^-(h^+ \cos\phi - h^-) \\[10pt] h^+ u^- \sin\phi \end{bmatrix} \Big/ \Delta v \ . \qquad 5.3.2$$

As a result, at each burn the quantities $\lambda_{u'}$, λ_h, and $\langle \lambda_{\hat{r}'},\ \hat{h} \rangle$ can be determined from this simple linear equation. These variables need to be computed for all η values between impulsive thrusts, in order to check that $S(\eta) \le 1$ for all η. To this end, consider first computing $\lambda_{u'}(\eta)$. Its value is known at the beginning and at the end of the coasting arc, but λ_{u0} is needed at the beginning of the arc because it appears in (from Eq. 5.2.4)

$$\lambda_{u'}(\eta) \;=\; -\lambda_{u0}\sin\eta + \lambda_{u'0}\cos\eta \ . \qquad 5.3.3$$

Since

$$\lambda_{\mathrm{h}}(\eta) \;=\; \frac{2\mu}{\mathrm{h}^3}\,\lambda_{\mathrm{u0}}\,(\cos\eta - 1) \;+\; \frac{2\mu}{\mathrm{h}^3}\,\lambda_{\mathrm{u'0}}\,\sin\eta \;+\; \lambda_{\mathrm{h0}}\;,\qquad\qquad 5.3.4$$

then, with subscript "o" referring to the beginning of a coasting arc, "*f*" referring to the end of a coasting arc, and η_f denoting the total coasting angle,

$$\lambda_{\mathrm{u0}} \;=\; \frac{\mathrm{h}^3}{2\mu(\cos\eta_f - 1)}(\lambda_{\mathrm{h}f} - \lambda_{\mathrm{h0}}) \;-\; \frac{\sin\eta_f}{(\cos\eta_f - 1)}\lambda_{\mathrm{u'0}}\;.\qquad\qquad 5.3.5$$

This λ_{u0} and the given $\lambda_{\mathrm{u'0}}$ provide $\lambda_{\mathrm{u'}}(\eta)$ for all η.

It is interesting and significant to note, however, that given arbitrary values of $\Delta\bar{\mathrm{v}}^l$ at both ends, and hence arbitrary values of $\lambda_{\mathrm{u'0}}$, $\lambda_{\mathrm{u'}f}$, λ_{h0}, and $\lambda_{\mathrm{h}f}$, the functional form of $\lambda_{\mathrm{u'}}(\eta)$ (i.e., Eq. 5.3.3) evaluated at η_f will not necessarily equal the given $\lambda_{\mathrm{u'}f}$. As a result, if a coasting arc between two burns on a proposed optimal trajectory is not such that $\lambda_{\mathrm{u'}f}$, from the $\overline{\mathrm{S}} = \dfrac{\Delta\bar{\mathrm{v}}^l}{\Delta\mathrm{v}}$ relationship, matches the value from the functional form of $\lambda_{\mathrm{u'}}(\eta_f)$, then the trajectory *cannot be optimal*. This is so because the Maximum Principle states[31,32] that if the trajectory is optimal, then there does exist a non-trivial adjoint response satisfying the conditions mentioned previously; but, the mismatch of the final functional value of $\lambda_{\mathrm{u'}}$ and that obtained from the requisite $\overline{\mathrm{S}} = \dfrac{\Delta\bar{\mathrm{v}}^l}{\Delta\mathrm{v}}$ relationship indicates that there is no such adjoint response. This fact provides an *additional test of optimality*, even before the requirement that $\mathrm{S}(\eta) \leq 1$ for all η is checked. This test can be put in the analytical form $\delta = 0$, where

$$\boxed{\;\delta \;\triangleq\; \lambda_{\mathrm{u'}f} \;+\; \lambda_{\mathrm{u0}}\sin\eta_f \;-\; \lambda_{\mathrm{u'0}}\cos\eta_f \;=\; 0.\;}\qquad\qquad 5.3.6$$

As a reminder, $\lambda_{u'0}$ and $\lambda_{u'f}$ are determined from Eq. 5.3.2 at each end of the coasting arc in question, λ_{u0} comes from Eq. 5.3.5, and η_f is the coasting angle.

Returning to analyzing $\overline{S}(\eta)$, evaluating $\lambda_h(\eta)$ is straightforward, after λ_{u0} is computed from Eq. 5.3.5, since it is function of only λ_{u0} , $\lambda_{u'0}$, λ_{h0} , and η (see Eq. 5.3.4). The last quantity to be considered is $\langle \lambda_{\hat{r}'} , \hat{h} \rangle$. For notational convenience, define $\lambda_{\hat{r}N} \triangleq \langle \lambda_{\hat{r}} , \hat{h} \rangle$ and $\lambda_{\hat{r}'N} \triangleq \langle \lambda_{\hat{r}'} , \hat{h} \rangle$ (where subscript "N" stands for normal, since the component of these vectors in the $\hat{h}$ direction is the out-of-plane component, normal to the plane of motion). Then,

$$\lambda_{\hat{r}'N}(\eta) \;=\; -\lambda_{\hat{r}N0} \sin\eta \;+\; \lambda_{\hat{r}'N0} \cos\eta \tag{5.3.7}$$

so that, evaluating Eq. 5.3.7 at η_f and solving for $\lambda_{\hat{r}N0}$ yields

$$\lambda_{\hat{r}N0} \;=\; \lambda_{\hat{r}'N0} \cot\eta_f \;-\; \lambda_{\hat{r}'Nf} \csc\eta_f \;. \tag{5.3.8}$$

This equation can be used to find $\lambda_{\hat{r}N0}$ as long as $\sin\eta_f \neq 0$ (i.e., $\eta_f \neq n\pi$ for any integer n). This value of $\lambda_{\hat{r}N0}$, along with the $\lambda_{\hat{r}'N0}$ given from the $\overline{S} = \dfrac{\Delta\overline{v}^I}{\Delta v}$ at the beginning of the coasting arc, yields $\lambda_{\hat{r}'N}(\eta)$ for all η through Eq. 5.3.7.

Thus, all variables in the equation for $\overline{S}(\eta)$ can be determined as functions of the independent variable η, so that the necessary condition $S(\eta) \leq 1 \ \forall \ \eta \in [0,\eta_f]$ can be checked. Along the way to unearthing the method for computing $\overline{S}(\eta)$, a new test of optimality along a coasting arc was discovered as an artifact of the functional form of the adjoint variables, the fact that $\lambda_h(\eta)$ and $\lambda_{u'}(\eta)$ are related through the initial value of $\lambda_u(\eta)$, λ_{u0}.

5.4 Computation of $S'(\eta)$

Now that $\overline{S}(\eta)$, and hence $S(\eta)$, can be evaluated on coasting arcs, the functional form
for $S'(\eta)$ is required for two purposes. Firstly, and primarily, it is required in order to test the
$S' = 0$ conditions at the appropriate burn times, as mentioned in Section 5.1. Secondly,
the condition $S'(\eta) = 0$ can be used to find the points η_i^* where the maxima of $S(\eta)$ occur, in
order to check the condition $S(\eta_i^*) \leq 1$ at these critical points in order to verify that $S(\eta) \leq 1$
everywhere on the trajectory.

To this end, consider that if $S(\eta) \neq 0$, then the zeros of $S'(\eta)$ are the same as the zeros
of $S(\eta) \cdot S'(\eta) = \langle \overline{S}(\eta) , \overline{S}'(\eta) \rangle$. Since h and $u(\eta)$ do not go to zero on any of the trajectories of
interest, the zeros of $\sigma(\eta) \triangleq h^2 u(\eta)^3 S(\eta) \cdot S'(\eta)$ will be the same as the zeros of $S'(\eta)$. Taking
straightforward derivatives of $\overline{S}(\eta)$ yields

$$
\overline{S}'(\eta) \;=\;
\begin{bmatrix}
\dfrac{\lambda_u}{h} \\[3mm]
\dfrac{(\frac{\mu u}{h^2} + u^2 + u'^2)\lambda_{u'} \;+\; uu'\lambda_u \;-\; hu'\lambda_h}{hu^2} \\[3mm]
-\dfrac{(u\langle \lambda_{\hat{r}} , \hat{h} \rangle + u'\langle \lambda_{\hat{r}'} , \hat{h} \rangle)}{hu^2}
\end{bmatrix} .
\qquad 5.4.1
$$

Therefore,

$$
\sigma(\eta) \;=\; -u^3 \lambda_u \lambda_{u'} \;+\; (h\lambda_h - u'\lambda_{u'})[(\tfrac{\mu u}{h^2} + u^2 + u'^2)\lambda_{u'} \;+\; uu'\lambda_u \;-\; hu'\lambda_h]
$$

$$
5.4.2
$$

$$- (u\lambda_{\hat{r}N}\lambda_{\hat{r}'N} + u'\lambda_{\hat{r}'N}^2) \, .$$

In these previous two equations, all quantities on the right hand side are evaluated at η.

5.5 Review

A two step check is suggested for checking the optimality of a trajectory consisting of impulsive burns instead of thrusting arcs. First, on each coasting arc between burns, the $\delta = 0$ test (Eq. 5.3.6) is evaluated. If $\delta \neq 0$ on any arc, then the trajectory is not optimal. If $\delta = 0$ on all arcs, then the classical optimality conditions on the primer vector must be checked. If $S(\eta) > 1$ for any η on any coasting arc, or if $S'(\eta) \neq 0$ at interior burns or after an initial coast or before a final coast, then the trajectory is not optimal. Otherwise, the trajectory is still a candidate for an optimal trajectory.

6.0 VERIFICATION OF IMPULSIVE THRUST TRAJECTORIES – TIME SPECIFIED

6.1 Introduction

The problem of verifying optimal trajectories when a maximum final time is given is nearly as easy as the open time case. As far as primer vector theory is concerned, very little is different from the time open case. The solution, however, of the Schumacher adjoint variables is slightly more complicated, since $\lambda_t \neq 0$ in general for time specified trajectories. This extra degree of freedom in the adjoint variables (the λ_t parameter) unfortunately means that the new $\delta = 0$ test for optimality does not apply for the time specified case. In other words, recall that unless $\delta = 0$, the functional form of $\lambda_{u'}(\eta_f)$ propagated from η_0 does not match the value of $\lambda_{u'f}$ determined from the $\overline{S} = \dfrac{\Delta \overline{v}^l}{\Delta v}$ requirement the Maximum Principle places on the control. But, for the time specified case, the parameter λ_t is now part of the $\lambda_{u'}$ solution, so this extra degree of freedom essentially allows $\delta = 0$ to be true always.

Effectively what has happened is that knowledge of the time of flight on the coasting arc has replaced the condition $\delta=0$, as will be shown later in this chapter. When there are more coasting arcs than one (i.e., more burns than two for rendezvous or more than one for intercept), more conditions are required to replace $\delta = 0$ on each coast. The appropriate condition is $\lambda_{t,m} = \lambda_{t,m-1}$ for each coasting arc m after the first one, resulting from the solution λ_t=constant over the whole trajectory.

The extant conditions on the primer vector, however, still hold, of course, in the time specified case. With the solutions and procedures developed in this chapter, these conditions can be easily checked by propagating the primer vector transformed to Schumacher space, $\overline{S}$, as well

as its derivative, $\bar{S}'$, and the derivative of its magnitude, S'.

6.2 *Solution of Adjoint Variables*

The adjoint variables were solved for coasting arcs in Section 5.2 for the case when $\lambda_t = 0$. Examination of Eqs. 4.2.7 reveals that only λ_u, $\lambda_{u'}$, and λ_h are changed when $\lambda_t \neq 0$. The $\lambda_t = 0$ solutions to these equations are homogeneous solutions, and λ_t multiplied by its factors are forcing functions, the consideration of which leads to complementary solutions.

Consider first the solution of $\lambda_{u'}$. The equation from Eq. 4.2.7 , on coasting arcs, is

$$\frac{d}{d\eta}\lambda_{u'} = -\lambda_u.$$

<div align="right">6.2.1</div>

Taking a derivative of this equation gives

$$\frac{d^2}{d\eta^2}\lambda_{u'} = -\frac{d}{d\eta}\lambda_u.$$

<div align="right">6.2.2</div>

Using

$$\frac{d}{d\eta}\lambda_u = \lambda_{u'} + \frac{2\lambda_t}{hu^3}$$

<div align="right">6.2.3</div>

from Eq. 4.2.7 produces, after appropriate rearrangement,

$$\frac{d^2}{d\eta^2}\lambda_{u'} + \lambda_{u'} = -\frac{2\lambda_t}{hu^3}.$$

<div align="right">6.2.4</div>

When $\lambda_t = 0$, this is the homogeneous equation solved before. Since λ_t is a constant, let the right hand side be $\lambda_t \cdot f(\eta)$; i.e.,

$$f(\eta) = -\frac{2}{hu^3}.$$

6.2.5

Then using the variation of parameters approach to the solution of this, the complementary solution is

$$\lambda_{u'c} = C_1(\eta)\cos\eta + C_2(\eta)\sin\eta$$

6.2.6

(since $\cos\eta$ and $\sin\eta$ are two independent solutions of the homogeneous equation). $C_1(\eta)$ and $C_2(\eta)$ are found from

$$C_1'(\eta) = -f(\eta)\sin\eta$$

6.2.7

and

$$C_2'(\eta) = f(\eta)\cos\eta.$$

6.2.8

These two equations can be integrated analytically, as is shown in appendix A.

In order to solve λ_{uc} next, recall that from Eq. 6.2.1

$$\lambda_{uc} = -\frac{d}{d\eta}\lambda_{u'c}.$$

6.2.9

Therefore,

$$\lambda_{uc} = -[C_1'(\eta) + C_2(\eta)] \cos\eta + [C_1(\eta) - C_2'(\eta)] \sin\eta. \qquad 6.2.10$$

Finally, λ_{hc} is to be solved. The differential equation of λ_h is

$$\frac{d\lambda_h}{d\eta} = \frac{2\mu}{h^3}\lambda_{u'}(\eta) + \frac{\lambda_t}{h^2 u^2(\eta)}. \qquad 6.2.11$$

Substituting both homogeneous and complementary solutions of $\lambda_{u'}$ into this equation gives

$$\frac{d\lambda_h}{d\eta} = \frac{2\mu}{h^3}(\lambda_{u'h} + \lambda_t \lambda_{u'c}) + \frac{\lambda_t}{h^2 u^2(\eta)}. \qquad 6.2.12$$

Since the right hand side of this equation contains only known functions of η, λ_h is solved by integrating both sides. Doing this, and subtracting the homogeneous solution from both sides yields the complementary solution of λ_h:

$$\lambda_{hc}(\eta) - \lambda_{hc}(0) = \int_0^\eta \left[\frac{2\mu}{h^3}\lambda_{u'c}(x) + \frac{1}{h^2 u(x)^2}\right] dx. \qquad 6.2.13$$

The first term on the right side of the equation requires the integral $\int_0^\eta \lambda_{u'c}(x)\,dx$, which is solved analytically in appendix A. For solving the second term on the right hand side, recall that $\frac{dt}{d\eta} = \frac{1}{hu^2}$. This means that the integral of the second term is just $\frac{1}{h}$ times the time of flight of the coasting arc. Finally, choose $\lambda_{hc}(0) = 0$. Putting these together,

$$\lambda_{hc}(\eta) = \frac{2\mu}{h^3}\int_0^\eta \lambda_{u'c}(x)\,dx + \frac{(t - t_0)}{h}, \qquad 6.2.14$$

where $\lambda_t \cdot \lambda_{hc}(\eta)$ is the total complementary solution.

Adding these complementary solutions to the homogeneous equations, Eqs. 5.2.4, and including all of the adjoint equations for completeness,

$$\lambda_{\hat{r}}(\eta) = \lambda_{\hat{r}0}\cos\eta + \lambda_{\hat{r}'_0}\sin\eta$$

$$\lambda_{\hat{r}'}(\eta) = -\lambda_{\hat{r}0}\sin\eta + \lambda_{\hat{r}'_0}\cos\eta$$

$$\lambda_u(\eta) = \lambda_{u0}\cos\eta + \lambda_{u'_0}\sin\eta + \lambda_t\lambda_{uc}(\eta) \qquad\qquad 6.2.15$$

$$\lambda_{u'}(\eta) = -\lambda_{u0}\sin\eta + \lambda_{u'_0}\cos\eta + \lambda_t\lambda_{u'c}(\eta)$$

$$\lambda_h(\eta) = \frac{2\mu}{h^3}\lambda_{u0}(\cos\eta - 1) + \frac{2\mu}{h^3}\lambda_{u'_0}\sin\eta + \lambda_t\lambda_{hc}(\eta) + \lambda_{ho}$$

and

$$\lambda_t = \text{constant}.$$

6.3 The Time Specified Local Primer Vector

In order to be able to determine the values of the local primer vector, $\overline{S}(\eta)$, for all values of $\eta \in [0, \eta_f]$ on any coasting arcs between burns on a proposed optimal trajectory, the values of the adjoint variables comprising $\overline{S}$ must be determined from the $\overline{S} = \dfrac{\Delta\overline{v}^I}{\Delta v}$ condition at both ends of the coast as before. Now, however, the additional adjoint variable, λ_t, must also be computed. To this end, consider the two equations of the two adjoint variables (from Eqs. 6.2.15),

$$\lambda_{u'}(\eta) \; = \; -\lambda_{u0}\sin\eta + \lambda_{u'_0}\cos\eta + \lambda_t \, \lambda_{u'c}(\eta) \qquad\qquad 6.3.1$$

$$\lambda_h(\eta) \; = \; \frac{2\mu}{h^3} \lambda_{u0} \, (\cos\eta - 1) \; + \; \frac{2\mu}{h^3} \lambda_{u'_0} \, \sin\eta \; + \lambda_t \, \lambda_{hc}(\eta) + \lambda_{h0}. \qquad\qquad 6.3.2$$

When these expressions, Eqs. 6.3.1 and 6.3.2 are evaluated at η_f, the left-hand-sides become $\lambda_{u'_f}$ and λ_{h_f}. These are known from the $\overline{S} = \dfrac{\Delta \overline{v}^I}{\Delta v}$ condition at the final burn on the coasting arc of interest. Similarly, $\lambda_{u'_0}$ and λ_{h0} are determined from the first burn. η_f is the known coasting angle, and $\lambda_{u'c}(\eta_f)$ and $\lambda_{hf}(\eta_f)$ can be computed from η_f and the state variable. The only unknowns, therefore, are λ_{u0} and λ_t. Eqs. 6.3.1 and 6.3.2 are two linear equations in two unknowns, so the solutions are readily determined.

Before solving these equations, reflect on the fact that when λ_t was specified to be zero, these two equations gave the $\delta = 0$ additional test of optimality, since they were two equations in the one unknown, λ_{u0}. Now, however, knowledge of the time of flight has replaced the $\delta = 0$ condition, since a specific time of flight yields a specific λ_t on a given coast between two burns, with the previous and subsequent orbits fully known. In other words, in view of Lambert's theorem[2], if the previous and subsequent orbits are known, then one parameter will suffice to specify the trajectory between these two orbits. Let this parameter be called ψ. In the next chapter it will be shown that when it is desired to compute (as opposed to merely checking) trajectories which satisfy the Maximum Principle, the parameter of choice ψ chosen in this work is u'_0. If the time of flight is free, then $\delta(\psi) = 0$ specifies the trajectory. If the time of flight is specified, then the value of ψ which yields this time of flight is the desired one as long as the time open solution ($\delta(\psi) = 0$) has time of flight longer than the specified maximum time.

On trajectories with more than two burns, the fact that λ_t must be constant gives an

additional check for each burn beyond two. That is, $\lambda_{t,n} = \lambda_{t,n+1}$ for coasting arcs n and

n+1. If n_b is the number of burns, then these $n_b - 2$ conditions on matching values of λ_t on all

coasting arcs, plus the one additional total time of flight condition (for a total of $n_b - 1$

conditions), replace the $n_b - 1$ conditions $\delta_i = 0$, $i = 1, \ldots, n_b - 1$, whenever the time free

solution has time of flight longer than the specified maximum. Note that if a time specified

solution was forced even though the time open trajectory had shorter time of flight, then λ_t

would become positive.

Returning to solving Eqs. 6.3.1 and 6.3.2, solve the first for $\lambda_{uo} \sin\eta$:

$$\lambda_{uo} \sin\eta = \lambda_{u'0} \cos\eta - \lambda_{u'f} + \lambda_t \lambda_{u'c}(\eta). \qquad 6.3.3$$

Next, multiply Eq. 6.3.2 by $\sin\eta$ and substitute for $\lambda_{uo} \sin\eta$ from above, then solve for λ_t to

yield

$$\lambda_t = \frac{(\lambda_{hf} - \lambda_{ho}) \sin\eta + \dfrac{2\mu}{h^3}(\lambda_{u'0} + \lambda_{u'f})(\cos\eta - 1)}{\lambda_{hc}(\eta) \sin\eta + \dfrac{2\mu}{h^3} \lambda_{u'c}(\eta)(\cos\eta - 1)}. \qquad 6.3.4$$

Finally, use this value of λ_t in Eq. 6.3.2 to solve for λ_{uo}:

$$\lambda_{uo} = \frac{\dfrac{h^3}{2\mu}[\lambda_{ho} - \lambda_{hf} + \lambda_t \lambda_{hc}(\eta)] + \lambda_{u'0} \sin\eta}{(1 - \cos\eta)}. \qquad 6.3.5$$

The computation of $\lambda_{r'N}(\eta)$ is the same as in the time open case, since it is not affected by λ_t.

With all of these values of the adjoint variables, $\overline{S}(\eta)$ can be computed in order to check that

$S(\eta) \leq 1$ for all $\eta \in [\,0\,, \eta_f\,]$.

6.4 Computation of $S'(\eta)$

The computation of $S'(\eta)$ for the time specified case is accomplished in exactly the same way as in the time open case. As already shown above, $\overline{S}(\eta)$ is the same regardless of the dispensation of the final time; hence, $S'(\eta)$ is the same as before except that the derivative of one of the adjoint variables now contains a term with λ_t in it. To this end, again taking straightforward derivatives of the local primer vector $\overline{S}(\eta)$ (Eq. 3.4.37), and using Eqs. 4.2.7 for the derivatives of the adjoint variables (with zero thrust and nonzero λ_t),

$$
\overline{S}'(\eta) \;=\; \left[\begin{array}{c} \dfrac{\lambda_u}{h} \\[3ex] \dfrac{(\frac{\mu u}{h^2} + u^2 + u'^2)\lambda_{u'} \;+\; uu'\lambda_u \;-\; hu'\lambda_h \;+\; \dfrac{\lambda_t}{hu}}{hu^2} \\[4ex] -\,\dfrac{(u\langle \lambda_{\hat{r}}\, ,\, \hat{h}\rangle + u'\langle \lambda_{\hat{r}'}\, ,\, \hat{h}\rangle)}{hu^2} \end{array}\right].
\qquad 6.4.1
$$

The only difference between this vector and the time open vector, Eq. 5.4.1, is the addition of the term $\dfrac{\lambda_t}{h^2 u^3}$ in the direction of $\hat{r}'$. The function $\sigma(\eta) \overset{\triangle}{=} h^2 u(\eta)^3 S(\eta) S'(\eta)$ defined in Section 5.4, which has the same zeros as does $S'(\eta)$ when $S(\eta) \neq 0$, is therefore

$$
\sigma(\eta) \;=\; -u^3\lambda_u\lambda_{u'} \;+\; (h\lambda_h - u'\lambda_{u'})[(\tfrac{\mu u}{h^2} + u^2 + u'^2)\lambda_{u'} \;+\; uu'\lambda_u \;-\; hu'\lambda_h \;+\; \tfrac{\lambda_t}{hu}]
$$

$$- \left(u\lambda_{\hat{r}N}\lambda_{\hat{r}'N} + u'\lambda_{\hat{r}'N}^2 \right).$$

So, with the knowledge of λ_t obtained by the methods of the previous section, as well as the other adjoint variables, $\sigma(\eta)$ can be calculated in order to check the necessary condition $\sigma(\eta) = 0$ where it applies.

7.0   USING THE NEW OPTIMALITY TEST TO COMPUTE TWO-BURN IMPULSIVE TRAJECTORIES

7.1   Introduction

The new optimality test, Eq. 5.3.6, can be used not only to verify optimality of impulsive burn trajectories, but also to compute trajectories which satisfy the Maximum Principle. First, in this chapter, the two burn case will be considered to a fixed position, then from this foundation a more general procedure will be built in the following chapter. The first several sections, Sections 7.2–7.6, will be devoted to the time free case. Section 7.7 will then treat the time specified two burn rendezvous and one burn intercept problems.

7.2   Two-Burn Time-Free Rendezvous Trajectories, No Initial Coast

Consider, first, the impulsive burn rendezvous optimal control problem where it is known *a priori* that the interceptor space vehicle will burn immediately at its current position (no coast), and that there will only be two burns, the initial one and the final one. This is indeed a simple subset of all the problems of interest. Many real problems, however, do fall into this category, and the new optimality test, Eq. 5.3.6, allows the solution to be easily computed.

As a matter of notation, let index subscripts denote the number of the coasting arc; e.g., $\hat{r}_n(0)$ and $\hat{r}_n(\eta_f)$ are the values of the element $\hat{r}$ at the beginning and at the end of the nth coasting arc. Thus, for rendezvous problems, $n \in \{0 , 1 , \ldots , n_{burn}\}$, where n_{burn} is the number of burns. For intercept problems, $n \in \{0 , 1 , \ldots , n_{burn} - 1\}$. Hence, for the two burn problem,

n=0 is the initial trajectory of the interceptor, n=1 is the intermediate trajectory, and n=2 is the target trajectory. Although this general notation need not be used when there are only two burns as is presently being considered, the ensuing results are more generally applicable and hence will also be used in later chapters.

Using this notation for the coasting arc between the two burns (i.e., $n = 1$), consider that the full set of elements are known at the end of the original interceptor trajectory: $\hat{r}_{n-1}(\eta_f)$, $u_{n-1}(\eta_f)$, $\hat{r}'_{n-1}(\eta_f)$, $u'_{n-1}(\eta_f)$, and h_{n-1}. Similarly, the full set of elements at the beginning of the target trajectory are known: $\hat{r}_{n+1}(0)$, $u_{n+1}(0)$, $\hat{r}'_{n+1}(0)$, $u'_{n+1}(0)$, and h_{n+1}. From elementary geometry, the vectors $\hat{r}_n(0)$, and $\hat{r}'_n(0)$ can be easily computed when $\eta_f \neq (2m-1)\pi$ for any integer m: $\hat{r}_n(0) = \hat{r}_{n-1}(\eta_f)$, and $\hat{r}'_n(0) = \hat{h}_n \times \hat{r}_n(0)$, where $\hat{h}_n = sgn(\sin\eta_f)\,\hat{r}_n(0) \times \hat{r}_{n+1}(0)$. Also, $u_n(0) = u_{n-1}(\eta_f)$.

On the other hand, if $\eta_f = (2m-1)\pi$ for some integer m, then the plane of motion of the coasting arc is not uniquely determined. Since $\lambda_{\hat{r}'N0} = -\lambda_{\hat{r}'Nf}$ when $\eta_f = (2m-1)\pi$ (see Eq. 5.3.7), the third component of the $\overline{S} = \dfrac{\Delta\overline{v}^l}{\Delta v}$ equation,

$$\frac{\lambda_{\hat{r}'N}}{hu} = \frac{h^+u^-\sin\phi}{\Delta v}, \qquad\qquad 7.2.1$$

can be used at the endpoints of the coasting trajectory to determine the plane of motion (namely, ϕ determines the plane of motion). That is,

$$\frac{h_n^2 u_n^2(0)\sin\phi_0}{\Delta v_0} = -\frac{h_n h_{n+1} u_n^2(\eta_f)\sin\phi_f}{\Delta v_f}. \qquad\qquad 7.2.2$$

Notice that Δv_0 and Δv_f are functions of ϕ_0 and ϕ_f, also. This is only one equation for the two unknowns ϕ_0 and ϕ_f, so another equation relating the two must be found. The requisite

relationship comes from the fact that since the planes of motion before and after this current one are known, once ϕ_0 is given, ϕ_f can be immediately determined. Since $\hat{r}_n(\pi) = -\hat{r}_n(0)$, the $n-1$ and the $n+1$ planes can be related by an angle α defined by:

$$\sin\alpha \;=\; \langle \hat{h}_{n+1}, \hat{r}'_{n-1}(\eta_f) \rangle \qquad\qquad 7.2.3$$

and

$$\cos\alpha \;=\; \langle \hat{h}_{n+1}, \hat{h}_{n-1} \rangle. \qquad\qquad 7.2.4$$

Then $\phi_f \;=\; \phi_0 + \alpha$. Substituting this into Eq. 7.2.2 gives

$$\frac{h_n^2 u_n^2(0)\sin\phi_0}{\Delta v_0} \;=\; -\,\frac{h_n h_{n+1} u_n^2(\eta_f)\sin(\phi_0 + \alpha)}{\Delta v_f}. \qquad\qquad 7.2.5$$

This is an implicit function of ϕ_0, which can be solved numerically.

Now, the only remaining undetermined elements are $u'_n(0)$, and h_n. These two elements are not independent, either, for since η_f is known, the following equation (Eq. 5.2.2) can be used to find h_n in terms of $u'_n(0)$ (or vice versa):

$$u_n(\eta_f) \;=\; \frac{\mu}{h_n^2} \;+\; \left(u_n(0) - \frac{\mu}{h_n^2}\right)\cos\eta_f \;+\; u'_n(0)\,\sin\eta_f \qquad\qquad 7.2.6$$

Hence, either $u'_n(0)$ or h_n can be considered to be the parameter of choice for defining trajectories between the two positions, so all trajectories between these two positions can be parameterized in terms of this single parameter. Since $u'_n(0)$ will be referred to often, define $\psi \triangleq u'_n(0)$. It is better to keep ψ as the parameter of choice instead of h_n, and hence define h_n in terms of ψ, because ψ in Eq. 7.2.6 is multiplied by $\sin\eta_f$. As a result, ψ could not be

determined from h_n when $\eta_f = \pi$ (or any multiple of π); on the other hand, h_n can be determined in terms of ψ from Eq. 7.2.6 for all $\eta_f \in (0, 2\pi)$. (Obviously, neither variable can be uniquely determined for trajectories with $\eta_f = 2\pi m$, where m is any integer, because $\underline{all}$ trajectories will repeat the same elements after traversing an angle of 2π.) The result of solving for h_n in terms of ψ from Eq. 7.2.6 is

$$h_n = \sqrt{\frac{\mu(1 - \cos\eta_f)}{u_n(\eta_f) - u_n(0)\cos\eta_f - \psi\sin\eta_f}} \qquad 7.2.7$$

The positive root is chosen since the specific angular momentum, h, is a non-negative quantity. Thus, all coasting trajectories between the initial interceptor position and the target position can be parameterized in terms of the single parameter ψ. When Eq. 7.2.7 is evaluated at $\eta_f = \pi$, h_n is a constant for all ψ values since $\sin\pi = 0$. In other words, $\underline{all}$ trajectories which fly from u_0 to u_f in a transfer angle of π will have the same angular momentum. This is why h cannot be an iteration variable near $\eta_f = \pi$.

The only remaining unknown, then, is the value of ψ which yields an optimal trajectory. Perhaps the most straightforward means of obtaining the value of ψ which satisfies the Maximum Principle is to numerically find the zero(s) of δ, Eq. 5.3.6, which should now be written functionally as $\delta(\psi)$. That is, each choice of ψ gives a coasting trajectory, and the elements of the trajectory along with the known elements of the initial interceptor trajectory and of the target trajectory are used to compute $\Delta \bar{v}^l$ at the beginning and at the end of the coasting arc. Then the values of the adjoint variables $\lambda_{u'}$ and λ_h can be determined at both ends of the trajectory from Eq. 5.3.2 (i.e., $\bar{S} = \frac{\Delta \bar{v}^l}{\Delta v}$). These, in turn, are used in Eq. 5.3.5 to determine λ_{u0}. Finally, λ_{u0} , $\lambda_{u'0}$, $\lambda_{u'f}$, and η_f are used to determine $\delta(\psi)$ for this value of ψ. In this manner, a suitable numerical technique can iterate on ψ to determine the value(s) ψ^* such that

$$\delta(\psi^*) = 0.$$

7.3 Domain of ψ

It must be observed, in order for $\delta(\psi)$ to be successfully manipulated, that not all values of ψ yield physically valid trajectories. These limits on ψ, which restrict its domain, are derived in Appendix B. Summarizing the results of Appendix B, when $\sin\eta_f > 0$, ψ has a lower bound,

$$\psi > -u_0 \frac{\sin\eta}{1 - \cos\eta_f} - \sqrt{\frac{2u_0 u_f}{1 - \cos\eta_f}}, \qquad 7.3.1$$

and an upper bound,

$$\psi < \frac{u_n(\eta_f) - u_n(0)\cos\eta_f}{\sin\eta_f}. \qquad 7.3.2$$

On the other hand, when $\sin\eta_f \le 0$, the lower bound on ψ is Eq. 7.3.1, but there is no upper bound.

7.4 Rendezvous Solutions as Roots of a Polynomial

Careful examination of the $\delta(\psi)$ equation, Eq. 5.3.6, together with each of the functions of ψ contained within it ($\lambda_{u'_f}$, λ_{u0}, $\lambda_{u'0}$, and the functions within them), reveals that $\delta(\psi) = 0$ is an algebraic equation in ψ. Therefore, by appropriate algebraic manipulations, $\delta(\psi)$ can be converted to a polynomial in ψ such that the zeros of $\delta(\psi)$ are also zeros of the polynomial (though the polynomial also has extraneous roots). For the rendezvous problem,

this yields a twelfth degree polynomial. The numerical difficulties of obtaining accurate solutions with such a high degree polynomial, however, make the numerical usefulness of this fact dubious. Theoretically speaking, it is nice to know the maximum number of possible real roots, but in practice it has proven better to work directly with $\delta(\psi)$ to find its zeros for rendezvous problem. Intercept problems, on the other hand, yield a polynomial in ψ which is only a quartic, which can be solved analytically. This is indeed useful. The derivation of this intercept polynomial will be given in Section 7.6.

7.5 Addition of an Initial Coast

In the course of analyzing optimal trajectories, it may become necessary to add an initial coast to the trajectory before the first burn. This may be necessary, for example, when $S > 1$ on the no initial coast solution (particularly when $S' > 0$ at $\eta = 0$). Since it is a requirement that $S' = 0$ on both sides of an interior burn; since S' is just a function of the state, the adjoint variables, and the independent variable η (as shown in Section 5.4); and, since all of these quantities are known between burns as derived above, $S'(0) = 0$ between the two burns gives an extra condition which can be used to determine the initial coast angle, η_0. As in Section 5.4, the quantity $\sigma(0)$ (Eq. 5.4.2) will be used in place of $S'(0)$ in actual computations.

The whole solution process for two-burn trajectories, therefore, consists of two steps. First, assume $\eta_0 = 0$, and solve the one dimensional problem $\delta(\psi) = 0$ for ψ. If $S(\eta) > 1$ for some η on the resulting trajectory, then solve the two nonlinear functions $\delta(\psi, \eta_0)$ and $\sigma(\psi, \eta_0; 0)$ for the two unknowns ψ and η_0.

7.6 Intercept Trajectories Between Fixed Positions

The intercept problem analogous to the two burn rendezvous problem is the one burn case. The reason for this is that, unlike the rendezvous problem, the optimal intercept trajectory will never thrust at the end of the trajectory (the intercept point), as demonstrated in Section 4.3. Therefore, the adjoint variables $\lambda_{u'_f}$, λ_{h_f}, and $\lambda_{\hat{r}'N_f}$ are set equal to zero as mandated by the transversality condition at the endpoint, instead of being determined from the final burn $\overline{S} = \frac{\Delta \overline{v}^l}{\Delta v}$ condition. Apart from this difference, the solution procedure for finding the values of ψ which are zeros of $\delta(\psi)$ is basically the same as in the rendezvous case. $\delta(\psi)$ is a simpler function, since the terms with adjoint variables at the end of the coasting arc vanish:

$$\delta(\psi) = \lambda_{u0} \sin\eta_f - \lambda_{u'_0} \cos\eta_f . \qquad 7.6.1$$

Since $\delta(\psi)$ is a simpler expression, a polynomial which is only a quartic can be derived from it. Evaluating λ_{u0} with $\lambda_{h_f} = 0$,

$$\lambda_{u0} = \frac{h^3 \lambda_{h0}}{2\mu(1 - \cos\eta_f)} + \frac{\sin\eta_f}{(1 - \cos\eta_f)} \lambda_{u'_0} . \qquad 7.6.2$$

In this equation and in what follows, $h \triangleq h_n$, $u_0 \triangleq u_n(0)$, and $u_f \triangleq u_n(\eta_f)$. With this expression $\delta(\psi)$ becomes, after simplification of the total factor of $\lambda_{u'_0}$,

$$\delta(\psi) = \frac{\sin\eta_f}{(1 - \cos\eta_f)} \frac{h^3}{2\mu} \lambda_{h0} + \lambda_{u'_0} \qquad 7.6.3$$

λ_{h0} and $\lambda_{u'_0}$ are determined from the $\overline{S} = \frac{\Delta \overline{v}^l}{\Delta v}$ requirement, Eq. 5.3.2.,

$$\lambda_{u'0} = \frac{h^2\psi - hh_{n-1}u'_{n-1} \quad (\eta_f)}{\Delta v_1}.$$ (7.6.4)

$$\lambda_{h0} = \frac{h\psi^2 - h_{n-1}u'_{n-1} \quad (\eta_f)\,\psi + u_0^2(h\cos\phi - h_{n-1})}{\Delta v_1}.$$ (7.6.5)

Then, $\dfrac{\Delta v_1\,\delta(\psi)}{h^4} = 0$ is the same requirement as $\delta(\psi)=0$, so that

$$\frac{\sin\eta_f}{2\mu(1-\cos\eta_f)}[\psi^2 + u_0^2\cos\phi - \frac{1}{h}(h_{n-1}u'_{n-1} \quad (\eta_f)\,\psi + h_{n-1}u_0^2)]$$

$$+ \frac{1}{h^2}\psi - \frac{1}{h^3}h_{n-1}u'_{n-1} \quad (\eta_f) = 0.$$ (7.6.6)

Since

$$\frac{1}{h} = \sqrt{\frac{u_n(\eta_f) - u_n(0)\cos\eta_f - \psi\sin\eta_f}{\mu(1-\cos\eta_f)}},$$ (7.6.7)

it and its factors must be isolated on one side of Eq. 7.6.6, then both sides must be squared and once again combined on one side of the equation to yield a quartic polynomial. Proceeding in this manner, Eq. 7.6.6 becomes

$$-\frac{\omega}{2}\psi^2 + \alpha\psi + \frac{\omega}{2}u_0^2\cos\phi = \frac{1}{h}\left\{-\frac{\omega}{2}h_{n-1}u'_{n-1} \quad (\eta_f)\,\psi + h_{n-1}(\frac{\omega}{2}u_0^2 + \alpha u'_{n-1} \quad (\eta_f))\right\}$$ (7.6.8)

where $\omega = \dfrac{\sin\eta_f}{\mu(1-\cos\eta_f)}$ and $\alpha = \dfrac{u_f - u_0\cos\eta_f}{\mu(1-\cos\eta_f)}$, so that $\dfrac{1}{h} = \sqrt{\alpha - \omega\psi}$. Next, for simplicity, rewrite Eq. 7.6.8 in generic terms,

$$a_2\psi^2 + a_1\psi + a_0 = \sqrt{\alpha - \omega\psi}\,(b_1\psi + b_0); \qquad\qquad 7.6.9$$

where,

$$a_0 = \tfrac{\omega}{2}u_0^2\cos\phi, \qquad\qquad 7.6.10$$

$$a_1 = \alpha, \qquad\qquad 7.6.11$$

$$a_2 = -\tfrac{\omega}{2}, \qquad\qquad 7.6.12$$

$$b_0 = h_{n-1}(\tfrac{\omega}{2}u_0^2 + \alpha u'_{n-1}\ (\eta_f)), \qquad\qquad 7.6.13$$

and

$$b_1 = \tfrac{\omega}{2}h_{n-1}u'_{n-1}\ (\eta_f). \qquad\qquad 7.6.14$$

Squaring Eq. 7.6.9 and combining all terms on one side of the equation results in the quartic

$$\boxed{\begin{aligned} &a_2^2\psi^4 + (2a_1a_2 + \omega b_1^2)\psi^3 + (2a_0a_2 + a_1^2 + 2\omega b_0b_1 - \alpha b_1^2)\psi^2 \\ &\quad + (2a_0a_1 + \omega b_0^2 - 2\alpha b_0b_1)\psi + (a_0^2 - \alpha b_0^2) = 0 \end{aligned}} \qquad 7.6.15$$

All the real roots of Eq. 7.6.15 are easily obtained analytically or numerically, so that all the zeros of Eq. 7.6.6 (which are a subset of the roots of the polynomial) are easily verified by substitution. So, the $\delta = 0$ condition takes on a particularly simple form for the case of one

burn intercept trajectories -- the test has reduced to the solution of a quartic.

7.7 Time-Specified Two-Burn Trajectories

Consider, again, the problem where the orbital transfer will occur between two fixed positions using only two burns (or one burn for intercept), with no initial coast. Since the transfer time is specified, the problem is just a Lambert's problem. ψ can be used as the iteration parameter for the solution process for Lambert's problem, just as it was presented as the iteration parameter for the $\delta(\psi) = 0$ equation in Section 7.2. The same arguments hold here as they do there, since a given ψ will uniquely specify the trajectory between the fixed positions. The only difference is that the requirement that time of flight be a specified value, $t(\psi) - t_0 - \Delta t_{\text{specified}} = 0$, replaces $\delta(\psi) = 0$.

It is of interest to note how this Lambert's solution compares with other popular Lambert's solution techniques, especially the p-iteration method[1]. Since $p = \frac{h^2}{\mu}$, this method is essentially an h-iteration method. In section 7.2 it was shown that iterating in ψ is much better in general than iterating in h, because when $\eta_f = \pi$, h is a constant over all trajectories, so that it cannot be used as an iterative parameter at that value of the transfer angle. Battin's latest Lambert problem solution technique[2], a modification of Gauss' original solution method, is generally reputed to be the most robust method available. In comparing Battin's method to an implementation of the ψ-iteration technique, Battin's method in general seemed a little more robust, though the ψ-iteration technique was generally competitive.

After Lambert's problem has been solved by whatever method, the solution must be checked for satisfying the necessary conditions on the primer vector, as in the time open case. In

this case, λ_t is computed first, then the Schumacher adjoint variables and hence the local primer vector $\bar{S}(\eta)$ can be propagated to check the requirement $S(\eta) \leq 1 \; \forall \; \eta \in [0, \eta_f]$. If this test fails, an initial coast can be added, and exactly as in the time open case, the value of the initial coasting angle which causes the condition $S' = 0$ to be satisfied immediately after the first burn is the proper choice. Again, as stated above, for the two burn rendezvous problem (or the one burn intercept problem), the only difference in the solution process is the replacement of the $\delta(\psi) = 0$ condition with the $t(\psi) - t_0 - \Delta t_{\text{specified}} = 0$ condition.

8.0 COMPUTATION OF GENERAL IMPULSIVE TRAJECTORIES

8.1 *Introduction*

In the previous chapter, it was shown that candidate solutions to the impulsive fuel-optimal two-burn rendezvous and one-burn intercept problems could be computed by solving either one nonlinear equation (if no initial coast was required), or two nonlinear equations (if an initial coast was required). In this chapter, these results will be extended to the general n-burn case. As before, two distinct cases occur for the general problem: the no initial coast and the initial coast cases.

First in order of development in this chapter is an explanation of the additional nonlinear equations which must be solved when additional burns beyond two are added. Next, two slight modifications to the solution process are introduced. These modifications are necessary to simplify the numerical solution process, especially to make the iteration process in searching for candidate optimal trajectories more smooth. Finally, changes to the algorithm when time is specified are presented.

8.2 *Additional Unknowns*

If an additional burn is added to a two-burn trajectory, making it a three-burn trajectory, then new unknowns crop up in the problem. Consider first motion restricted to a plane. In order to specify where the burn will take place, the coasting angle between the first burn and the additional burn, η_1, must be determined. Next, u_2, the reciprocal radius at the

intermediate burn point, is unknown. Once these are specified for the planar problem, and it is assumed that the subsequent trajectory is specified (in some solution process), then the only remaining unknown on the new trajectory is, as before, ψ (because, as in the two burn case, the flight is between two fixed positions specified by η_1 and ψ). It is easily shown by examining the equations of coasting motion ($u(\eta)$ and $u'(\eta)$) and of $\overline{S}(\eta)$ that knowing these additional three quantities permits these equations to be determined. By the way, h on the new coasting trajectory could be used instead of u_2, if this is desirable.

Now, three additional equations must be found in order to solve for the three new unknowns. The most obvious equation to use is, of course, $\delta(\psi) = 0$ on the new coasting arc, as before. Since interior burns must have $S' = 0$ on both sides of the burn (as deduced by Lawden[31], and as was used in the two-burn case with initial coast), $\sigma_n(\eta_f) = \sigma_{n+1}(0) = 0$ provide the two remaining equations. For each additional burn beyond three, again the three quantities η_n, ψ_n, and u_{nf} (or h_n), must be determined, and the three equations above on this new trajectory provide a means for solving for them.

If the problem is not restricted to have only planar motion, as was assumed above, then the angle between the current and the previous trajectory, ϕ_n, must be determined for each new coasting arc before a new burn. Hence, another condition is required in order to determine ϕ_n for each additional burn. The extra equation to be satisfied comes from another necessary condition due to Lawden[30], which is related to the $S' = 0$ condition used extensively above. Lawden solves the impulsive thrust optimization problem using Calculus of Variations, with each burn being a corner of the trajectory (in Calculus of Variations parlance, a corner is a discontinuity in the derivative of the state). He extends the classical Weierstrass–Erdmann corner conditions to include problems with differential constraints and Lagrange multipliers (i.e., the adjoint variables), and shows that, among other things, the primer vector and the primer

vector rate must be continuous across an impulsive burn. Since the primer vector rate is $\dot{\lambda}_{\overline{V}} = -\lambda_{\overline{r}}$, the continuity of $\lambda_{\overline{r}}$ can be used in its stead.

$\dot{\lambda}_{\overline{V}}^+ = \dot{\lambda}_{\overline{V}}^-$ across the burn gives three equations to be satisfied. Two of these conditions have already been used above, in the $S'^+ = S'^- = 0$ equations. That is, $S' = 0$ because $\frac{d}{dt}|\lambda_{\overline{V}}| = 0$ on each side of the burn (as shown in chapter 5), but the fact that $\frac{d}{dt}|\lambda_{\overline{V}}| = 0$ at an interior burn is already derived from the continuity of $\dot{\lambda}_{\overline{V}}$ (together with the requirement $|\lambda_{\overline{V}}| \leq 1$). Hence one degree of freedom is all that is left from the continuity of $\dot{\lambda}_{\overline{V}}$ requirement. Since the continuity of $\lambda_{\overline{r}}$ is used in its place, the new equation chosen to be used is

$$\lambda_{\overline{r}}^+ \cdot \hat{r} = \lambda_{\overline{r}}^- \cdot \hat{r} . \qquad 8.2.1$$

This direction of $\lambda_{\overline{r}}$ is chosen since S' is effectively the component of $\dot{\lambda}_{\overline{V}}$ in the $\lambda_{\overline{V}}$ direction (i.e., the direction of thrust), and it should be rare to thrust in the radial direction. If $\lambda_{\overline{V}}$ is ever nearly aligned with $\hat{r}$, then another component should be used instead.

Now, all the adjoint variables in the analyses above are in Schumacher space, so the transformation between them and $\lambda_{\overline{r}}$ are needed to make Eq. 8.2.1 useful. The appropriate transformation equation is Eq. 3.4.40:

$$\lambda_{\overline{r}} = u(h\lambda_h - u'\lambda_{u'} - u\lambda_u)\hat{r} + [u(\lambda_{\hat{r}}^T \hat{r}' - \lambda_{\hat{r}'}^T \hat{r}) + hu'\lambda_h - (u^2 + u'^2)\lambda_{u'}]\hat{r}'$$
$$+ (u\lambda_{\hat{r}}^T \hat{h} + u'\lambda_{\hat{r}'}^T \hat{h})\hat{h} . \qquad 8.2.2$$

The inner product of this with $\hat{r}$ is

$$\lambda_{\hat{r}}^T \, \dot{r} \;\; = \;\; u(h\lambda_h - u'\lambda_{u'} - u\,\lambda_u) \tag{8.2.3}$$

so that the required equation to be solved is

$$\tau \;\; \triangleq \;\; h^-\lambda_h^- - u'^-\lambda_{u'}^- - u\lambda_u^- - h^+\lambda_h^+ + u'^+\lambda_{u'}^+ + u\lambda_u^+ \;\; = \;\; 0 \, . \tag{8.2.4}$$

The solution of this τ equation at every burn other than the first and the last burn, together with the solutions of the previously mentioned equations, yields a trajectory which is an extremal.

8.3 Further Considerations

The development of the equations which are to be solved in order to find impulsive burn approximations to the general n-burn intercept and rendezvous problems is nearly complete. There are, however, two additional considerations to be addressed, which simplify the numerical solution process. First, in Section 5.3 it was stated (immediately after Eq. 5.3.8) that $\lambda_{\hat{r}N0}$ could be solved for (at the beginning of any coasting trajectory) as long as $\sin\eta_f \neq 0$. There seems to be no reasonable method for solving for $\lambda_{\hat{r}N0}$ directly, however, when $\sin\eta_f = 0$. $\lambda_{\hat{r}N0}$ is, however, an integral member of the equations which must be solved numerically. Therefore, $\lambda_{\hat{r}N0}$ on each coasting arc can be added as an additional unknown in the problem, the correct choice of which (together with the other variables in the solution process) will solve the equation

$$\Delta\lambda_{\hat{r}'Nf} \; = \; -\lambda_{\hat{r}N0}\sin\eta + \lambda_{\hat{r}'N0}\cos\eta - \lambda_{\hat{r}'Nf} \; = \; 0. \tag{8.3.1}$$

This equation is the difference between the functional value of $\lambda_{\hat{r}'Nf}$ (the $[-\lambda_{\hat{r}N0}\sin\eta + \lambda_{\hat{r}'N0}\cos\eta]$ portion of Eq. 8.3.1) and the value obtained from the $\overline{S} = \frac{\Delta\overline{v}^l}{\Delta v}$ condition at the terminal end of the current coasting trajectory (denoted $\lambda_{\hat{r}'Nf}$ in Eq. 8.3.1), which must be equal. With one new variable and one new equation per coasting trajectory, there are now $n_b - 1$ new variables and equations in the solution process.

In doing this, the solution process for part of the rest of the equations is simplified. Recall from Section 7.2 that if η_f is an integer multiple of π, then the plane connecting the previous and the subsequent orbital planes is not uniquely determined by mere geometry. With the aid of the functional requirements of $\lambda_{\hat{r}'N}$, a nonlinear equation (Eq. 7.2.5) was found whose solution yielded ϕ_0, the angle between the previous and the current trajectory planes. With this current solution process, however, the solution of this equation is avoided since it is subsumed in Eq. 8.3.1. That is, solutions which satisfy Eq. 8.3.1 will satisfy Eq. 7.2.5 when η_f is an odd multiple of π, which is easily verified by direct substitution of π in Eq. 8.3.1. When $\eta_f = \pi$, Eq. 8.3.1 says that

$$\lambda_{\hat{r}'N0} = -\lambda_{\hat{r}'Nf}.$$ 8.3.2

Hence, only the correct choice of ϕ_0 and/or ϕ_f will satisfy Eq. 8.3.2 (since $\lambda_{\hat{r}'N0}$ and $\lambda_{\hat{r}'Nf}$ are functions of ϕ_0 and ϕ_f -- see Eq. 5.3.2), thus forcing the correct transfer plane to be chosen.

Of course, Eq. 8.3.1 is equal to zero when $\eta = \pi$ no matter what choice of $\lambda_{\hat{r}N0}$ is made (for the appropriate value of ϕ_0 and other parameters which make $\lambda_{\hat{r}'N0} = -\lambda_{\hat{r}'Nf}$), since $\lambda_{\hat{r}N0}$ is then multiplied by $\sin\pi = 0$. Since ϕ_0 is in the state of the optimization problem, a solution will yield the correct plane of motion as stated above, but will the correct choice of $\lambda_{\hat{r}N0}$ be made? This is important because $\lambda_{\hat{r}N0}$ is used in $S(\eta)$ is order to check that $S(\eta) \le 1$ for all η.

The answer is yes, the correct $\lambda_{\hat{r}N0}$ will be chosen because this quantity is in the $\sigma(\eta)$ equation, so that the requisite $\sigma(0) = 0$ (i.e., $S'(0) = 0$) and/or $\sigma(\eta_f) = 0$ will force the correct value of $\lambda_{\hat{r}N0}$ to be found. The only exception to this is in cases when no $\sigma(\eta) = 0$ condition is required; the only such case is the two burn trajectory with no initial coast. Even in that case, unless $\eta_f = \pi$, Eq. 5.3.8 can be used to compute $\lambda_{\hat{r}N0}$.

The second consideration mentioned at the beginning of this section has to do with smoothness of the numerical solution process. In the computational problem introduced so far, the position of the interceptor trajectory at the second to last burn is known. Since the position of the final burn is given (from the target elements), ϕ_{n-1} (the angle between the planes of motion at the next to last burn) and η_f (the final coasting angle) can be computed from geometry. There is, however, an ambiguity in determining these values. That is, if ϕ_{n-1} and η_f satisfy the geometric requirements, $\phi_{n-1} - \pi$ and $2\pi - \eta_f$ also transfer the trajectory to the same final position. Of course, both choices could be made, and the better of the two solutions could be selected as the proposed optimum.

But, in terms of a numerical solution process, this ambiguity is much more serious than that; it could lead to lack of smoothness at certain values of ϕ_{n-1} and η_f. For example, if the shortest η_f is always chosen (i.e., $\eta_f \leq \pi$ is always chosen), a slight variation in the η value of the second to last coast at a point such that η_f is near π may cause the direction of the trajectory to suddenly do a plane change of π! This kind of jump devastates the effectiveness of calculus based descent methods such as Quasi-Newton methods.

Therefore, ϕ_{n-1} and η_f are added to the variables in the numerical solution process. The resulting equation which must be satisfied is

$$\hat{r}_n(\eta_f) - \hat{r}_T = 0. \qquad\qquad 8.3.3$$

$\hat{r}_n(\eta_f)$ is the final position of the interceptor trajectory, and $\hat{r}_T$ is the target position. This equation is actually composed of three redundant equations, with only two degrees of freedom, in the two unknowns ϕ_{n-1} and η_f. These three equations could be transformed to the difference between two angles to rid the redundancy, but these angles would again have undesirable ambiguities which would again destroy smoothness in the numerical process. Since, with redundant equations, the system cannot be solved as a problem of n equations in n unknowns, a robust nonlinear least squares algorithm is used to solve the equations.

8.4 Maximum Time Specified

As briefly mentioned in chapter 3, when a maximum time constraint in which to perform the rendezvous or intercept is specified, the solution process is expanded to a two step procedure. First, the open time problem is solved as presented above; after that, the total time of flight of the solution trajectory is computed. If this time is less than the maximum, then it is the maximum time specified solution as well. On the other hand, if the total time of flight is greater than the maximum, then the solution process takes on a different form.

For the two burn rendezvous case with no initial coast, the resulting problem is merely a Lambert's problem (i.e., find the trajectory between two positions which has the specified time of flight). According to Lambert's theorem, one single parameter is sufficient to specify the trajectory between these two positions. In this case, the parameter of choice is ψ ($\psi \triangleq u_0'$). The solution is then the candidate optimal trajectory. As a check, Eq. 6.3.4 can be used to compute λ_t, which must be negative; a positive λ_t indicates that the time open solution requires less time

of flight and would hence be the candidate optimal solution.

As with the open time case, the resulting trajectory must be checked to ensure that $S(\eta) \leq 1$ for all η on that trajectory. If not, then the first thing to add to the two burn trajectory is an additional coast. The new condition to be satisfied in order to determine η_0 is, as with the time open problem, $\sigma(\eta_0) = 0$ (i.e., $S'(\eta_0) = 0$). The problem is now one of solving two nonlinear equations, Lamberts problem and $\sigma(\eta_0) = 0$, simultaneously for ψ and η_0.

Then, again, $S(\eta) \leq 1$ for all η must be checked. If the two burn trajectory with initial coast still is not optimal, then an additional burn must be added. In this case, the specified time of flight, and the fact that λ_t on the arc between the first two burns must equal λ_t on the arc between the middle and last burns, together replace the two conditions $\delta = 0$ for the two coasting arcs between burns. The rest of the equations in the solution process remain the same as in the open time case. For each subsequent addition of a burn, the $\delta = 0$ equation is replaced by $\lambda_{t,m} = \lambda_{t,m-1}$ (where the burn was added on the mth coasting arc). This process is continued until $S(\eta) \leq 1$ for the correct number of burns.

9.0 COMPUTATION OF FINITE THRUST TRAJECTORIES

9.1 Introduction

The ultimate goal of the analyses in this work is to obtain finite thrust trajectories for general three dimensional motion, because they are much closer to actual physical trajectories than are the instantaneous impulse thrust trajectories developed by the methods of the previous chapters.   The instantaneous impulse solutions, however, can be used as initial conditions in the finite thrust numerical solution process.   It is shown in this chapter that adjoint variable transformations are again useful to accomplish this goal.   The solutions from the instantaneous impulse formulation developed above allow both the state and the adjoint variables to be propagated along the candidate optimal interceptor trajectory in Schumacher coordinates; then, as will be shown below, it is desirable to transform the state and adjoint variables to $\bar{r}$, $\bar{v}$, $\lambda_{\bar{r}}$, and $\lambda_{\bar{v}}$ for use in a numerical differential equations solution method at several points along the trajectory.

9.2 The Boundary Value Problem

When finite thrust trajectories are to be propagated, the portion of the trajectory where the thrust is nonzero must be integrated numerically.   As was mentioned in Chapter 4, the optimal control problem is a boundary value problem, with some of the state and adjoint variables defined at the initial time, and some of them defined at the final time.   One of the most popular and successful numerical boundary value solution methods is the shooting method. In this technique, the unknown initial conditions are guessed, then the variables are integrated

to the final time. The endpoint variables are then compared with the specified values, and a Newton's method (or other method for solving nonlinear systems of equations) iterates on the unknown initial conditions until the difference between the final variable values and the required values is made zero.

A slight modification to this shooting method is very popular for finding numerical solutions to optimal control problems. It is called the multiple shooting method, because the whole time span of the trajectory is broken into multiple smaller intervals, then the functions to be made zero are not only the discrepancies in the final variable values, but also the discrepancies between the variables at the end of one interval and their values at the beginning of the next interval. This is an important technique for optimal control problems because often either the state or the adjoint variables are unstable (hence they have a positive Lyaponov exponent), which will cause the solution of nearby trajectories to diverge exponentially from each other. For example, if the state is a stable linear system (hence having negative eigenvalues), then the adjoint state is unstable (having positive eigenvalues). So, in order to minimize integration errors, the trajectories are integrated over smaller time spans.

Also, if the optimal control solution process yields a bang-bang control law (i.e, discontinuities in the control variables function occur, as is the case with minimum fuel space transfers), then a slight modification to the multiple shooting method greatly aids the numerical solution of these problems. The switching times can be made part of the multiple shooting method state, and conditions in the state and adjoint variables indicating a switching point become functions to be made zero. This way, discontinuities in the control variables over a Runge-Kutta integration step (which can cause significant errors) can be avoided. One popular computer program which contains all of these features is BOUNDSCO. This program was used to obtain the numerical finite thrust optimal control solutions for this research.

BOUNDSCO requires, by definition of the multiple shooting method, initial guesses for both the state and adjoint variables at several points along the trajectory, including the endpoints. Obtaining good initial guesses, sufficiently close to the solution to allow the locally convergent Quasi-Newton iteration process to converge, is an extremely difficult task in general (especially for the adjoint variables). Experience shows that "hand-made" guesses to the initial conditions for a high dimension problem like three dimensional space transfer problems often fail. This is one nice feature of the methods developed above for instantaneous impulse trajectories, since both the state and adjoint variables are determined in the solution process. This instantaneous impulse solution is used as an initial estimate of the multiple shooting method state. The impulsive burn solutions are used to propagate the trajectories to several points in Schumacher coordinates, then the state and adjoint variables are transformed to $\bar{r}$, $\bar{v}$, $\lambda_{\bar{r}}$ and $\lambda_{\bar{v}}$. The trajectory is then integrated in these Cartesian variables due to their simple form:

$$\dot{\bar{r}} = \bar{v}$$

$$\dot{\bar{v}} = -\frac{\mu}{r^3}\bar{r} + \bar{T}$$

9.2.1

$$\dot{\lambda_{\bar{r}}} = \frac{\mu}{r^3}\left[I - \frac{3}{r^2}\bar{r}\bar{r}^T\right]\lambda_{\bar{v}}$$

and

$$\dot{\lambda_{\bar{v}}} = -\lambda_{\bar{r}}.$$

These equations are much simpler on thrusting arcs than the Schumacher variables (compare these with Eqs. 4.2.7), so there is much less likelihood of programming errors and accumulation

of roundoff errors using these Cartesian variables.

The thrust control, $\bar{T}$, is of course determined from the Maximum Principle to be

$$
\bar{T} \;=\; \begin{cases} T_{max} \dfrac{\lambda_{\bar{v}}}{|\lambda_{\bar{v}}|} \,, & |\lambda_{\bar{v}}| > 1 \\[2mm] 0 \,, & |\lambda_{\bar{v}}| < 1 \end{cases} \,. \qquad\qquad 9.2.2
$$

Hence the condition for determining a switching time is $|\lambda_{\bar{v}}| = 1$. In converting from the instantaneous solution to the finite burn case, the burn times in general become the center of a thrusting arc. Then the magnitude of the $\Delta\bar{v}$ in the instantaneous burn case is used to determine an approximate burn time Δt_b, so that the switching times become the instantaneous burn time plus and minus $\Delta t_b/2$. The exceptions to this are the initial burn if there is no initial coast, and the final burn. In the initial burn case with no initial coast, the trajectory is initiated with $|\bar{T}| = T_{max}$, and the first switching time is at Δt_{b1}. Similarly, the final switching time for rendezvous problems is $t_f - \Delta t_{bf}$.

The magnitude for each Δt_b is determined from the impulse equation resulting from the derivative of the velocity vector:

$$
\Delta\bar{v} \;=\; \int_{t_{b0}}^{t_{bf}} \left(-\frac{\mu}{r^3}\bar{r} + \bar{T} \right) dt \,. \qquad\qquad 9.2.3
$$

t_{b0} and t_{bf} here denote the initial and final burn times for the current thrusting arc. If the thrust acceleration magnitude is sufficiently large as compared to the gravity acceleration, then $\Delta\bar{v}$ can be approximated by

$$
\Delta\bar{v} \;\approx\; \int_{t_{b0}}^{t_{bf}} \bar{T} \, dt \,. \qquad\qquad 9.2.4
$$

Furthermore, if the time duration is sufficiently short such that motion in the direction of $\bar{T}$ can be ignored (this is essentially the instantaneous impulse approximation), then an approximation for the magnitude of $\Delta\bar{v}$ is

$$\Delta v \approx |\bar{T}| (t_{bf} - t_{b0}).$$ 9.2.5

From this, the approximate burn duration used to guess the switching times is

$$\Delta t_b = \frac{\Delta v}{T_{max}}.$$ 9.2.6

9.3 Transformation of Adjoints

The transformation equations for the adjoint variables have already been given in Chapter 3. The primer vector transformation equation, which has been used extensively to this point, again is, from Eq. 3.4.35,

$$\lambda_{\bar{v}} = -\frac{\lambda_{u'}}{h} \hat{r} + \frac{(h\lambda_h - u'\lambda_{u'})}{hu} \hat{r}' + \frac{\hat{h}^T \lambda_{\hat{r}'}}{hu} \hat{h}.$$ 9.3.1

The quantities $\lambda_{u'}$, λ_h, and the component of $\lambda_{\hat{r}'}$ in the $\hat{h}$ direction are known on coasting trajectories between burns as determined in Chapters 5 and 6, $\lambda_{\bar{v}}$ is completely known on the instantaneous impulse trajectory, except possibly on an initial coast before the first burn. The values to be used on an initial coast will be derived in the next section.

As far as $\lambda_{\bar{r}}$ is concerned, the relevant equation is Eq. 3.4.40:

$$\lambda_{\bar{r}} = u(h\lambda_h - u'\lambda_{u'} - u\lambda_u)\hat{r} + [u(\lambda_{\hat{r}}^T \hat{r}' - \lambda_{\hat{r}'}^T \hat{r}) + hu'\lambda_h - (u^2 + u'^2)\lambda_{u'}]\hat{r}'$$
$$+ (u\lambda_{\hat{r}}^T \hat{h} + u'\lambda_{\hat{r}'}^T \hat{h})\hat{h}.$$

9.3.2

All of these quantities are known as functions of η from the analyses in Chapters 5 and 6 except for $\lambda_{\hat{r}}^T \hat{r}'$ and $\lambda_{\hat{r}'}^T \hat{r}$. These can be determined on an optimal trajectory by using the fact that the Hamiltonian is zero, even for time specified problems, because even time specified problems have η free. Now, from Eq. 4.2.6, the Hamiltonian on coasting arcs is

$$H = \lambda_{\hat{r}}^T \hat{r}' - \lambda_{\hat{r}'}^T \hat{r} + u'\lambda_u - (u - \frac{\mu}{h^2})\lambda_{u'} + \frac{\lambda_t}{hu^2} = 0.$$

9.3.3

Rearranging this equation gives the unknown quantity in $\lambda_{\bar{r}}$ in terms of known quantities:

$$\lambda_{\hat{r}}^T \hat{r}' - \lambda_{\hat{r}'}^T \hat{r} = -u'\lambda_u + (u - \frac{\mu}{h^2})\lambda_{u'} - \frac{\lambda_t}{hu^2}.$$

9.3.4

Thus, $\lambda_{\bar{r}}$ and $\lambda_{\bar{v}}$ can be computed anywhere on coasting arcs between burns, to then be written to a file which is read as input by the program which uses the BOUNDSCO routines. How to compute the adjoints on an initial coasting arc is the subject of the next section.

9.4 Computation of the Adjoints on an Initial Coasting Arc

On an initial coasting arc, there is a burn on only one side of the arc, so the previous

methods cannot be used. From the $\overline{S} = \frac{\Delta \overline{v}^l}{\Delta v}$ condition (Eq. 5.3.2) at the end of the coast, however, some of the adjoint values can be determined:

$$
\begin{bmatrix} \dfrac{-\lambda_{u'f}}{h_0} \\[3mm] \dfrac{h_0 \lambda_{hf} - u'_0(\eta_0)\lambda_{u'f}}{h_0 u_1} \\[3mm] \dfrac{\lambda_{\hat{r}'Nf}}{h_0 u_1} \end{bmatrix} = \begin{bmatrix} h_0 u'_0(\eta f) - h_1 \psi_1 \\[3mm] u_1(h_1 \cos\phi_1 - h_0) \\[3mm] h_1 u_1 \sin\phi_1 \end{bmatrix} / \Delta v . \qquad 9.4.1
$$

Subscript "0" here denotes a quantity at the beginning of the first arc after the first burn, and "f" denotes a quantity at the final point of the initial coast. As a reminder, Δv in the denominator on the right side of the equation is the magnitude of the vector in the numerator. Since the quantities in this equation are evaluated on the initial intercept trajectory, at the end of the initial coast, the elements on the left side of the equation are for the initial interceptor trajectory. The right side contains the change in elements over the first impulsive burn. Hence, $\lambda_{u'f}$, λ_{hf}, and $\lambda_{\hat{r}'Nf}$ are known for the the initial coasting arc. If these can be propagated to the beginning of the arc, then the primer vector, $\lambda_{\overline{v}}$, will be known there since it is a function of these three adjoints and the orbital elements (see Eq. 9.3.1). Eqs. 5.2.4 (for time free) or Eqs. 6.2.15 (for time specified) can be used to find these values, as well as λ_{u0} and $\lambda_{\hat{r}N0}$ required by the $\lambda_{\overline{r}}$ transformation equation (Eq. 9.3.2 with Eq. 9.3.4), if only λ_t, λ_{uf} and $\lambda_{\hat{r}Nf}$ are also known.

First of all, λ_t is known because it is a constant over the entire trajectory, so it is computed between subsequent burns. This leaves two unknowns, λ_{uf} and $\lambda_{\hat{r}Nf}$. Lawden's

corner condition used in Section 8.2, $\dot{\lambda}_{\bar{v}}^{+} = \dot{\lambda}_{\bar{v}}^{-}$, can be used to obtain these two values. Using Eq. 8.2.2, λ_{uf} and $\lambda_{\hat{r}Nf}$ appear in readily usable forms in the $\hat{r}$ and in the $\hat{h}$ directions. From the continuity of the $\hat{r}$ component of Eq. 9.3.2,

$$\lambda_{uf} = \frac{1}{u_1}\left(h_0\lambda_{hf} - u'_f\lambda_{u'f} - h_1\lambda_{h0} + \psi_1\lambda_{u'0} + u_1\lambda_{u0}\right). \qquad 9.4.2$$

For determining $\lambda_{\hat{r}Nf}$ it must be recalled that

$$\hat{r}'^{+} = \cos\phi\,\hat{r}'^{-} + \sin\phi\,\hat{h}^{-} \qquad 9.4.3$$

and

$$\hat{h}^{+} = -\sin\phi\,\hat{r}'^{-} + \cos\phi\,\hat{h}^{-}. \qquad 9.4.4$$

Using these with the inner product of Eq. 9.3.2 (with Eq. 9.3.4 substituted in) with $\hat{h}^{-}$ on both sides of the burn, then solving for $\lambda_{\hat{r}Nf}$ yields

$$\lambda_{\hat{r}Nf} = \frac{b_2\sin\phi_1 + b_3\cos\phi_1 - u'_f\lambda_{\hat{r}'Nf}}{u_1}, \qquad 9.4.5$$

where

$$b_2 = u_1\left(-\psi_1\lambda_{u0} + (u_1 - \frac{\mu}{h_1^2})\lambda_{u'0} - \frac{\lambda_t}{h_1 u_1^2}\right) + h_1\psi_1\lambda_{h0} - (u_1^2 + \psi_1^2)\lambda_{u'0} \qquad 9.4.6$$

and

$$b_3 = u_1\lambda_{\hat{r}N0} + \psi_1\lambda_{\hat{r}'N0}. \qquad 9.4.7$$

So, with values obtained for all of the relevant adjoint variables at the final point of the initial coast, the equations for the adjoint variables on coasting arcs (Eqs. 6.2.15) can be used to determine their values at the beginning of the coasting arc:

$$\lambda_{\hat{r}N0} = \cos\eta_0\ \lambda_{\hat{r}Nf} - \sin\eta_0\ \lambda_{\hat{r}N'f} \qquad\qquad 9.4.8$$

$$\lambda_{\hat{r}N'0} = \sin\eta_0\ \lambda_{\hat{r}Nf} + \cos\eta_0\ \lambda_{\hat{r}N'f} \qquad\qquad 9.4.9$$

$$\begin{bmatrix} \lambda_{u0} \\ \lambda_{u'0} \end{bmatrix} = \begin{bmatrix} \cos\eta_0 & -\sin\eta_0 \\ \sin\eta_0 & \cos\eta_0 \end{bmatrix} \begin{bmatrix} \lambda_{uf} - \lambda_t\lambda_{uc}(\eta_0) \\ \lambda_{u'f} - \lambda_t\lambda_{u'c}(\eta_0) \end{bmatrix} \qquad 9.4.10$$

and

$$\lambda_{h0} = \lambda_{hf} - \frac{2\mu}{h_0^3}\lambda_{u0}\ (\cos\eta_0 - 1) - \frac{2\mu}{h_0^3}\lambda_{u'0}\ \sin\eta_0 - \lambda_t\lambda_{hc}(\eta_0)\ . \qquad 9.4.11$$

These values are then transformed to $\lambda_{\overline{r}}$ and $\lambda_{\overline{v}}$, then written to an input file to be read and used by BOUNDSCO.

10.0 NUMERICAL EXAMPLES

10.1 Introduction

In order to illustrate the algorithm derived in the preceding chapters, various solutions of extremals using this algorithm are given in this chapter. Two and three burn solutions are shown for both time open and time specified rendezvous problems to a fixed set of target elements. Two burn solutions are presented in the next section, and three burn solutions are presented in the subsequent section. In both sections, some classical results are investigated first, followed by variations in these problems, and concluding with other more general problems.

In each case where the solution of the impulsive thrust algorithm satisfied the condition that the primer vector magnitude be no greater than one over the entire trajectory, the state and adjoint trajectories from the solution were fed as initial conditions into the multiple shooting computer program BOUNDSCO. These initial conditions are automatically written to the input file used by the computer routines which call BOUNDSCO. The shooting points generated by the impulsive thrust program are the initial and final points of the trajectory, and the points one third of the transfer angle and two thirds of the transfer angle between each burn.

In order to ensure close comparison between the impulsive thrust results and the finite thrust results, the magnitude of the finite thrust was chosen to be large: ten times the gravitational acceleration. Good results have also been obtained from BOUNDSCO when the thrust was as low as one times the gravitational acceleration with the initial conditions obtained from the impulsive thrust routines, but the larger number should help guarantee convergence of

BOUNDSCO. If the thrust is low enough for there to be a large discrepancy between the finite burn and the impulsive burn trajectories, then the impulsive approximation is probably not good for that problem. In actual engineering applications, a large number such as the one used here would likely be used to obtain an initial finite thrust solution, then thrust would be (perhaps slowly) reduced to the correct level. Also, other slight variations would potentially have to be made to some other parameters until the solution was exactly the desired one. For example, for time open problems, both λ_t and the common Hamiltonian in Cartesian coordinates would have to be zero, but the Hamiltonian would be slightly nonzero due to variations in time of flight between infinite and finite thrust solutions; hence, time of flight would need to be adjusted until the Hamiltonian became zero. For the results presented here, only the initial BOUNDSCO solution is given without these (probably minor) adjustments.

For all the results presented, three tables are given for each problem investigated. The first contains the interceptor and the target elements; the second contains the initial guess and converged solution for the iteration parameters in the impulsive thrust algorithm; and the third contains various iteration characteristics such as number of iterations for both the impulsive thrust algorithm and for BOUNDSCO, the cost function for the converged results for both programs, the values of λ_t and of the finite thrust Hamiltonian in Cartesian coordinates, and the time of flight of the extremal trajectory. Also included in this last table is the initial error of the norm used by the Quasi-Newton method in BOUNDSCO; this gives a measure of how good the initial conditions from the impulsive thrust routines are. For most of the problems presented, the iteration parameters for the plane change at the second to last burn (ϕ_1 or ϕ_2) and for the final coasting angle (η_1 or η_2) are missing from the tables because the computer program will, on option, automatically generate values for these parameters which will cause the final trajectory position to match the targets position. Finally, a plot of the primer magnitude

history is given for both the impulsive thrust trajectory and the finite thrust trajectory.

10.2 Two-Burn Trajectories

The most obvious two burn optimal trajectory to check the algorithm against is the Hohmann transfer. Tables 10.2.1 through 10.2.3 contain the data for a sample Hohmann solution from a circular orbit of radius one to a second circular orbit of radius two. Time is open in the solution process shown. For most two burn problems, the first three iteration parameters (see Table 10.2.2) are usually set to zero. In this case, those values are the solution to the Hohmann transfer when the rendezvous point is already 180° away from the interceptor, so the parameters had to be made nonzero in order to obtain any iterations. In other runs made without this initial lineup, the algorithm quickly creates an initial coast until the interceptor is 180° from the target, at which point the first burn commences. Table 10.2.3 shows that for the Hohmann problem, when BOUNDSCO is fed initial conditions from the impulsive burn solution, the error is already very small, so that only six iterations are required to obtain convergence (the relative precision tolerances in the impulsive burn software and in BOUNDSCO were set to 10^{-6} in the runs presented here). Figures 10.2.1 and 10.2.2 both show the well known attribute that $S' = 0$ at the beginning and at the end of the transfer orbit for the impulsive thrust solution. The finite thrust solution has the primer magnitude $p > 0$ whenever a thrust is occurring, which is at the beginning and end of the trajectory in this case.

Tables 10.2.4 through 10.2.6 show the results when the two space vehicles have the same initial elements as in the preceding problem, but the transfer time is now specified to be 5.0 TU (the time open transfer time is 5.77 TU). In order to reduce the transit time, an initial coast of 0.33 rad was added by the algorithm, since the original radius is smaller and hence has a faster

Table 10.2.1. Elements for Hohmann Transfer.

	$\hat{r}$			u	$\hat{r}'$			u'	h
Interceptor	1.000000	0.000000	0.000000	1.000000	0.000000	1.000000	0.000000	0.000000	1.000000
Target	-1.000000	0.000000	0.000000	0.500000	0.000000	-1.000000	0.000000	0.000000	1.414000

Table 10.2.2. Iteration Parameters for Hohmann Transfer.

	ψ_1	η_0	$\lambda_{\hat{r}N01}$	ϕ_1	η_1
initial	0.010000	0.500000	0.000000	—	—
final	3×10^{-13}	4×10^{-10}	0.000000	0.000000	3.141593

Table 10.2.3. Iteration Characteristics for Hohmann Transfer.

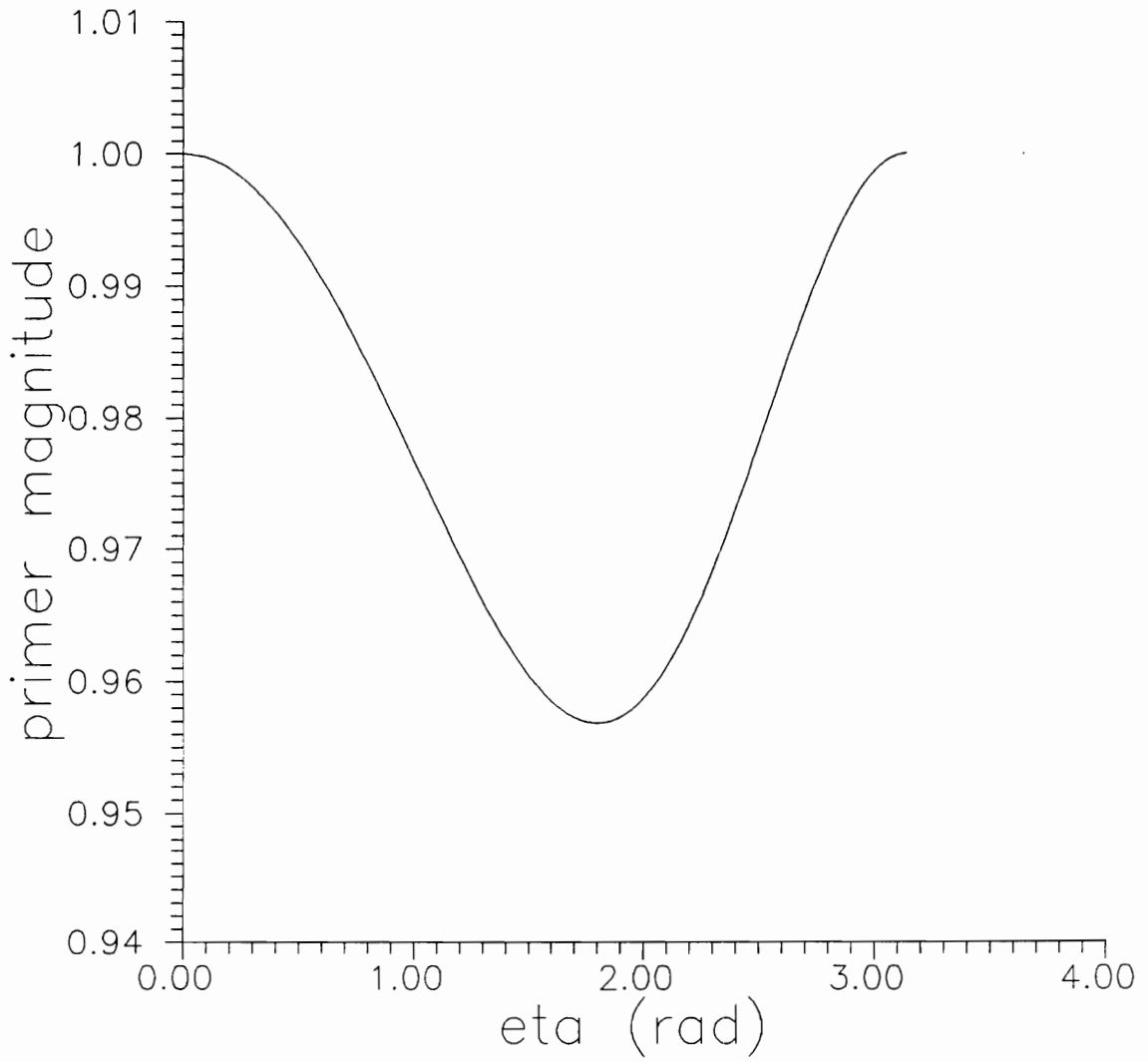| number iters.	char. vel. (du/tu)	λ_t	flight time (tu)	BOUNDSCO init. error	BOUNDSCO iterations	$\int \mid \bar{T} \mid dt$ (du/tu)	Hamiltonian
3	0.284350	$-6. \times 10^{-13}$	5.771474	0.00002	6	0.2843673	-9.31×10^{-4}

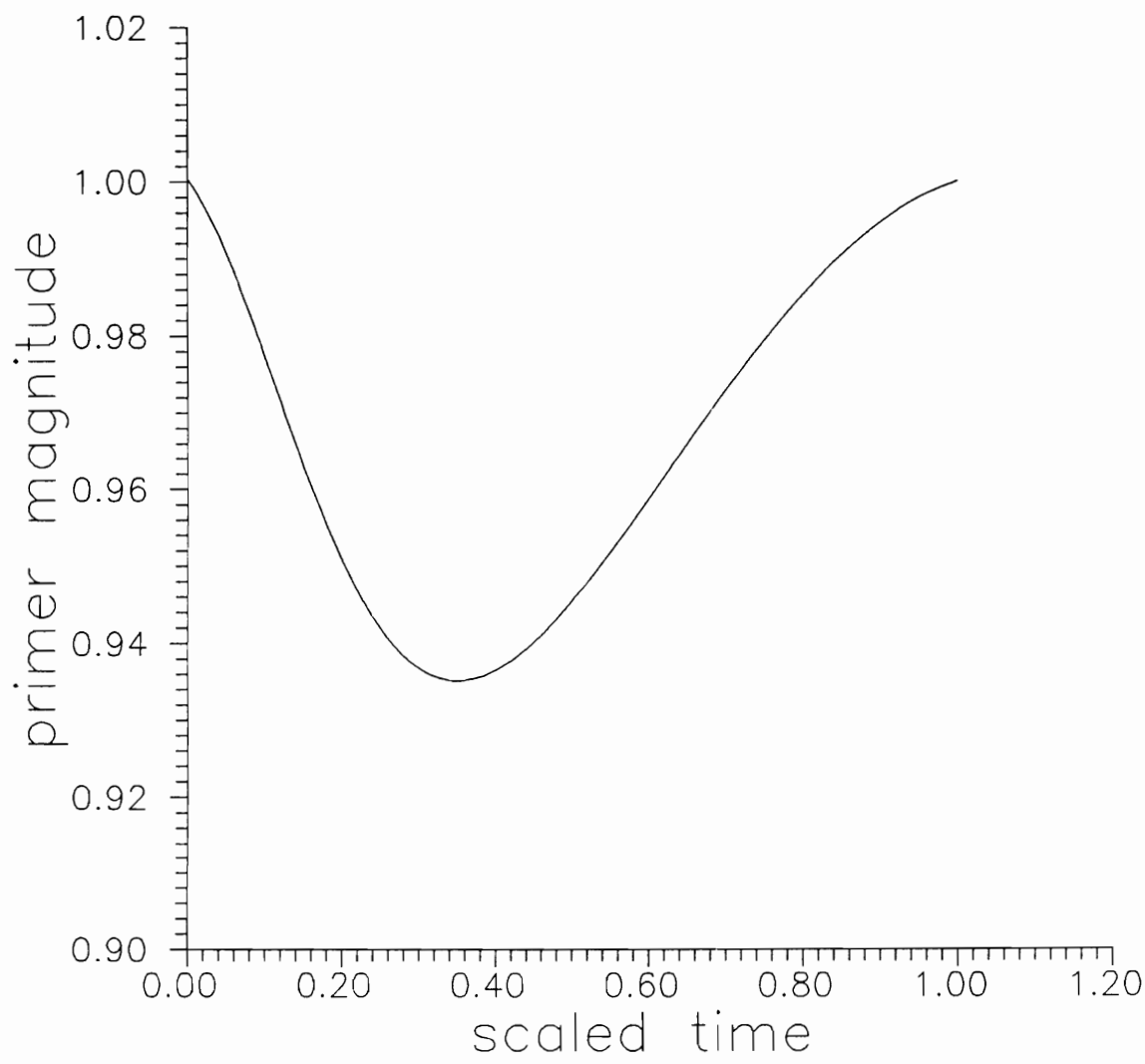Figure 10.2.1. Impulsive Thrust Primer Magnitude for Hohmann Transfer.

Figure 10.2.2. Finite Thrust Primer Magnitude for Hohmann Transfer.

Table 10.2.4. Elements for Hohmann-Like Transfer with Max. Time = 5.0 TU.

	$\hat{r}$			u	$\hat{r}'$			u'	h
Interceptor	1.000000	0.000000	0.000000	1.000000	0.000000	1.000000	0.000000	0.000000	1.000000
Target	-1.000000	0.000000	0.000000	0.500000	0.000000	-1.000000	0.000000	0.000000	1.414000

Table 10.2.5. Iteration Parameters for Hohmann-Like Transfer with Max. Time = 5.0 TU.

	ψ_1	η_0	$\lambda_{\hat{r}N01}$	ϕ_1	η_1
initial	0.000000	0.000000	0.000000	—	—
final	0.011238	0.332034	0.000000	0.000000	2.809558

Table 10.2.6. Iteration Characteristics for Hohmann-Like Transfer with Max. Time = 5.0 TU.

number iters.	char. vel. (du/tu)	λ_t	flight time (tu)	BOUNDSCO init. error	BOUNDSCO iterations	$\int |\bar{T}| \, dt$ (du/tu)	Hamiltonian
5	0.329793	-0.131951	5.000000	0.020	7	0.330514	0.133648

angular rate. While the Hohmann transfer has no radial component of thrust at either burn, this lower time trajectory required a small component of thrust in the radial direction (i.e., $\psi > 0$) since the burn could not occur at the 180° separation point. Notice in Table 10.2.6 that λ_t is now nonzero and negative as it must be. Recall that the Hamiltonian used in the BOUNDSCO software is equal to $-\lambda_t$ according to the theory in Section 3.4. In Table 10.2.6 these two quantities are nearly equal in magnitude; the difference is mainly due to the fact that the corresponding finite thrust trajectory has higher cost. Figures 10.2.3 and 10.2.4 show that $S' = 0$ at the first burn since it is after an initial coast, but it is nonzero at the terminal (rendezvous) point.

Both of the previous examples have both the initial and the final orbits as circular orbits. Tables 10.2.7 through 10.2.9, together with Figures 10.2.5 and 10.2.6, present the characteristics of a circular to non-circular in-plane transfer through an angle of two radians, with time unspecified. When this solution was attempted the first time, the initial coasting angle went negative. With time open problems this really is not a problem, since adding 2π to the original coasting angle yields a valid trajectory. Hence, the algorithm was run again with η_0 set to 6.28 for an initial guess; the algorithm converged with $\eta_0 = 5.19$ rad. The characteristic velocity shown in Table 10.2.9 is very low. In fact, it is less than the Hohmann characteristic velocity to the same radius (Table 10.2.3) because the rendezvous orbit has a small outward component of radial velocity ($u' < 0$), so the interceptor need not expend as much fuel as it would if rendezvous was to a circular orbit. This is also why the final coasting angle, η_1, is now slightly less than π.

The next set of tables and figures (Tables 10.2.10 through 10.2.12 and Figures 10.2.7 and 10.2.8) start with the same set of elements, but the time of transfer is now specified to be 3.0 TU (as opposed to 10.8 TU of the previous solution). The first burn now occurs right away
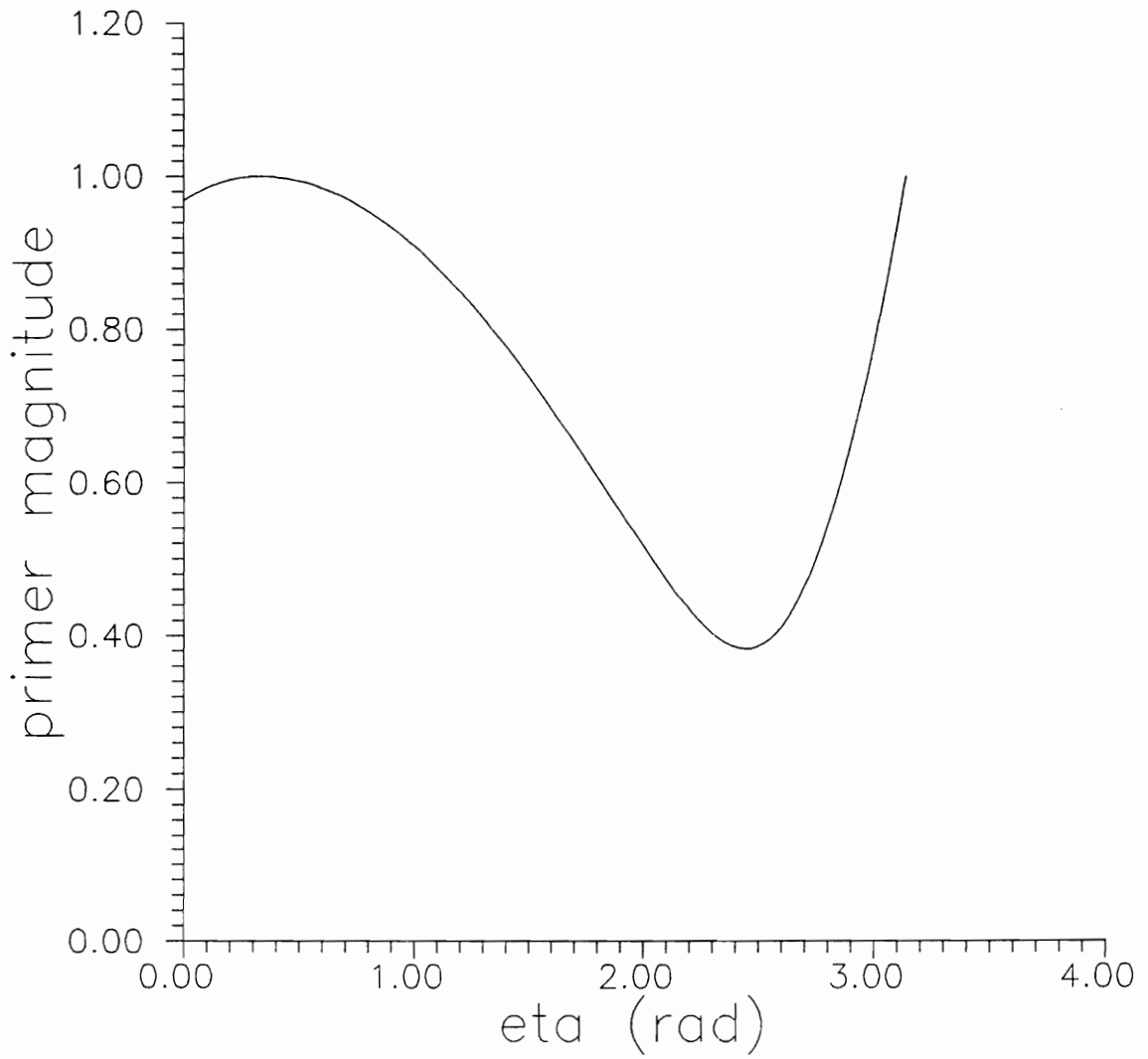
Figure 10.2.3. Impulsive Thrust Primer Magnitude for Hohmann-Like Transfer with Max. Time = 5.0 TU.
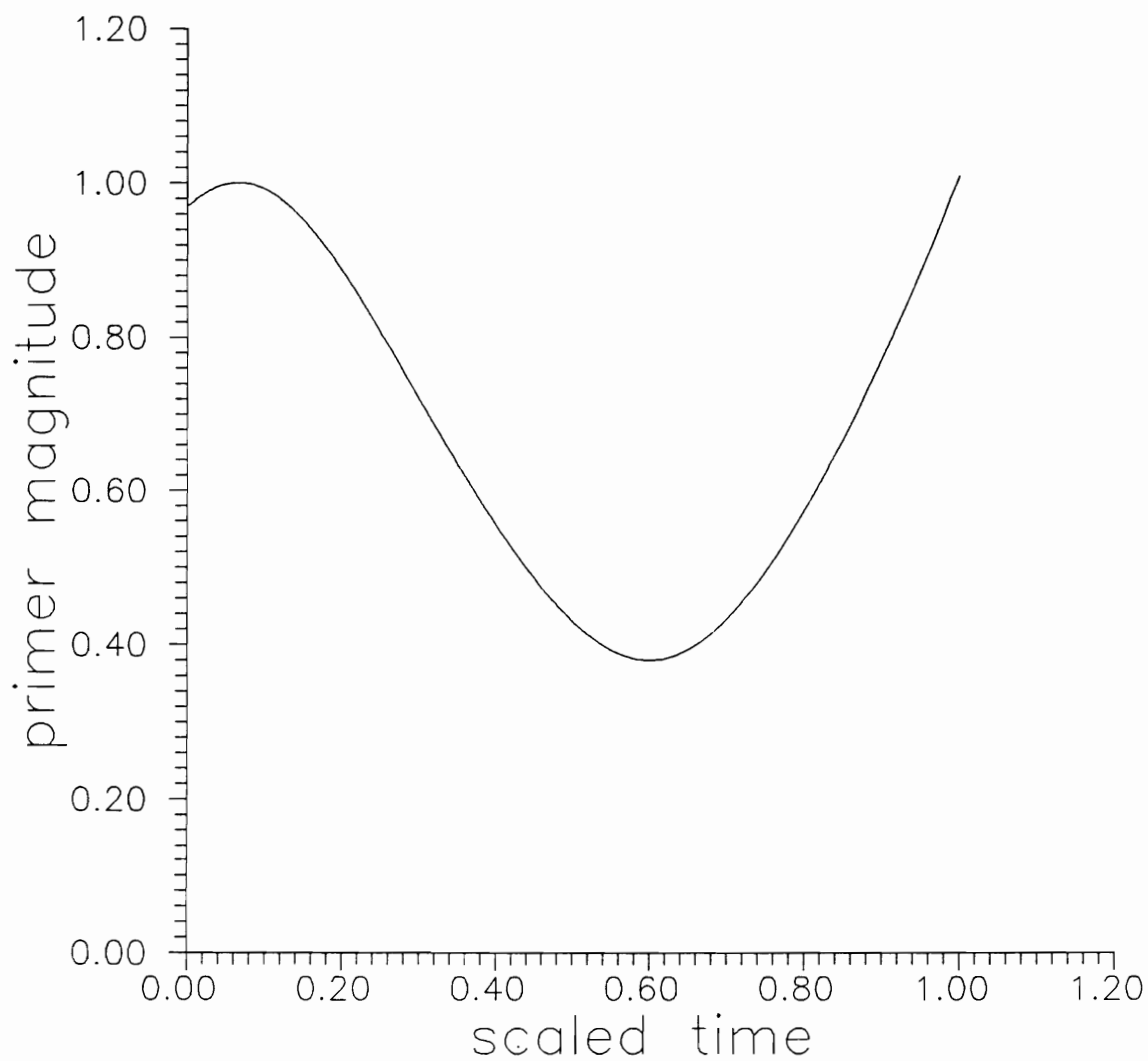
Figure 10.2.4. Finite Thrust Primer Magnitude for Hohmann-Like Transfer with Max. Time = 5.0 TU.

Table 10.2.7. Elements for Circular to Non-Circular in-Plane Transfer.

	$\hat{r}$			u	$\hat{r}'$			u'	h
Interceptor	1.000000	0.000000	0.000000	1.000000	0.000000	1.000000	0.000000	0.000000	1.000000
Target	-0.416147	0.909297	0.000000	0.500000	-0.909297	-0.414614	0.000000	-0.010000	1.400000

Table 10.2.8. Iteration Parameters for Circular to Non-Circular in-Plane Transfer.

	ψ_1	η_0	$\lambda_{\hat{r}N01}$	ϕ_1	η_1
initial	0.000000	6.280000	0.000000	—	—
final	3×10^{-10}	5.186872	0.000000	0.000000	3.096313

Table 10.2.9. Iteration Characteristics for Circular to Non-Circular in-Plane Transfer.

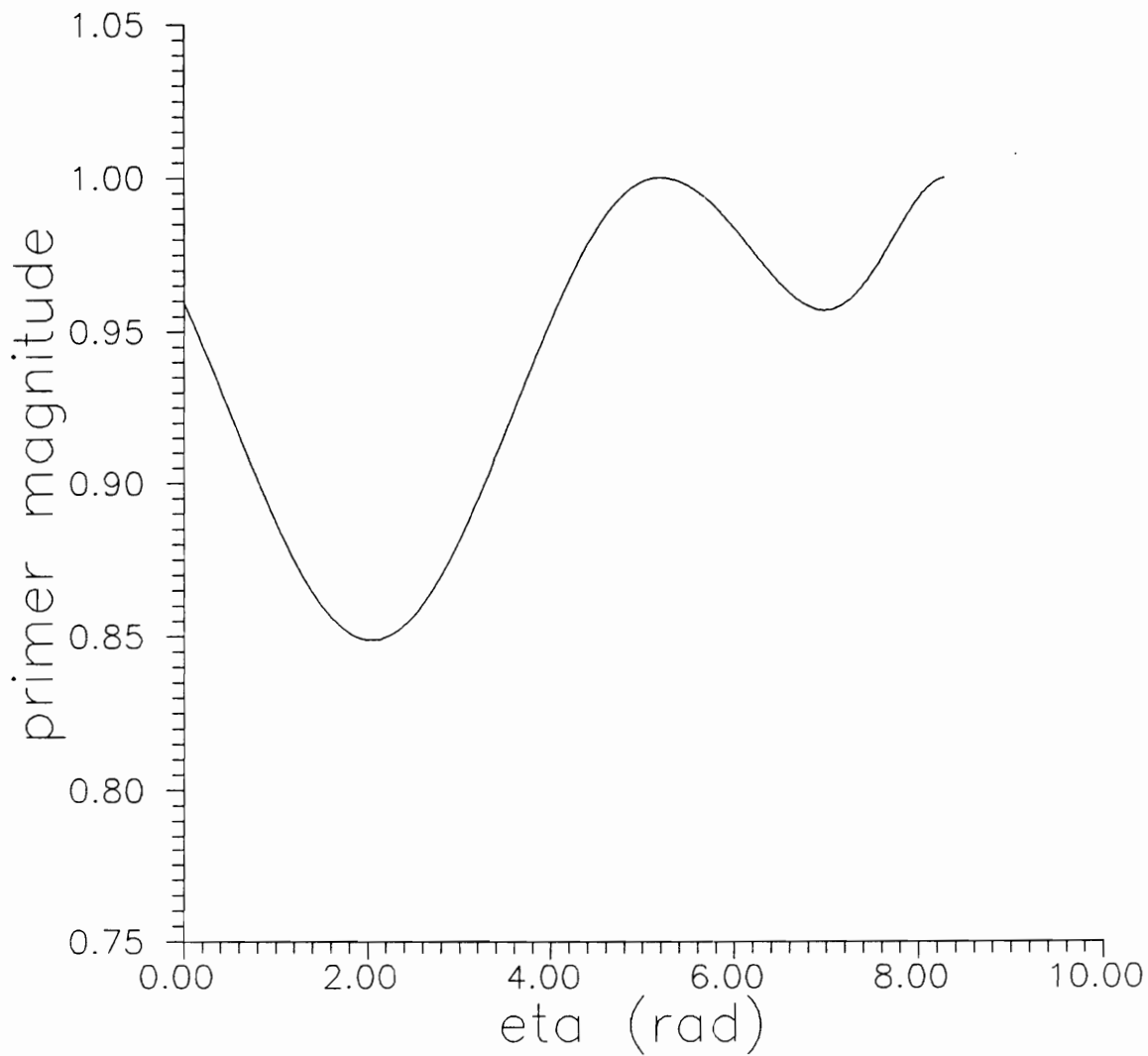| number iters.	char. vel. (du/tu)	λ_t	flight time (tu)	BOUNDSCO init. error	BOUNDSCO iterations	$\int \lvert \bar{T} \rvert \, dt$ (du/tu)	Hamiltonian
4	0.277403	$2. \times 10^{-10}$	10.80436	0.005	6	0.277405	4.68×10^{-4}

Figure 10.2.5. Impulsive Thrust Primer Magnitude for Circular to Non-Circular in-Plane Transfer.
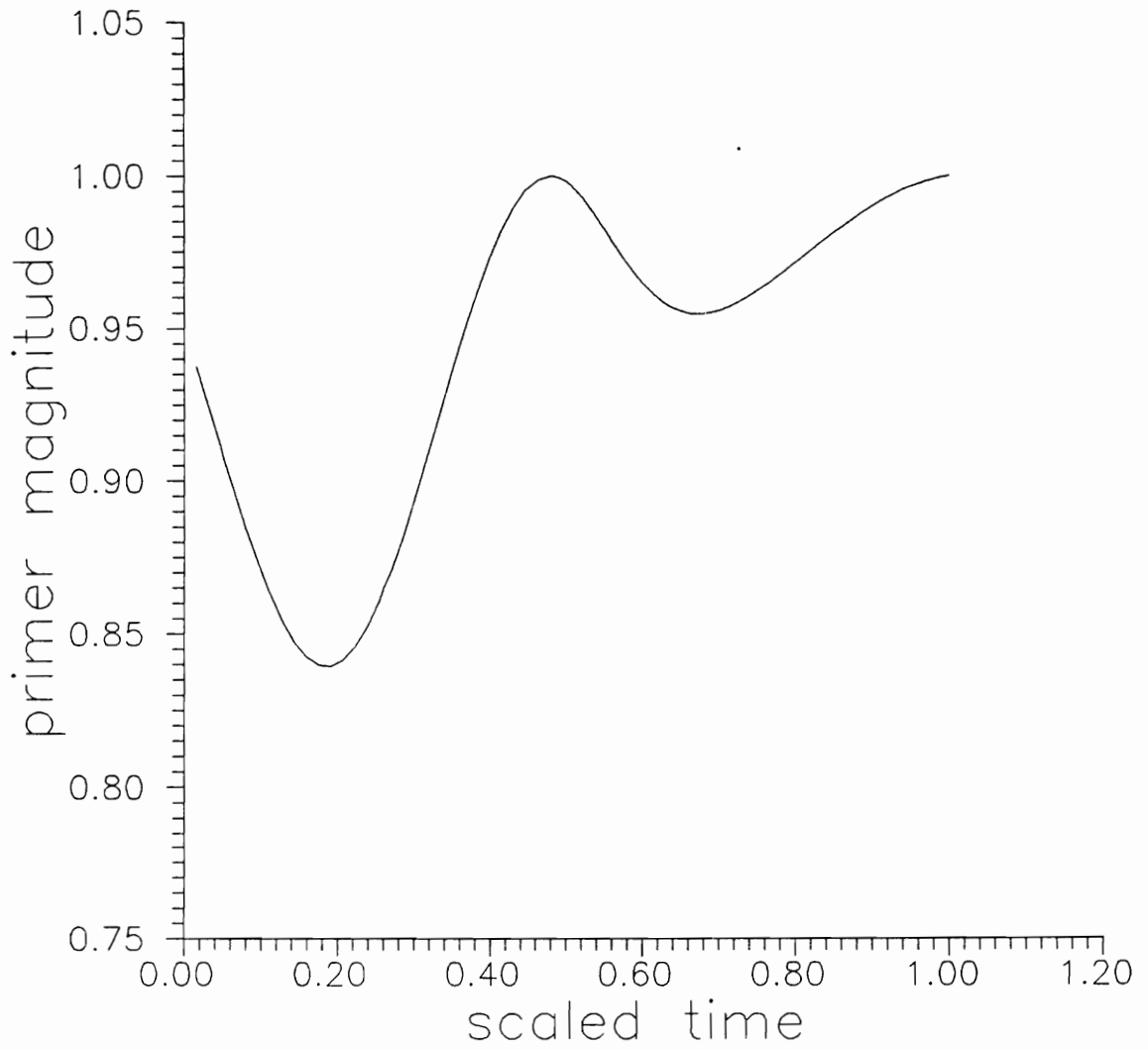
Figure 10.2.6. Finite Thrust Primer Magnitude for Circular to Non-Circular in-Plane Transfer.

Table 10.2.10. Elements for Circular to Non-Circular in-Plane Transfer (Time Specified).

	$\hat{r}$			u	$\hat{r}'$			u$'$	h
Interceptor	1.000000	0.000000	0.000000	1.000000	0.000000	1.000000	0.000000	0.000000	1.000000
Target	-0.416147	0.909297	0.000000	0.500000	-0.909297	-0.414614	0.000000	-0.010000	1.400000

Table 10.2.11. Iteration Parameters for Circular to Non-Circular in-Plane Transfer (Time Specified).

	ψ_1	η_0	$\lambda_{\hat{r}N01}$	ϕ_1	η_1
initial	0.000000	0.000000	0.000000	—	—
final	-0.04429	0.000000	0.000000	0.000000	2.000000

Table 10.2.12. Iteration Characteristics for Circular to Non-Circular in-Plane Transfer (Time Specified).

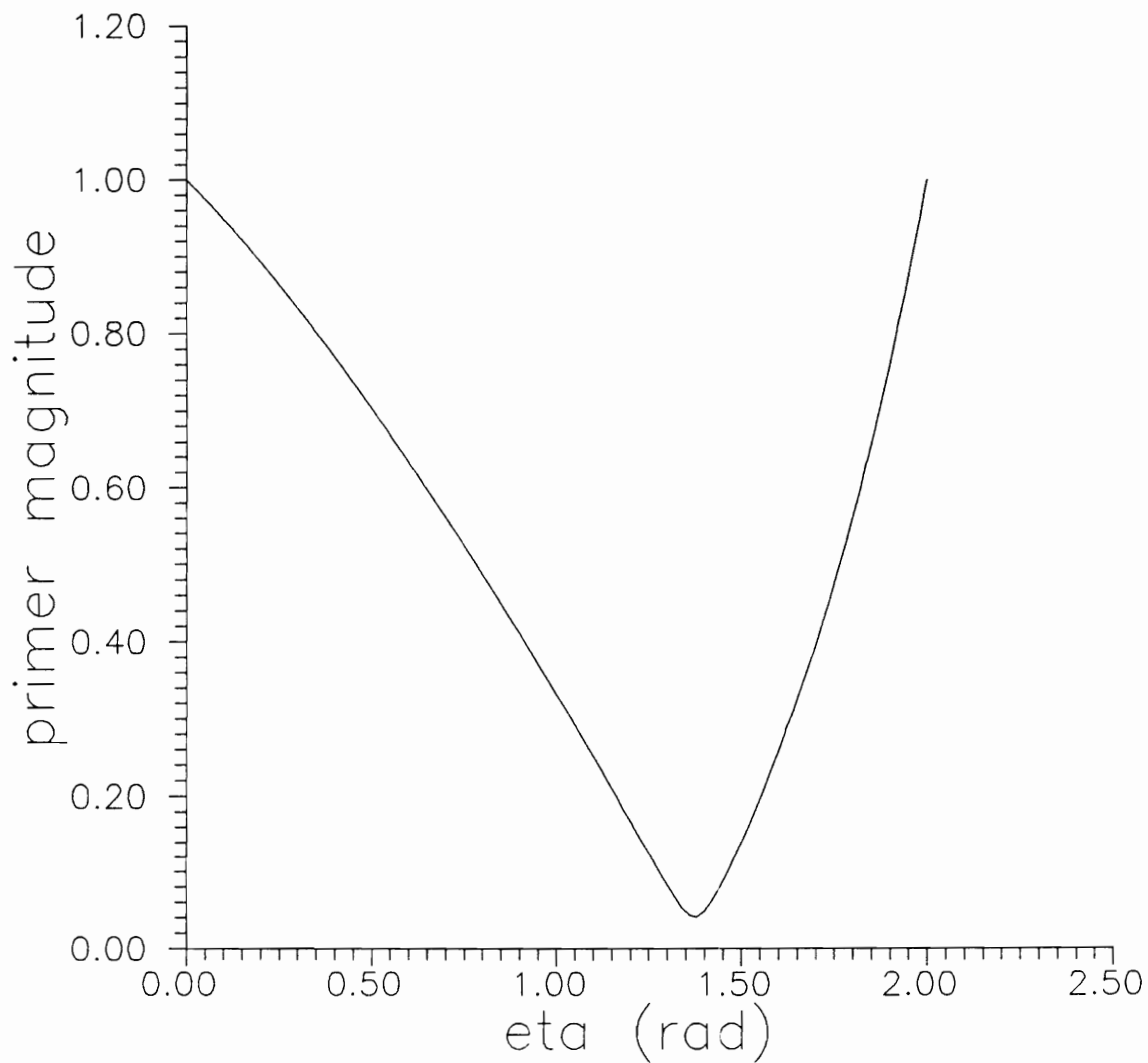| number iters.	char. vel. (du/tu)	λ_t	flight time (tu)	BOUNDSCO init. error	BOUNDSCO iterations	$\int |\bar{T}| dt$ (du/tu)	Hamiltonian
4	0.558938	-0.36792	3.000000	0.0001	6	0.565132	0.376713

Figure 10.2.7. Impulsive Thrust Primer Magnitude for Circular to Non-Circular in-Plane Transfer (Time Specified).
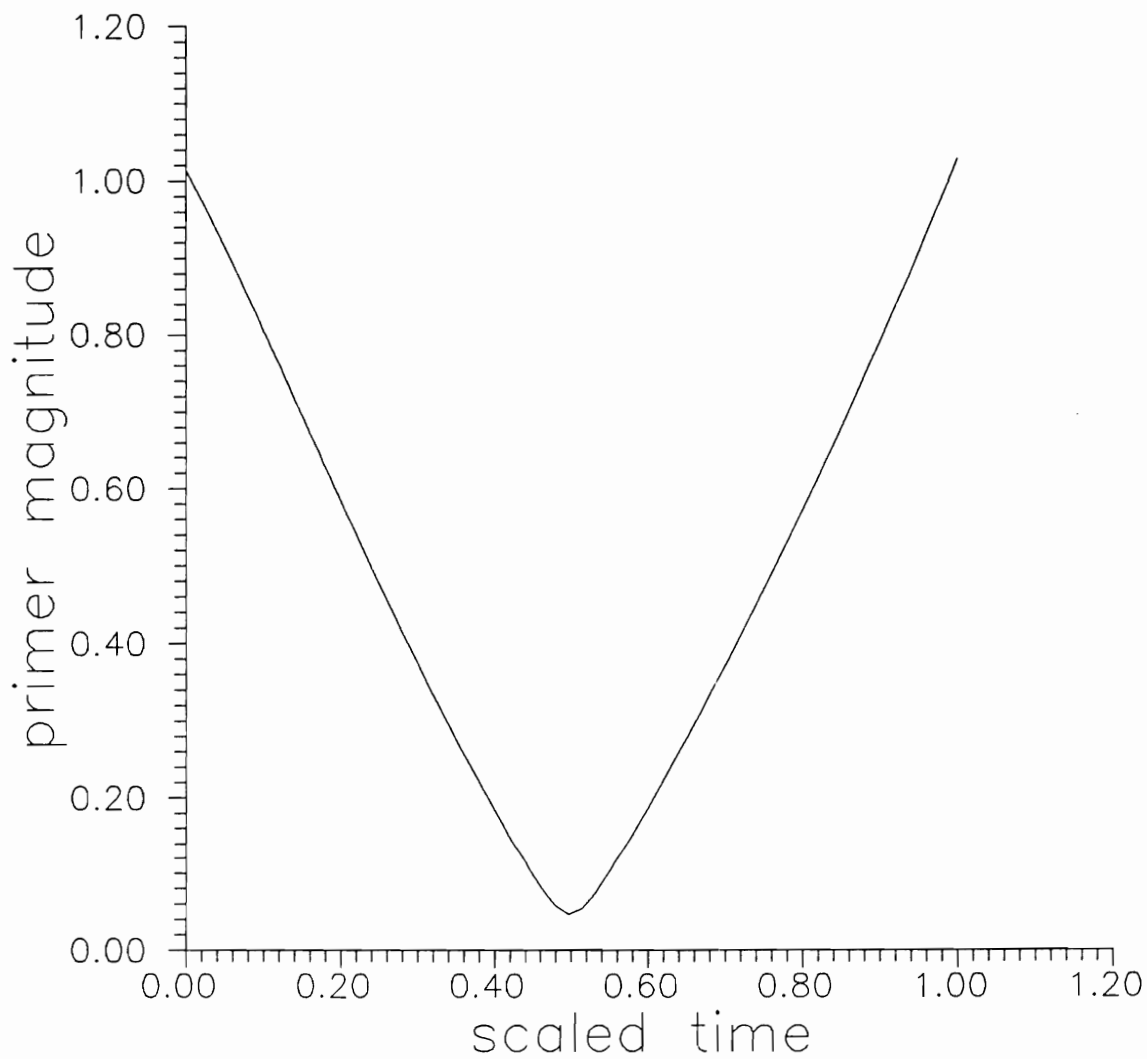
Figure 10.2.8. Finite Thrust Primer Magnitude for Circular to Non-Circular in-Plane Transfer (Time Specified).

since there is no time for a long coast, resulting in a characteristic velocity which is of course much higher. λ_t also now has a substantial magnitude. Furthermore, S' is far from zero at both ends of the trajectory.

The final two burn trajectory presented (see Tables 10.2.13 through 10.2.15 and Figures 10.2.9 and 10.2.10) is a time specified out-of-plane transfer between two non-circular orbits. Since the two orbit positions are at a distance of at least two DU, and since the specified time is so short, the characteristic velocity is quite large. When the specified time was relaxed from 3 DU to 4.65 DU in another run, the characteristic velocity decreased from 2.15 to 1.13 DU/TU.

In all of the runs presented, and indeed in nearly all of the two burn problems attempted, the algorithm seems to be quite robust. Non-circular and out-of-plane solutions are generally no more difficult to obtain than are circular and in-plane solutions. Of course, if the orbits are sufficiently non-circular, or if the required plane changes are large, more burns than two are generally required. Three burn solutions are the topic of the next section.

10.3 Three-Burn Trajectories

Just as the Hohmann transfer is the most common and most significant time open two-burn transfer, so also are the bi-elliptic and bi-parabolic transfers for three-burn time open in-plane maneuvers.[21,11,34] It has been analytically shown that bi-elliptic transfers are lower in cost than Hohmann transfers (between circular orbits) when the ratio of the larger orbit to the

Table 10.2.13. Elements for Non-Circular to Non-Circular Time Specified Out-of-Plane Transfer.

	$\hat{r}$			u	$\hat{r}'$			u'	h
Interceptor	-0.414563	0.905837	-0.087156	0.500000	-0.901781	-0.396063	0.172987	-0.00100	1.400000
Target	-0.482969	-0.836515	-0.258819	0.350000	0.851451	-0.517633	0.084186	0.002000	1.500000

Table 10.2.14. Iteration Parameters for Non-Circular to Non-Circular Time Specified Out-of-Plane Transfer.

	ψ_1	η_0	$\lambda_{\hat{r}N01}$	ϕ_1	η_1
initial	0.000000	0.000000	0.000000	—	—
final	0.375991	0.000000	0.480898	-0.54592	2.135270

Table 10.2.15. Iteration Characteristics for Non-Circular to Non-Circular Time Specified Out-of-Plane Transfer.

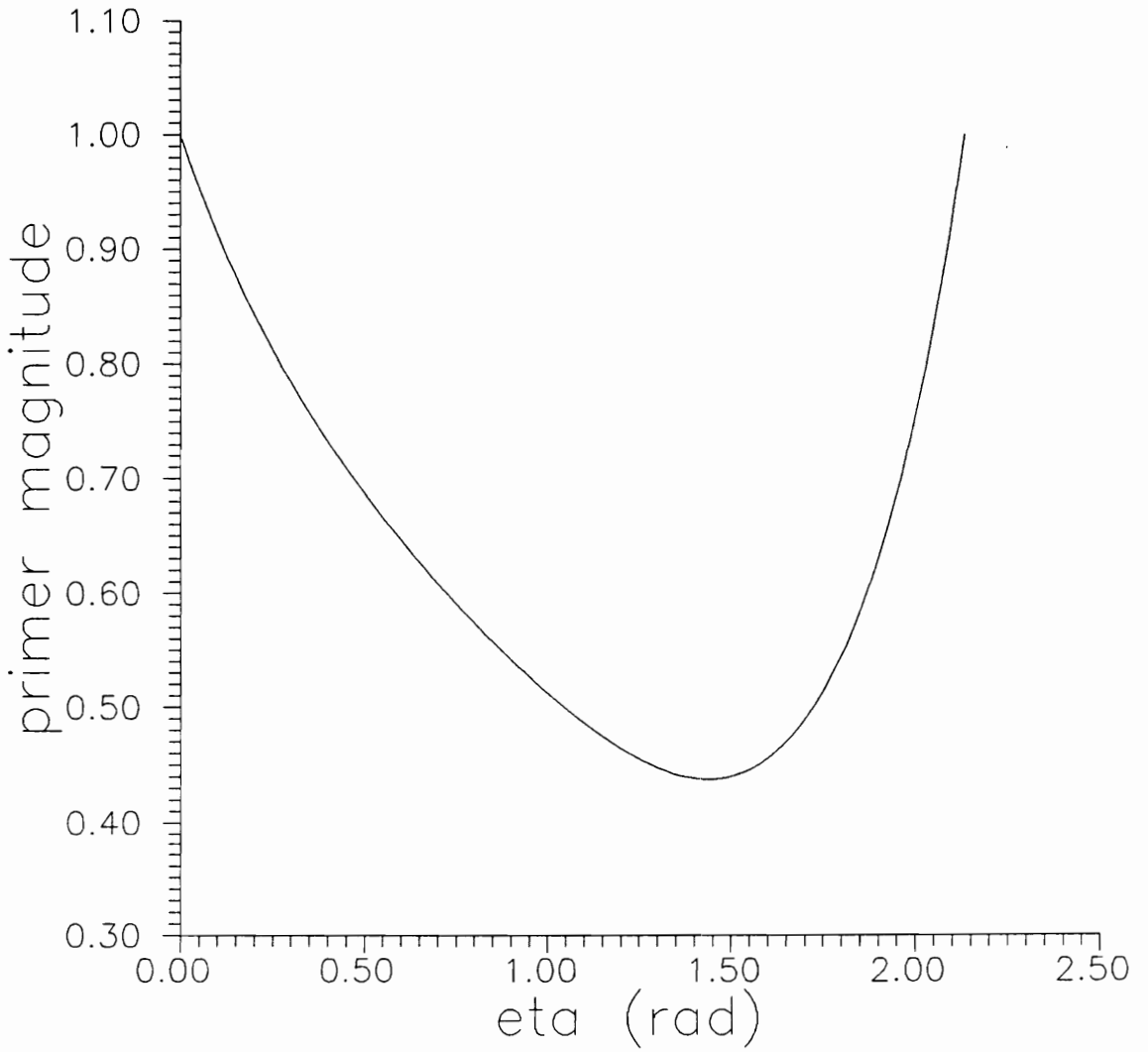| number iters.	char. vel. (du/tu)	λ_t	flight time (tu)	BOUNDSCO init. error	BOUNDSCO iterations	$\int \mid \bar{T} \mid dt$ (du/tu)	Hamiltonian
7	2.150220	-0.927518	3.000000	1.59	9	2.230903	1.091184

Figure 10.2.9. Impulsive Thrust Primer Magnitude for Non-Circular to Non-Circular Time Specified Out-of-Plane Transfer.
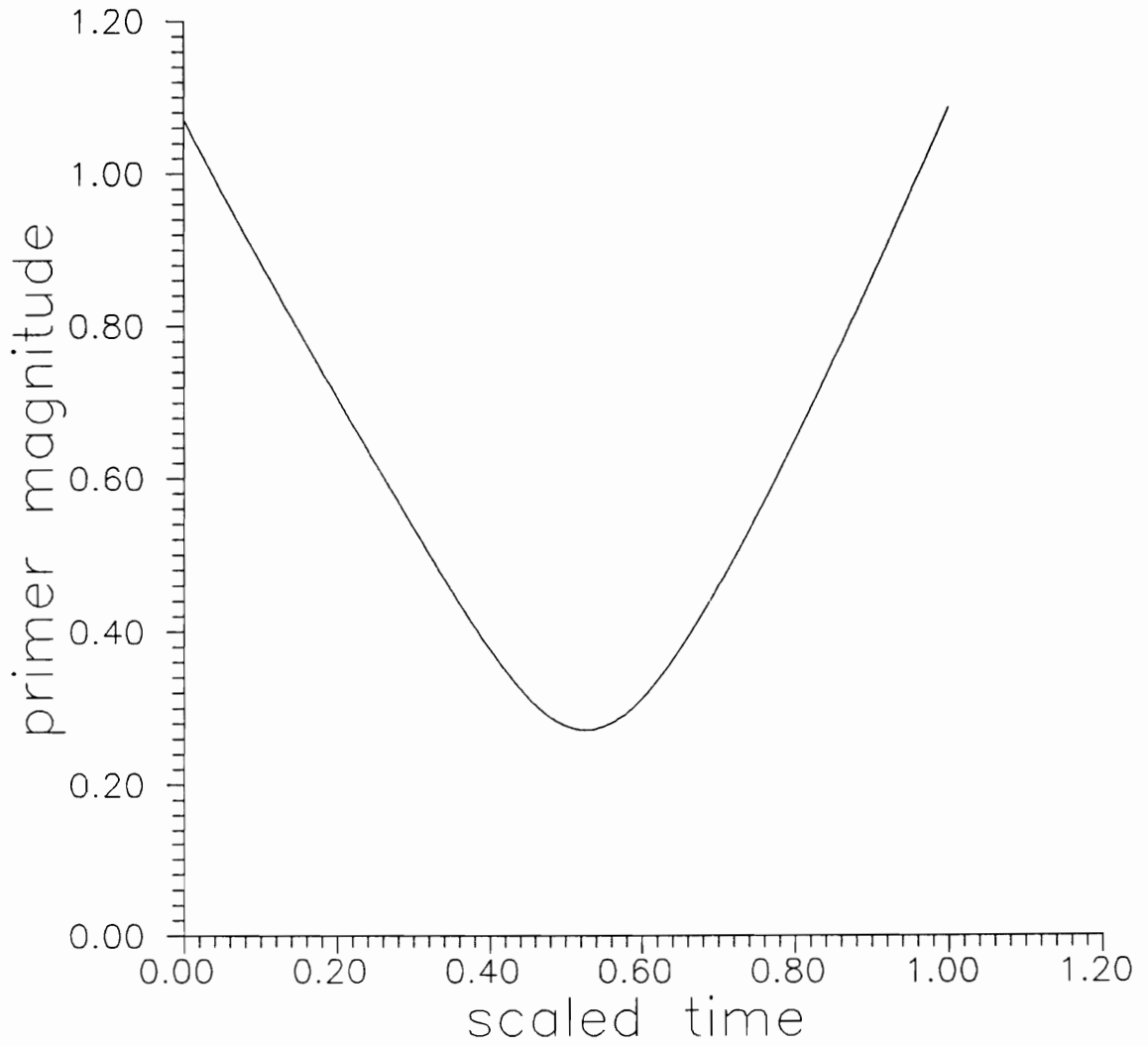
Figure 10.2.10. Finite Thrust Primer Magnitude for Non-Circular to Non-Circular Time Specified Out-of-Plane Transfer.

smaller orbit is greater than about 15.56. The bi-elliptic transfer burns initially purely in the transverse direction to carry the interceptor to a radius greater than the larger of the two circular orbits through an angle of π rad, then a transverse burn is again accomplished go bring the trajectory back to the target trajectory. The bi-elliptic transfer is not optimal in theoretical terms because there is no radius of the intermediate burn which furnishes a minimum; the cost continues to decrease as that radius is increased. In the limit as the intermediate radius approaches infinity, a so-called bi-parabolic transfer is obtained.

An interesting feature of Schumacher coordinates is that as an infinite radius is approached, the value of the reciprocal radius merely approaches zero. So, as long as time is not involved in the problem (since the limiting bi-parabolic orbit requires an infinite amount of transfer time), a bi-parabolic orbit presents no problems for Schumacher coordinates. Although the algorithm using the primer vector theory has some difficulty fully converging to the bi-parabolic orbit since u occurs in the denominator of some of the expressions, the solution was nonetheless attempted. The results are shown in Tables 10.3.1 through 10.3.3 and Figure 10.3.1. They are termed bi-elliptical there because u never quite reached zero in the solution process. No BOUNDSCO solution was attempted since time is the independent variable used in the routines called by BOUNDSCO.

The way the target elements were aligned required an initial coast of 270°. λ_t is very small, as it should be since this is a time open solution. Notice that the initial condition is a bi-elliptic orbit, but the algorithm causes u to approach zero. Since the bi-elliptic orbit consists of two Hohmann-like maneuvers, it is of interest to determine which of the equations is not

Table 10.3.1. Elements for Bi-Elliptic Transfer.

	$\hat{r}$			u	$\hat{r}'$			u'	h
Interceptor	1.000000	0.000000	0.000000	1.000000	0.000000	1.000000	0.000000	0.000000	1.000000
Target	0.000000	-1.00000	0.000000	0.040000	1.000000	0.000000	0.000000	0.000000	0.200000

Table 10.3.2. Iteration Parameters for Bi-Elliptic Transfer.

	ϕ_1	ψ_1	η_0	$\lambda_{\hat{r}N01}$	u_2	ψ_2	η_1	$\lambda_{\hat{r}N02}$	ϕ_2	η_f
initial	0.000000	0.000000	4.710000	0.000000	0.010000	0.000000	3.140000	0.000000	—	—
final	-1×10^{-19}	-0.000518	4.709942	5×10^{-17}	0.000071	-0.000044	3.140121	-5×10^{-14}	-9×10^{-14}	3.141551

Table 10.3.3. Iteration Characteristics for Bi-Elliptic Transfer.

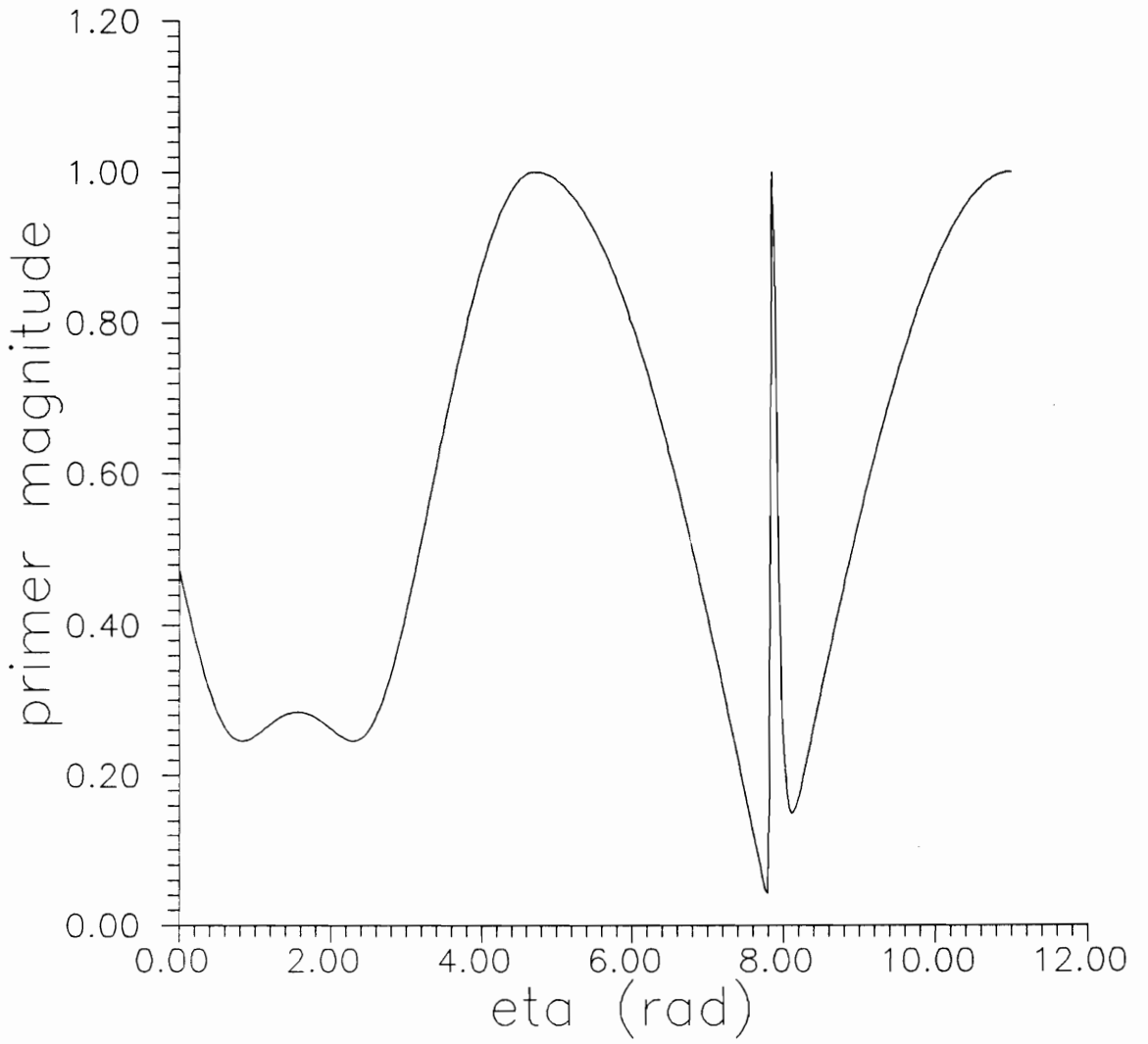| number iters.	char. vel. (du/tu)	λ_t	flight time (tu)	BOUNDSCO init. error	BOUNDSCO iterations	$\int \mid \bar{T} \mid dt$ (du/tu)	Hamiltonian
45	0.689157	-1×10^{-12}	3.7×10^7	—	—	—	—

Figure 10.3.1. Impulsive Thrust Primer Magnitude for Bi-Elliptic Transfer.

initially satisfied, causing u→0. All of the equations are initially satisfied if the coasting angles are exactly correct, except for the τ equation (Eq.8.2.4) from Lawden's corner condition. It is easy to see by examination of the components of the τ equation that u must be zero to satisfy $\tau = 0$ at the middle burn of a bi-elliptic transfer (thus actually making it a bi-parabolic transfer). The actual transfer time of this almost converged trajectory, which has a maximum radius of 14,000 DU (u $= 7.1 \times 10^{-5}$), is 3.7×10^{7} TU (1009 years).

Another classical three burn transfer occurs when the inclination of a circular orbit is to be changed, without changing the semi-major axis or the eccentricity of the orbit. Of course, this can be accomplished through one burn at the node of the common axis of the two orbits, but it has been shown that a three burn transfer always requires less fuel than the one burn maneuver. The three burn transfer burns at the common axis of the two planes; this burn chiefly raises the apo-apsis of the trajectory, while producing just a small portion of the total required plane change. The second burn produces most of the requisite plane change at a large radius (plane changes are less expensive at greater distances from the attracting body). For 45° plane change in a circular orbit of radius one, for example, this radius is about 1.6 DU. The third and final burn produces the last little bit of plane change, while making the orbit circular again, at the common axis of the two orbits.

It is shown by this current analysis, however, that this classical transfer is not optimal from the point of view of optimal control theory. A parameter optimization routine which seeks to minimize the characteristic velocity of the three burn trajectory will, on the other hand, converge quite rapidly to this classical solution. When time open transfers with the algorithm developed in this dissertation failed to obtain the classical solution (in fact, it always diverged away from it), the solution was obtained by a parameter optimization routine. The optimal control necessary conditions of Lawden, and the new $\delta = 0$ necessary condition developed herein,

were then applied to this converged trajectory; it was non-optimal on both counts. Lawden's corner condition at impulsive burns (the $\tau = 0$ condition in this work, Eq. 8.2.4) is violated by the trajectory ($\tau = 0.304$), and also $\delta \neq 0$. The former condition must hold even if the solution was a time specified extremal. To numerically confirm that this conundrum is not just some analysis gone astray, the parameter-optimal solution was fed into BOUNDSCO to see how it behaved. It also diverged away from that solution, converging to a totally different solution.

Tables 10.3.4 through 10.3.9, with Figures 10.3.2 through 10.3.5, show two time specified attempts at attaining an optimal solution for this problem, when the plane change angle is 45°, through the algorithm developed in this work. The times of flight for the two cases are 20 TU and 19 TU, respectively. While both solutions have characteristic velocities less than the one burn case (which is 0.765 DU/TU), they are also higher than the classical solution (0.703 DU/TU). The 19 TU solution has nearly zero λ_t , so it is approximately an open time extremal (BOUNDSCO converges to effectively the same solutions). The most probable explanation for this conundrum is that a four impulse solution probably exists which has lower characteristic velocity than all of the solutions mentioned above.

One final three burn solution will be shown to demonstrate the algorithm on problems with non-circular orbits (see Tables 10.3.10 through 10.3.12 and Figures 10.3.6 and 10.3.7) when time is unspecified. The initial interceptor elements in this case are the most commonly used

Table 10.3.4. Elements for Time Restricted Classical Three Burn Plane Change.

	$\hat{r}$			u	$\hat{r}'$			u'	h
Interceptor	1.000000	0.000000	0.000000	1.000000	0.000000	1.000000	0.000000	0.000000	1.000000
Target	1.000000	0.000000	0.000000	1.000000	0.000000	0.707107	0.707107	0.000000	1.000000

Table 10.3.5.   Iteration Parameters for Time Restricted Classical Three Burn Plane Change.

	ϕ_1	ψ_1	η_0	$\lambda_{\hat{r}N01}$	u_2	ψ_2	η_1	$\lambda_{\hat{r}N02}$	ϕ_2	η_f
initial	0.050000	0.000000	0.000000	0.000000	0.300000	0.000000	3.140000	0.000000	-0.78000	3.140000
final	0.057001	-2×10^{-15}	0.000000	-2×10^{-14}	0.300502	-2×10^{-14}	3.141593	-5×10^{-14}	-0.656319	3.141593

Table 10.3.6. Iteration Characteristics for Time Restricted Classical Three Burn Plane Change.

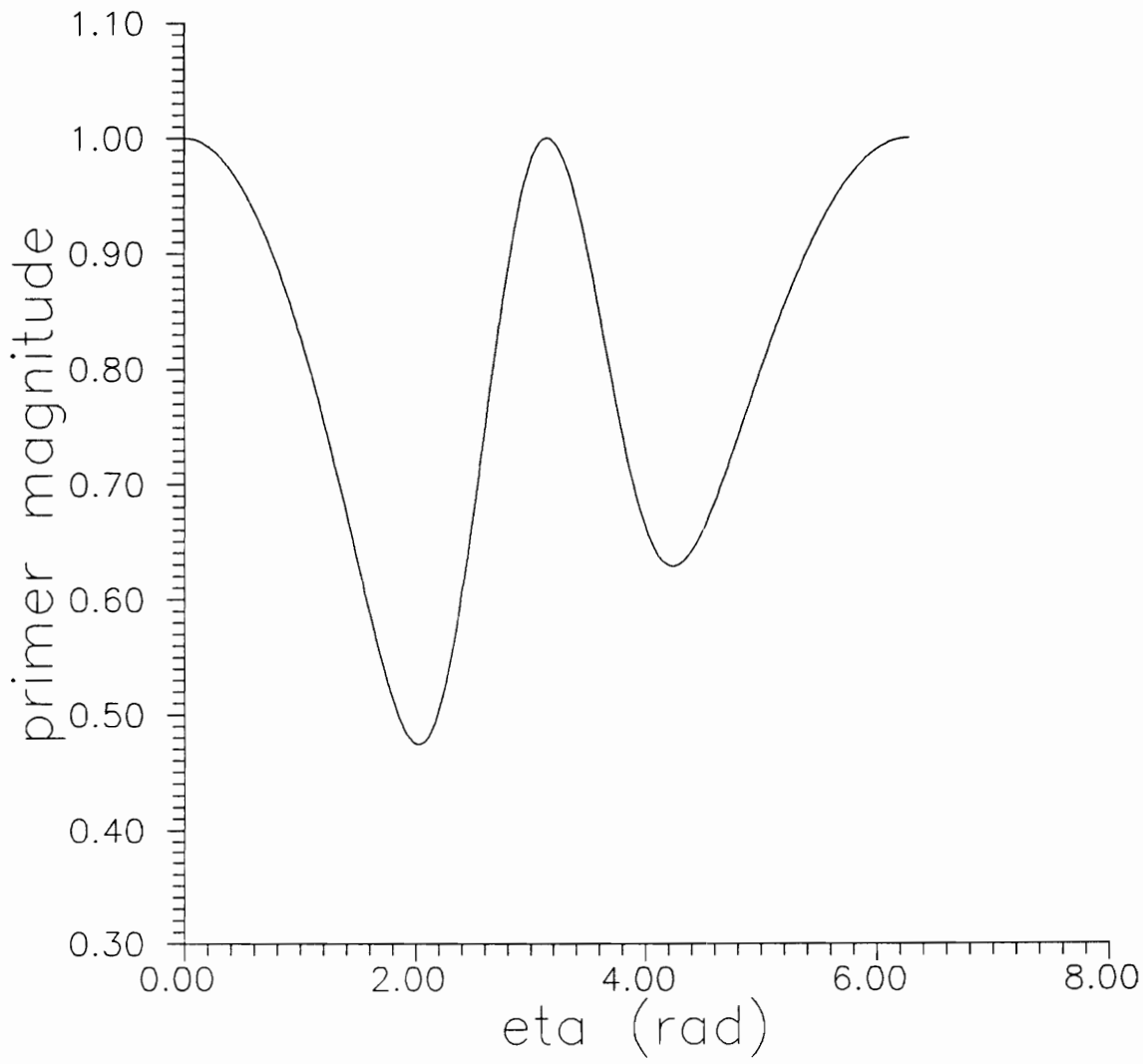| number iters.	char. vel. (du/tu)	λ_t	flight time (tu)	BOUNDSCO init. error	BOUNDSCO iterations	$\int \lvert \bar{T} \rvert \, dt$ (du/tu)	Hamiltonian
7	0.741732	1×10^{-16}	20.00000	2.21	16	0.741179	-2.92×10^{-3}

Figure 10.3.2. Impulsive Thrust Primer Magnitude for Time Restricted Classical Three Burn Plane Change.
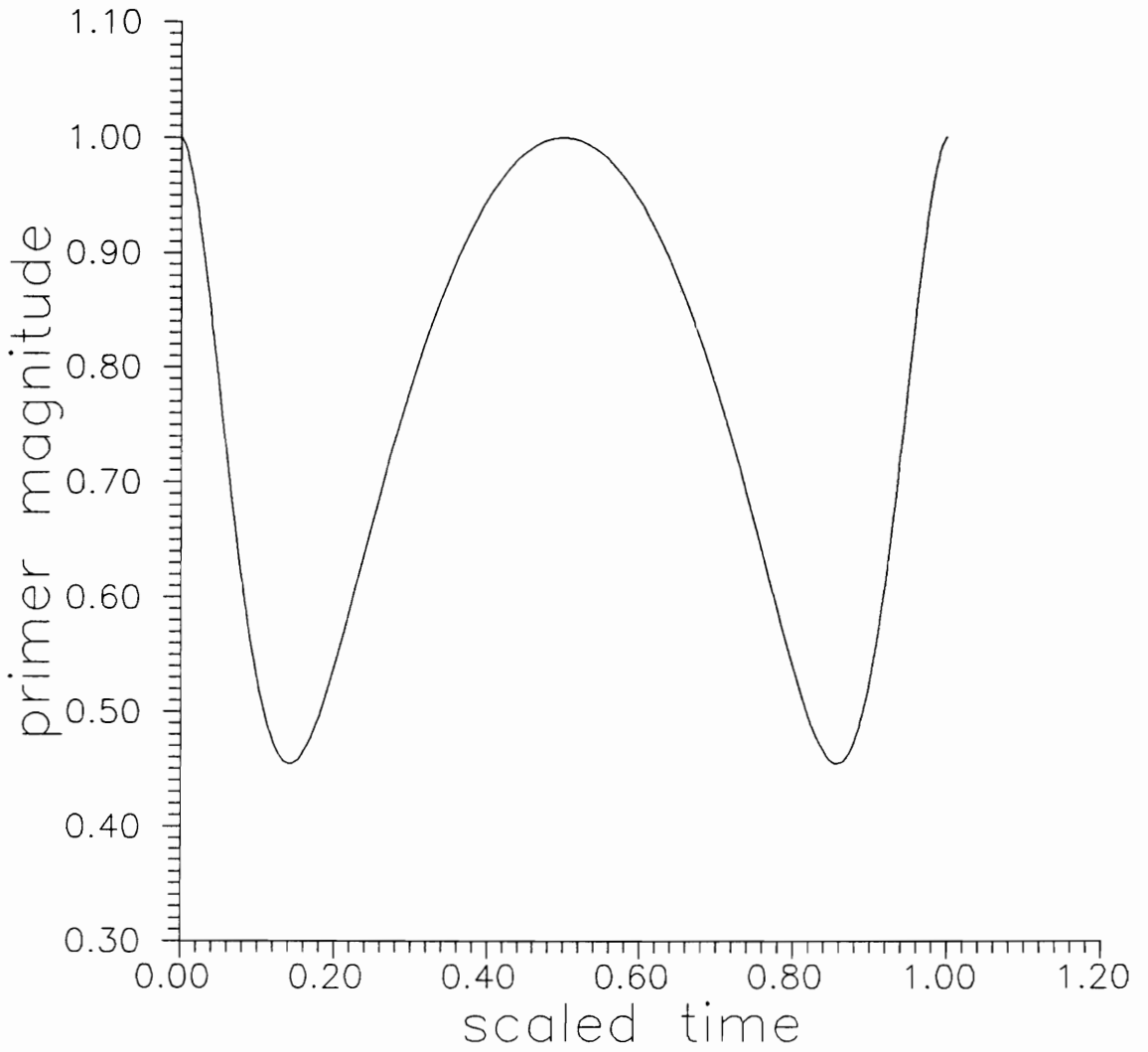
Figure 10.3.3. Finite Thrust Primer Magnitude for Time Restricted Classical Three Burn Plane Change.

Table 10.3.7. Elements for Further Restricted Time.

	$\hat{r}$			u	$\hat{r}'$			u'	h
Interceptor	1.000000	0.000000	0.000000	1.000000	0.000000	1.000000	0.000000	0.000000	1.000000
Target	1.000000	0.000000	0.000000	1.000000	0.000000	0.707107	0.707107	0.000000	1.000000

Table 10.3.8. Iteration Parameters for Further Restricted Time.

	ϕ_1	ψ_1	η_0	$\lambda_{\hat{r}N01}$	u_2	ψ_2	η_1	$\lambda_{\hat{r}N02}$	ϕ_2	η_f
initial	0.050000	0.000000	0.000000	0.000000	0.300000	0.000000	3.140000	0.000000	-0.78000	3.140000
final	0.058538	-5×10^{-15}	0.000000	-1×10^{-13}	0.314241	1×10^{-14}	3.141593	1×10^{-14}	-0.653115	3.141593

Table 10.3.9. Iteration Characteristics for Further Restricted Time.

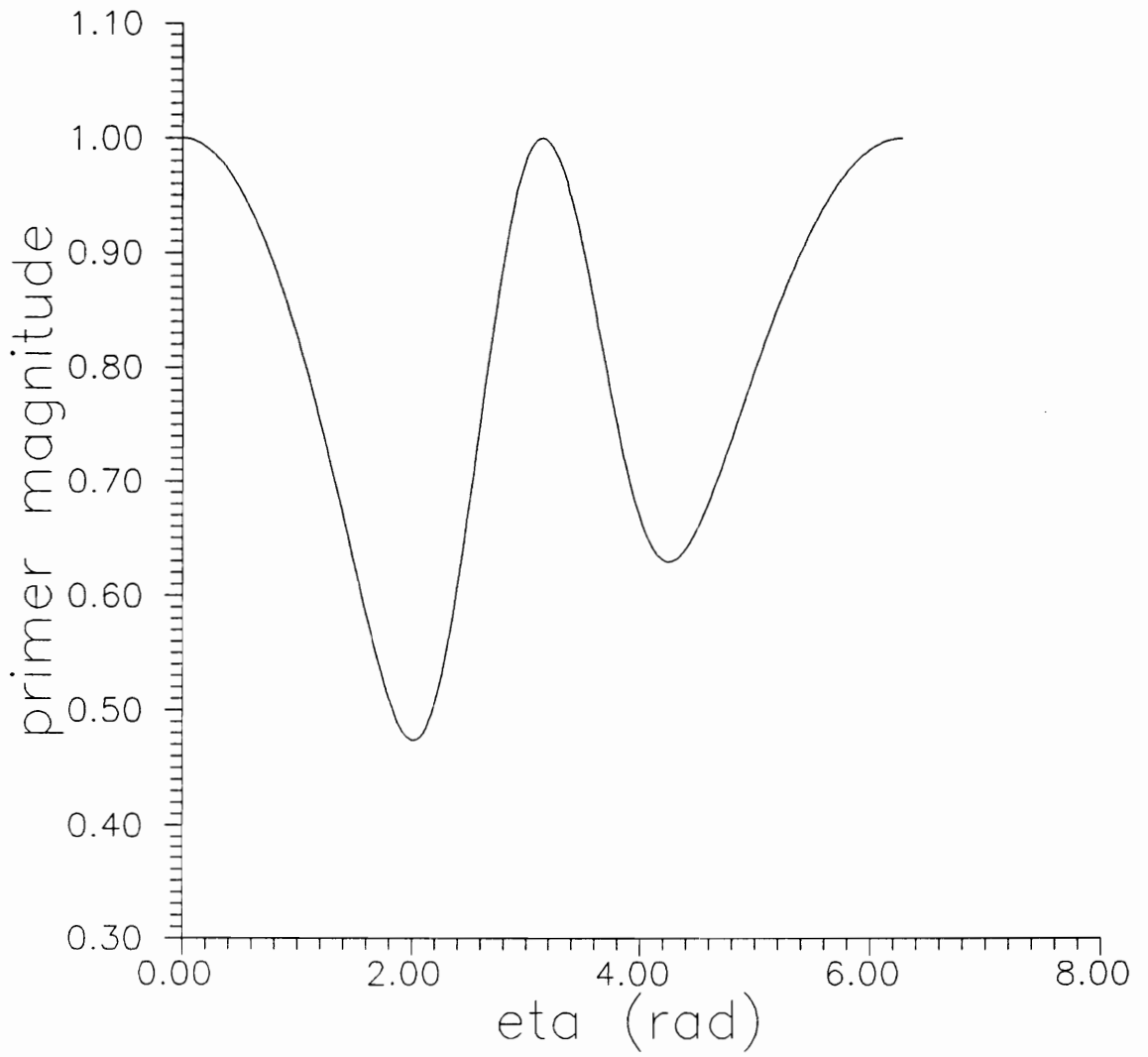| number iters.	char. vel. (du/tu)	λ_t	flight time (tu)	BOUNDSCO init. error	BOUNDSCO iterations	$\int |\bar{T}| dt$ (du/tu)	Hamiltonian
11	0.738735	-3×10^{-17}	19.00000	2.10	11	0.738157	-3.13×10^{-3}

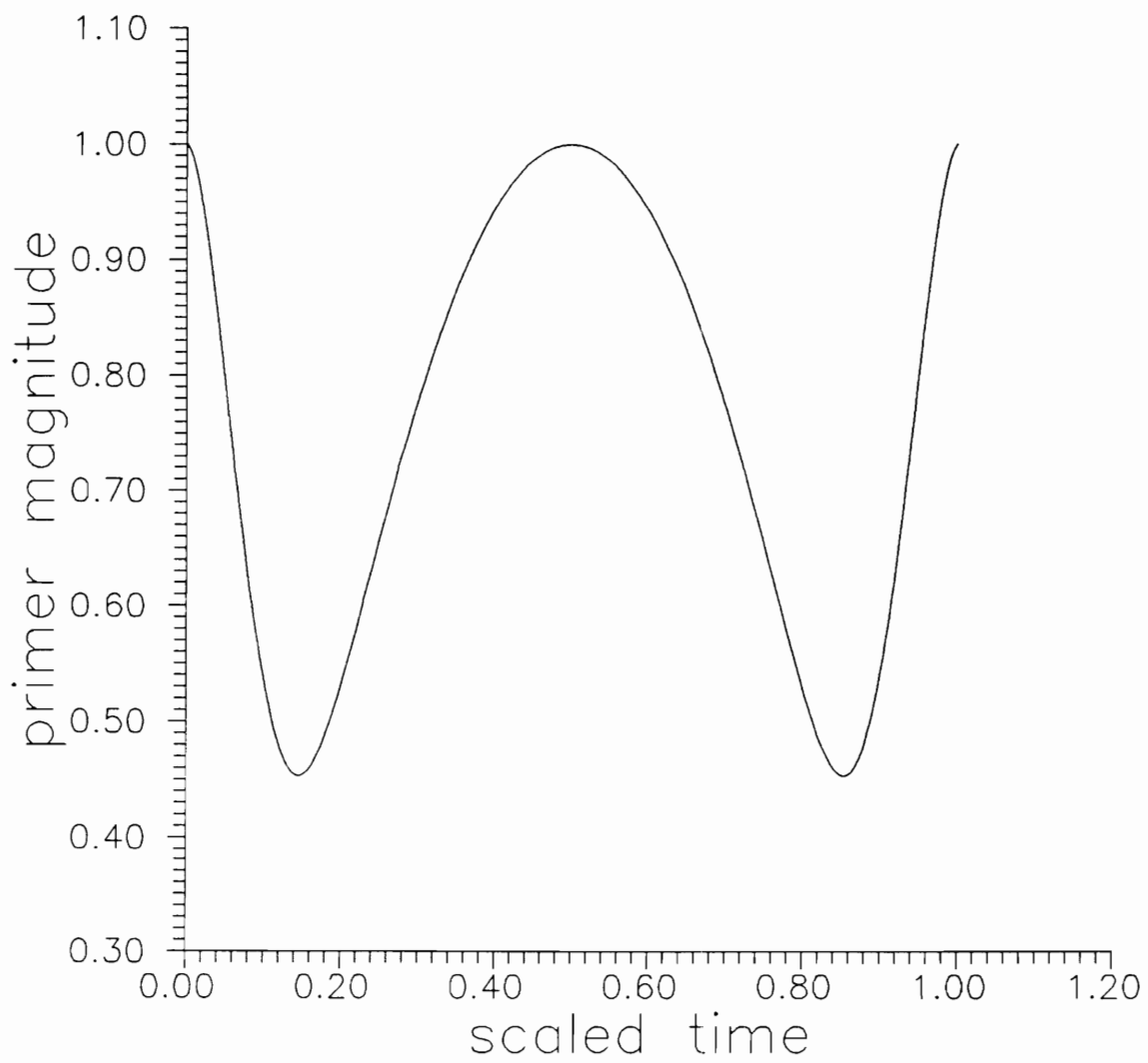Figure 10.3.4. Impulsive Thrust Primer Magnitude for Further Restricted Time.

Figure 10.3.5. Finite Thrust Primer Magnitude for Further Restricted Time.

Table 10.3.10. Elements for General Three Burn Trajectory.

	$\hat{r}$			u	$\hat{r}'$			u'	h
Interceptor	1.000000	0.000000	0.000000	1.000000	0.000000	1.000000	0.000000	0.000000	1.000000
Target	0.816035	-0.571394	0.0871557	0.800000	0.456063	0.543879	0.704416	0.010000	1.100000

Table 10.3.11.   Iteration Parameters for General Three Burn Trajectory.

	ϕ_1	ψ_1	η_0	$\lambda_{\hat{r}N01}$	u_2	ψ_2	η_1	$\lambda_{\hat{r}N02}$	ϕ_2	η_f
initial	0.000000	0.000000	0.000000	0.000000	0.700000	0.000000	3.000000	0.000000	—	—
final	0.039508	0.003868	0.000000	0.085565	0.908730	-0.022867	2.993129	0.015861	-0.143233	2.672594

Table 10.3.12. Iteration Characteristics for General Three Burn Trajectory.

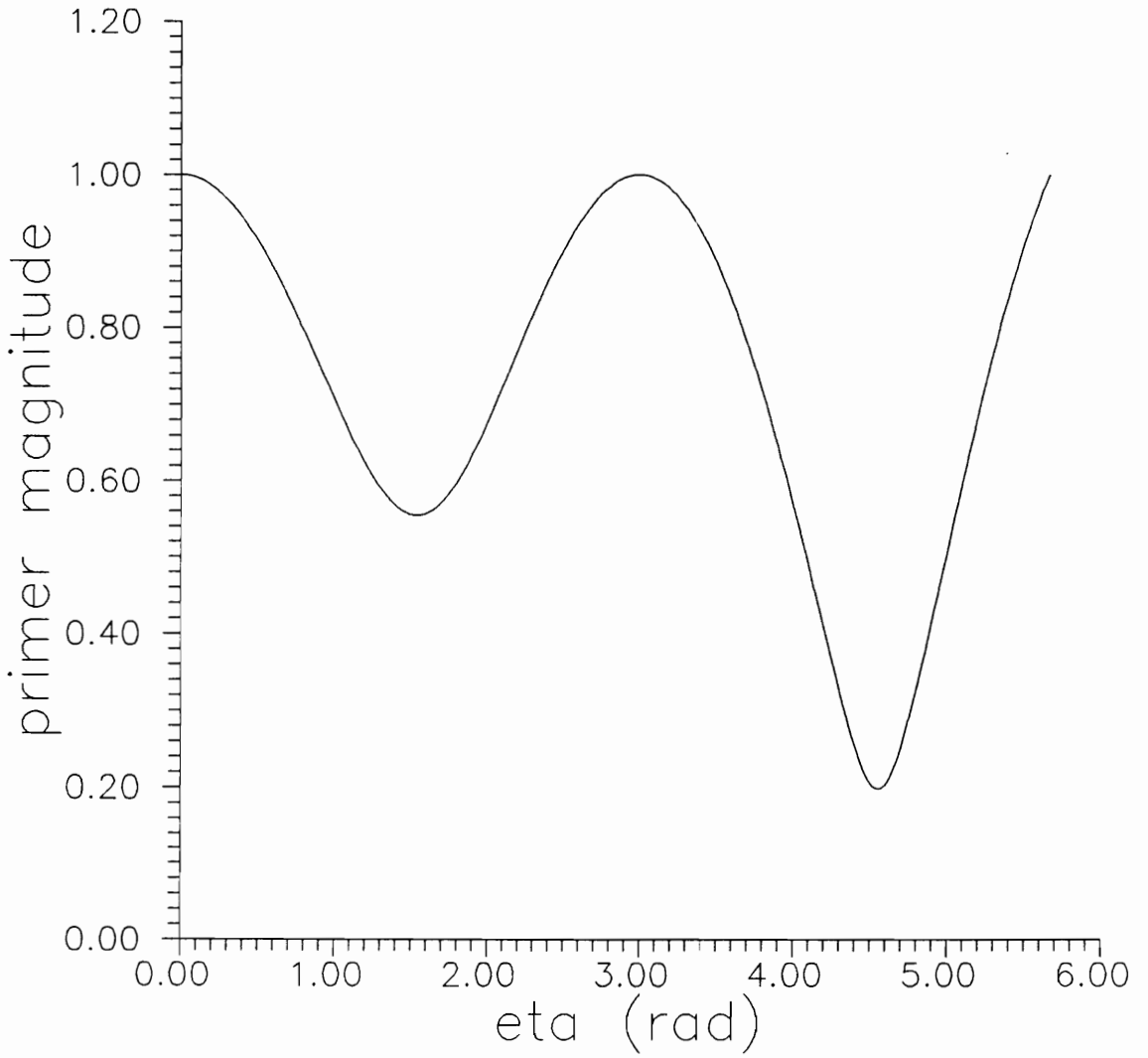| number iters.	char. vel. (du/tu)	λ_t	flight time (tu)	BOUNDSCO init. error	BOUNDSCO iterations	$\int |\bar{T}| dt$ (du/tu)	Hamiltonian
7	0.730182	$2. \times 10^{-12}$	6.638881	0.0743	9	0.732539	-3.45×10^{-3}

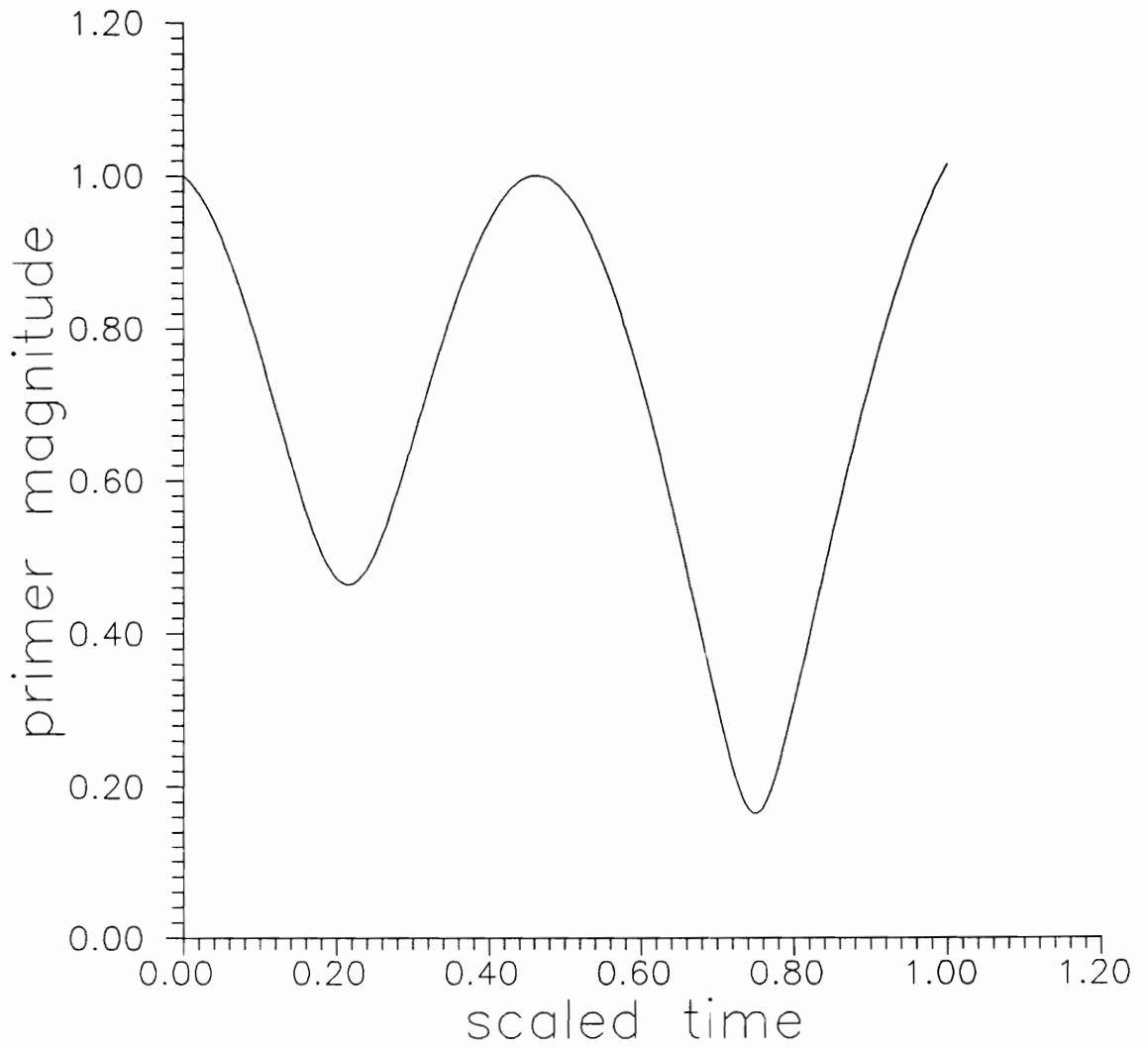Figure 10.3.6. Impulsive Thrust Primer Magnitude for General Three Burn Trajectory.

Figure 10.3.7. Finite Thrust Primer Magnitude for General Three Burn Trajectory.

above starting at a radius of 1 DU. The target elements were picked by hand to have characteristics common to many problems which require three burn solutions, specifically a planar orientation very different from the original interceptor orbit. The $\hat{r}$ and $\hat{r}'$ elements can be obtained by rotating the $\hat{r}$, $\hat{r}'$, $\hat{h}$ basis from the interceptor elements through a 3-2-1 rotation with angles of 315°, 5°, and 45°, respectively (in the order of rotation). Both the impulsive burn routine and BOUNDSCO converge very well to the extremal.

11.0 CONCLUSIONS

The use of redundant adjoint variable transformations has proven to be a very valuable tool as applied to the transformation between Cartesian adjoint variables and Schumacher adjoint variables. Several benefits result from the application of this transformation. First, the transformation has provided a useful means of propagating the primer vector of classical theory along coasting arcs, since for time open problems the Schumacher adjoint variables are simple harmonic oscillators. Second, the application of the classical primer vector theory in the transformed Schumacher space led to the development of a new necessary condition for time open minimum-fuel transfer. Furthermore, the transformation led to a convenient check of Lawden's corner condition at burns on optimal trajectories; specifically, the time rate of change of the primer vector must be continuous across a burn. Since it proved convenient to do the propagating of the adjoint variables in Schumacher space, using the local primer vector $\bar{S}$, and since $\bar{S}'$ itself is not in general continuous across a burn, the derivative of the primer vector was transformed into Schumacher adjoints. Finally, it proved convenient to propagate extremal impulsive thrust trajectories in Schumacher variables and adjoint variables, then transform them to Cartesian position, velocity, and the adjoint variables associated with these, in order to use them as initial conditions in a finite thrust boundary value solver. Then these Cartesian variables were used in the boundary value solver since the differential equations associated with them are more convenient than the Schumacher variables on thrusting arcs.

The conclusion is that adjoint variable transformations are very useful; some properties or conditions may be used in one space, then the adjoint variables may be transformed to another space to take advantage of salient features in that system. In this specific application, some necessary conditions for fuel-optimal space flight transfer exist in one adjoint space, and

others exist in the second adjoint space. Also, the Schumacher adjoints are easily propagated on coasting arcs, while the Cartesian adjoints are much simpler for propagation along thrusting arcs. The redundant adjoint variable transformation derived in this dissertation proved to be a valuable means of simultaneously tapping both resources.

When all of the equations derived from the necessary conditions of both systems were put into a computer program which simultaneously solves the system of equations, a useful numerical tool resulted. The program seems to be robust, generally finding candidate optimal control solutions with a minimum of effort.

REFERENCES AND SELECTED BIBLIOGRAPHY

1.   Bate, R.R., Mueller, D.D., and White, J.E., *Fundamentals of Astrodynamics*, Dover Publications, Inc., New York, 1971.

2.   Battin, R.H., *An Introduction to the Mathematics and Methods of Astrodynamics*, American Institute of Aeronautics and Astronautics, Inc., New York, 1987.

3.   Broucke, R., Lass, H., and Ananda, M., "Redundant Variables in Celestial Mechanics," *Astron. and Astrophys.*, Vol. 13, pp 390-398, 1971.

4.   Bryson, A.E., and Ho, Y.C., *Applied Optimal Control*, Hemisphere Publishing Company, 1975.

5.   Bryson, A.E., Denham, W.F., and Dreyfus, S.E., "Optimal Programming Problems with Inequality Constraints I: Necessary Conditions for Extremal Solutions," *AIAA Journal*, Vol 1., No. 11, pp. 2544-2550, 1963.

6.   Burdet, C.A., "Regularization of The Two Body Problem," *Zeitschritt für Angevandte Matehematik und Physik*, Vol. 18, pp. 434-438, 1967.

7.   Chiu, Jeng-Hua, *Optimal Multiple-Impulse Nonlinear Orbital Rendezvous*, Ph.D. Thesis, University of Illinois at Urbana-Champaign, 1984

8.   Churchill, R.V., *Complex Variables and Applications*, MacGraw-Hill Book Company, New York, 1960.

9.   Clohessy, W.H. and Wiltshire, R.S., "Terminal Guidance System for Satellite Rendezvous," *J. Aerosp. Sc.*, Vol 27, pp. 653-658, 1960.

10.   Dennis, J.E., jr. and Schnabel, R.B., *Numerical Methods for Unconstrained Optimization and Nonlinear Equations*, Prentice Hall, Inc., New Jersey, 1983.

11.   Edelbaum, T.N., "How Many Impulses?," *Astronautics and Aeronautics*, Vol. 5, pp. 64-69, Nov. 1967.

12.   Geyling, F.T., and Westerman, H.R., *Introduction to Orbital Mechanics*, Addison-Wesley Publishing Co., Reading, MA, 1971.

13.   Gill, P.E., Murray, W., and Wright, M.H., *Practical Optimization*, Academic Press, New York, 1981.

14.   Glandorf, D.R., *Optimal Fixed-Time Orbital Transfer with a Radial Constraint*, Ph.D. Thesis, Iowa State University, 1967.

15.   Glandorf, D.R., "Lagrange Multipliers and the State Transition Matrix

for Coasting Arcs," *AIAA Journal*, Vol. 7, No. 2, pp. 363-365, 1969.

16. Gobetz, F.W., "Optimum Transfers Between Hyperbolic Asymptotes," *AIAA Journal*, Vol. 1, pp. 2034-2041, 1963.

17. Gobetz, F.W., and Doll, J.R., "A Survey of Impulsive Trajectories," *AIAA Journal*, Vol. 5, pp. 801-834, 1967.

18. Goldstein, H., *Classical Mechanics*, Addison-Wesley, Inc., 1950.

19. Gradsteyn, I.S., and Ryzhik, I.M., *Table of Integrals, Series, and Products*, Academic Press, New York, 1965.

20. Handelsman, M., "Optimal Free-Space Fixed-Thrust Trajectories Using Impulsive Trajectories as Starting Iteratives," *AIAA Journal*, Vol. 4, No. 6, pp. 1077-1082, 1966.

21. Hoelker, R.F. and Silber, R., "The Bi-Elliptical Transfer Between Co-Planar Circular Orbits," *Proc. 4th Symposium Ballistic Missile and space Technology*, Los Angeles, 1959.

22. Hohmann, W., *Die Erreichbarkeit der Himmelskörper*, Oldenbourg, Munich, 1925. "The Attainability of Heavenly Bodies," *NASA Technical Translation F.44*, 1960.

23. Jezewski, D.J., and Rozendaal, H.L., "An Efficient Method for Calculating Optimal Free-Space, N-Impulse Trajectories," *AIAA Journal*, Vol. 6, No. 1, 1968.

24. Jezewski, D.J., "Autonomous, Exoatmospheric, Trajectory Optimization," AAS/AIAA Astrodynamics Specialist Conference, August 7-10, 1989.

25. Junkins, J.L., and Turner, J.D., *Optimal Spacecraft Rotational Maneuvers*, Elsevier Scientific Publishing Co., New York, 1985.

26. Kelley, H.J., "Method of Gradients," *Optimization Techniques*, Chapter 6, Ed. by G. Leitmann, Academic Press, New York, 1962.

27. Komatsuzaki, T. "Equivalent Transformation of Optimal Control Problems," *Int. J. Control*, Vol. 26, No. 5, pp. 707-719, 1977.

28. Lawden, D.F., "Interplanetary Rocket Trajectories," *Advances in Space Sciences*, Ed. by F.I. Ordway, Chap. 1, Academic Press, New York, 1959.

29. Lawden, D.F., "Optimal Intermediate Thrust Arcs in a Gravitational Field," *Astronautica Acta*, Vol. 8, pp. 106-123, 1962.

30. Lawden, D.F., *Optimal Trajectories for Space Navigation*, Butterworth & Co. (Publishers) Ltd., London, 1963.

31. Lee, E.B., and Markus, L., *Foundations of Optimal Control Theory*, John

Wiley and Sons, Inc., 1986.

32. Leitmann, G., *The Calculus of Variations and Optimal Control*, Plenum Press, New York, 1981.

33. Lion, P.M. and Handelsmann, M., "Primer Vector on a Fixed-Time Impulsive Trajectories," *AIAA Journal*, Vol. 6, No. 1, pp. 127-132, 1968.

34. Lutze, F.H., Cliff, E.M., and Kelley, H.J., *Optimal Rendezvous with Cooperative Vehicles II*, VPI&SU Report, July 1985.

35. Marec, J.P., *Optimal Space Trajectories*, Elsevier, New York, New York, 1979.

36. Neustadt, L.W., "A General Theory of Minimum-Fuel Space Trajectories," *SIAM Journal on Control*, Vol. 3, pp. 317-356, 1966.

37. Pontryagin, *Differential Equations*

38. Pontryagin, L.S., Boltyanskii, V.G., and Gamkrelidze, R.V., *The Mathematical Theory of Optimal Processes*, Interscience Publishers, New York, 1962.

39. Pitkin, E.T., "A Regularized Approach to Universal Orbit Variables," *AIAA Journal*, Vol. 3, No. 8, pp 1508-1511, 1965.

40. Potter, J.E. and Stern, R.E., "Optimization of Midcourse Velocity Corrections," *Proceedings IFAC Symposium on Automatic Control in the Peaceful Uses of Space*, Stavanger, Norway, Plenum Press, N.Y., pp. 70-84, Jun 1965.

41. Prussing, J.E., "Optimal Four Impulse Fixed-Time Rendezvous in the Vicinity of a Circular Orbit," *AIAA Journal*, Vol. 7, pp. 928-935, 1969.

42. Prussing, J.E., "Optimal Two and Three Impulse Fixed-Time Rendezvous in the Vicinity of a Circular Orbit," *AIAA Journal*, Vol. 8, pp. 1221-1228, July 1970.

43. Prussing, J.E. and Chiu, Jeng-Hua, "Optimal Multiple-Impulse Time-Fixed Rendezvous Between Circular Orbits," *Journal of Guidance, Control and Dynamics*, Vol. 9, pp. 17-22, 1986.

44. Robbins, H.M., "An Analytical Study of the Impulsive Approximation," *AIAA Journal*, Vol. 4, No. 8, pp. 1417-1423, 1966.

45. Royden, H.L., *Real Analysis*, Macmillan Publishing Company, New York, 1988.

46. Schumacher, P.W., *Results of True-Anomaly Regularization in Orbital Mechanics*, Ph.D. Dissertation, Dept. of Aerospace and Ocean Engineering, VPI&SU, 1987.

47. Schumacher, P.W., "Universal True Anomaly Time Equations," AAS Paper No. 89-448,

AAS/AIAA Astrodynamics Specialist Conference, Stowe, Vermont, August 7-10, 1989.

48.   Schumacher, P.W., "Lambert Problem in True Anomaly Regularized Variables," AAS Paper No. 89-385, AAS/AIAA Astrodynamics Specialist Conference, Stowe, Vermont, August 7-10, 1989.

49.   Stiefel, E.L., and Scheifele, G., *Linear and Regular Celestial Mechanics*, Springer-Verlag, New York, 1971.

50.   Vasudevan, G., *Fuel Optimal Rendezvous Including a Radial Constraint*, M.S. Thesis, Dept. of Aerospace and Ocean Engineering, VPI & SU, 1986.

51.   Vasudevan, G., and Lutze, F.H., "On Verification of Fuel-Optimal Space Trajectories," *Opt. Cont. Appl. Meth.*, Vol. 9, pp. 285-302, 1988.

52.   Vasudevan, G., *A Homotopy Approach to the Solutions of Minimum-Fuel Space-Flight Rendezvous Problems*, Ph.D. Dissertation, Dept. of Aerospace and Ocean Engineering, VPI&SU, 1989.

53.   Vidali, S.R., "On the Euler Parameter Constraint," *Journal of the Astronautical Sciences*, Vol. 36, No. 3, pp. 259-265, 1988.

54.   Wellnitz, L.J., and Prussing, J.E., "Optimal Trajectories For Time-Constrained Rendezvous Between Arbitrary Conic Orbits," AAS/AIAA Astrodynamics Specialist Conference, Kalispell, Montana, 1987.

APPENDIX A: INTEGRATION OF VARIATION OF PARAMETERS VARIABLES

In this appendix, the variables $C_1(\eta)$ and $C_2(\eta)$ from the variation of parameters solution approach to $\lambda_{u'c}(\eta)$, as well as other related equations, are integrated analytically. Recall from Eqs. 6.2.7 and 6.2.8 that

$$C_1'(\eta) \; = \; \frac{2}{hu(\eta)^3}\sin\eta \qquad\qquad\qquad A.1$$

and

$$C_2'(\eta) \; = \; -\frac{2}{hu(\eta)^3}\cos\eta. \qquad\qquad\qquad A.2$$

Since $u(\eta) = \dfrac{\mu}{h^2} + (u_0-\dfrac{\mu}{h^2})\cos\eta + u_0'\sin\eta = \dfrac{\mu}{h^2}(1 + \alpha\cos\eta + \beta\sin\eta)$, with $\alpha = \dfrac{h^2u_0}{\mu}-1$, and $\beta = \dfrac{h^2u_0'}{\mu}$, A.1 leads to

$$C_1(\eta) \; = \; \frac{2\,h^5}{\mu^3}\int\frac{\sin\eta}{(1 + \alpha\cos\eta + \beta\sin\eta)^3}\,d\eta + \text{const.} \qquad\qquad A.3$$

When $1-\alpha^2-\beta^2 \neq 0$, this integral can be solved by applying formulae 2.558 of Gradshteyn and Ryzhik[17], page 149, successively. After the first application,

$$C_1(\eta) \; = \; \frac{2\,h^5}{\mu^3}\left\{\frac{-(\alpha + \cos\eta)}{2(1-\alpha^2-\beta^2)(1 + \alpha\cos\eta + \beta\sin\eta)^2}\right.$$

$$A.4$$

$$\left. + \; \frac{1}{2(1-\alpha^2-\beta^2)}\int\frac{\sin\eta - 2\beta}{(1 + \alpha\cos\eta + \beta\sin\eta)^2}\,d\eta\right\} + \text{const.}$$

Applying the formulae again to the integral in A.4,

$$C_1(\eta) = -\frac{h^5}{\mu^3}\left\{\frac{(\alpha+\cos\eta)(1-\alpha^2-\beta^2) + [\alpha+(1+2\beta^2)\cos\eta+2\alpha\beta\sin\eta](1+\alpha\cos\eta+\beta\sin\eta)}{(1-\alpha^2-\beta^2)(1+\alpha\cos\eta+\beta\sin\eta)^2}\right.$$

$$\left. + \frac{3\beta}{(1-\alpha^2-\beta^2)^2}\int\frac{d\eta}{(1+\alpha\cos\eta+\beta\sin\eta)}\right\} + \text{const.} \qquad\text{A.5}$$

The remaining integral in A.5 is

$$\int\frac{d\eta}{(1+\alpha\cos\eta+\beta\sin\eta)} = \frac{2}{\sqrt{1-\alpha^2-\beta^2}}\tan^{-1}\left(\frac{(1-\alpha)\tan\frac{\eta}{2}+\beta}{\sqrt{1-\alpha^2-\beta^2}}\right) + \text{const.} \qquad\text{A.6}$$

Since this expression involves $\tan\frac{\eta}{2}$, which is singular at $\frac{\eta}{2}=\frac{\pi}{2}$, the equation in this form is only valid up to $\eta=\pi$. However, η is typically required up to 2π. Therefore the form of Eq. A.6 needs to be modified.

Consider first the elliptical case ($1-\alpha^2-\beta^2 > 0$). Eq. A.6 for that case can be put in a more useful form by applying a technique similar to what Schumacher did to the true anomaly time equation in order to make it universal. First, define

$$\tan\frac{\theta}{2} = \frac{(1-\alpha)z+\beta}{\sqrt{1-\alpha^2-\beta^2}}, \qquad\text{A.7}$$

where

$$z = \tan\frac{\eta}{2}, \qquad\text{A.8}$$

so that

$$\int\frac{d\eta}{(1+\alpha\cos\eta+\beta\sin\eta)} = \frac{\theta}{\sqrt{1-\alpha^2-\beta^2}} + \text{const.} \qquad\text{A.9}$$

Then, defining $v = \tan\frac{\eta}{4}$, and using the trig identities

$$\tan\frac{\theta}{4} = \frac{\tan\frac{\theta}{2}}{1 + \sqrt{1 + \tan^2\frac{\theta}{2}}} \tag{A.10}$$

and

$$\tan\frac{\eta}{2} = \frac{2\tan\frac{\eta}{4}}{1 - \tan^2\frac{\eta}{4}} \qquad \Rightarrow \qquad v = \frac{2v}{1-v^2}, \tag{A.11}$$

it follows that

$$\tan\frac{\theta}{4} = \frac{2(1-\alpha)v + \beta(1-v^2)}{(1-v^2)\left(\sqrt{1-\alpha^2-\beta^2} + \sqrt{(1-\alpha^2-\beta^2) + \left(\frac{2(1-\alpha)v}{1-v^2}+\beta\right)^2}\right)}. \tag{A.12}$$

In other words, substituting for θ in Eq. A.9, where $\theta = 4\tan^{-1}\frac{\theta}{4}$,

$$\int \frac{d\eta}{(1 + \alpha\cos\eta + \beta\sin\eta)} = \tag{A.13}$$

$$\frac{4}{\sqrt{1-\alpha^2-\beta^2}}\tan^{-1}\left[\frac{2(1-\alpha)v + \beta(1-v^2)}{\left((1-v^2)\sqrt{1-\alpha^2-\beta^2} + \text{sgn}(1-v^2)\sqrt{(1-v^2)(1-\alpha^2-\beta^2) + \left(\frac{2(1-\alpha)v}{1-v^2}+\beta\right)^2}\right)}\right]$$

Since $v = \tan\frac{\eta}{4}$ is not singular until $\eta = 2\pi$, this equation is valid for $\eta < 2\pi$.

For the hyperbolic case ($1-\alpha^2-\beta^2 < 0$), the same basic approach is used. In fact, Eq. A.13 can be used directly if complex arithmetic is used. Complex arithmetic is necessary since $1-\alpha^2-\beta^2 < 0$, so that $\sqrt{1-\alpha^2-\beta^2}$ is complex. However, the result of the integration is real, so real manipulations are desired. First, note that $\sqrt{1-\alpha^2-\beta^2} = i\sqrt{\alpha^2+\beta^2-1}$ (with $i = \sqrt{-1}$), and for convenience, define

$$A = 2(1-\alpha)\,v + \beta(1-v^2) \qquad\qquad\qquad \text{A.14}$$

$$B = (1-v^2)\sqrt{1-\alpha^2-\beta^2} \qquad\qquad\qquad \text{A.15}$$

$$C = (1-v^2)\sqrt{\alpha^2+\beta^2-1} \qquad\qquad\qquad \text{A.16}$$

and

$$iD = \sqrt{B^2+A^2}\,. \qquad\qquad\qquad\qquad \text{A.17}$$

Then A.13 can be written

$$\int \frac{d\eta}{(1 + \alpha\cos\eta + \beta\sin\eta)} = \frac{4}{i\sqrt{\alpha^2+\beta^2-1}}\tan^{-1}\left[\frac{A}{B\pm\sqrt{B^2+A^2}}\right] \qquad \text{A.18}$$

where the $\pm$ is short for $\mathrm{sgn}(1-v^2)$. Now, B is complex, but the term $\sqrt{B^2+A^2}$ may or may not be complex.

Consider first the case where both B and $\sqrt{B^2+A^2}$ are complex. Note also, for simplicity of the manipulations which are to follow, that by multiplying the numerator and denominator of the argument of the arctangent above by the conjugate of the denominator there results

$$\frac{A}{B \pm \sqrt{B^2 + A^2}} = \frac{-B \pm \sqrt{B^2 + A^2}}{A} . \qquad \text{A.19}$$

Further, recall from complex analysis[6] that

$$\tan^{-1}x = \frac{1}{2i} \ln\left[\frac{1+ix}{1-ix}\right] . \qquad \text{A.20}$$

Then,

$$\tan^{-1}\left[i \frac{-C \pm D}{A}\right] = -\frac{i}{2} \ln\left[\frac{1 + C \mp D}{1 - C \pm D}\right] . \qquad \text{A.21}$$

So, plugging the right hand side of the above into Eq. A.18,

$$\int \frac{d\eta}{(1 + \alpha \cos\eta + \beta \sin\eta)} = \frac{1}{\sqrt{\alpha^2 + \beta^2 - 1}} \ln\left[\frac{A - C + \text{sgn}(1-v^2)D}{A + C - \text{sgn}(1-v^2)D}\right] + \text{const.} \qquad \text{A.22}$$

Consider next the case where B is complex but $\sqrt{B^2 + A^2}$ is real. Then

$$\tan^{-1}\left[\frac{-B \pm \sqrt{B^2 + A^2}}{A}\right] = \tan^{-1}\left[\frac{-iC \pm \sqrt{A^2 - C^2}}{A}\right] \qquad \text{A.23}$$

$$= -\frac{i}{2} \ln\left[\frac{1 + \frac{C}{A} \pm i\frac{1}{A}\sqrt{A^2 - C^2}}{1 - \frac{C}{A} \mp i\frac{1}{A}\sqrt{A^2 - C^2}}\right] \qquad \text{A.24}$$

$$= -\frac{i}{2} \ln\left[\frac{\sqrt{\left(1 + \frac{C}{A}\right)^2 + \frac{A^2 - C^2}{A^2}}}{\sqrt{\left(1 - \frac{C}{A}\right)^2 + \frac{A^2 - C^2}{A^2}}} \; e^{i[\theta - (-\pi + \theta)]}\right] , \qquad \text{A.25}$$

where $\theta = \arg\left(1 + \frac{C}{A} \pm i\frac{1}{A}\sqrt{A^2-C^2}\right)$. Using the fact that the log of a product is the sum of the logs,

$$\tan^{-1}\left[\frac{-B \pm \sqrt{B^2+A^2}}{A}\right] = -\frac{i}{2}\left[\frac{1}{2}\ln\left[\frac{\left(1 + \frac{C}{A}\right)^2 + \frac{A^2-C^2}{A^2}}{\left(1 - \frac{C}{A}\right)^2 + \frac{A^2-C^2}{A^2}}\right] + i\pi\right], \qquad \text{A.26}$$

$$= \frac{1}{4i}\ln\left[\frac{\left(A + C\right)^2 + A^2-C^2}{\left(A - C\right)^2 + A^2-C^2}\right] + \frac{\pi}{2}, \qquad \text{A.27}$$

$$= \frac{1}{4i}\ln\left[\frac{A + C}{A - C}\right] + \frac{\pi}{2}, \qquad \text{A.28}$$

so that

$$\int\frac{d\eta}{(1 + \alpha\cos\eta + \beta\sin\eta)} = \frac{1}{\sqrt{\alpha^2+\beta^2-1}}\ln\left[\frac{A-C}{A+C}\right] + \text{const.} \qquad \text{A.29}$$

When $1-\alpha^2-\beta^2 = 0$, the second of formulae 2.558 of Gradshteyn and Ryzhik is used to solve A.1. The result is

$$C_1(\eta) = \frac{h^5}{\mu^3}$$

$$\cdot\left(\frac{(\alpha+\cos\eta) + \frac{\beta}{5}(\alpha\sin\eta-\beta\cos\eta)\left\{7 + 6(\alpha\cos\eta+\beta\sin\eta) + 2(\alpha\cos\eta+\beta\sin\eta)^2\right\}}{(1 + \alpha\cos\eta + \beta\sin\eta)^3}\right)$$

$$+ \text{ const.}$$

Now that $C_1(\eta)$ is known, the solution to $C_2(\eta)$ is needed. Recall that

$$C_2(\eta) \;=\; -\frac{2\,h^5}{\mu^3} \int \frac{\cos\eta}{(\,1 + \alpha\cos\eta + \beta\sin\eta\,)^3}\, d\eta + \text{const.} \qquad \text{A.31}$$

Again using formulae 2.558 of Gradshteyn and Ryzhik successively for the case when $1-\alpha^2-\beta^2 \;\neq\; 0$, it is easily determined that

$$C_2(\eta) \;=\; -\frac{h^5}{\mu^3}\Bigg\{ \frac{(\beta+\sin\eta)(1-\alpha^2-\beta^2) + [\beta-2\alpha\beta\cos\eta+(1+2\alpha^2)\sin\eta](1+\alpha\cos\eta+\beta\sin\eta)}{(1-\alpha^2-\beta^2)^2(1 + \alpha\cos\eta + \beta\sin\eta)^2}$$

$$+ \frac{-3\alpha}{(1-\alpha^2-\beta^2)^2} \int \frac{d\eta}{(\,1 + \alpha\cos\eta + \beta\sin\eta\,)} \Bigg\} \;+\; \text{const.,} \qquad \text{A.32}$$

where the remaining integral is the same as A.13. When $1-\alpha^2-\beta^2 = 0$,

$$C_2(\eta) \;=\; \frac{h^5}{\mu^3}$$

$$\cdot \left(\frac{(\beta+\sin\eta) - \frac{\alpha}{5}(\alpha\sin\eta-\beta\cos\eta)\Big\{7 + 6(\alpha\cos\eta+\beta\sin\eta) + 2(\alpha\cos\eta+\beta\sin\eta)^2\Big\}}{(1 + \alpha\cos\eta + \beta\sin\eta)^3} \right)$$

$$\text{A.33}$$

$$+ \text{ const.}$$

The final integral to be addressed in this appendix is $\displaystyle\int_0^{\eta} \lambda_{u'c}(x)\, dx$. With

$$\lambda_{u'c} \;=\; C_1(\eta)\cos\eta + C_2(\eta)\sin\eta, \qquad \text{A.34}$$

the integral can be written

$$\int_0^{\eta} \lambda_{u'_c}(x)\,dx = \frac{2h^5}{\mu^3}\left(\int_0^{\eta}\cos y \int_0^{y}\frac{\sin x}{(1+\cos x+\sin x)^3}\,dx\,dy\right.$$

$$\left. -\int_0^{\eta}\sin y \int_0^{y}\frac{\cos x}{(1+\cos x+\sin x)^3}\,dx\,dy\right)$$

A.35

The first of the terms in the difference is

$$\int_0^{\eta}\int_0^{y}\frac{\cos y\,\sin x}{(1+\cos x+\sin x)^3}\,dx\,dy = \int_0^{\eta}\int_x^{\eta}\frac{\cos y\,\sin x}{(1+\cos x+\sin x)^3}\,dy\,dx$$

A.36

$$= \int_0^{\eta}\frac{(\sin\eta-\sin x)\,\sin x}{(1+\cos x+\sin x)^3}\,dx$$

A.37

$$= \sin\eta\int_0^{\eta}\frac{\sin x\,dx}{(1+\cos x+\sin x)^3} - \int_0^{\eta}\frac{\sin^2 x\,dx}{(1+\cos x+\sin x)^3}$$

A.38

Similarly,

$$-\int_0^{\eta}\int_0^{y}\frac{\sin y\,\cos x}{(1+\cos x+\sin x)^3}\,dx\,dy = -\int_0^{\eta}\int_x^{\eta}\frac{\sin y\,\cos x}{(1+\cos x+\sin x)^3}\,dy\,dx$$

A.39

$$= -\int_0^{\eta}\frac{(\cos x-\cos\eta)\,\cos x}{(1+\cos x+\sin x)^3}\,dx$$

A.40

$$= \cos\eta\int_0^{\eta}\frac{\cos x\,dx}{(1+\cos x+\sin x)^3} - \int_0^{\eta}\frac{\cos^2 x\,dx}{(1+\cos x+\sin x)^3}$$

A.41

Adding Eqs. A.38 and A.41, noting that $\cos^2 x+\sin^2 x=1$, and remembering the definitions of

$C_1(\eta)$ and $C_2(\eta)$,

$$\int_0^\eta \lambda_{u'c}(x)\,dx = \big[C_1(\eta)-C_1(0)\big]\sin\eta - \big[C_2(\eta)-C_2(0)\big]\cos\eta$$

<div style="text-align: right">A.42</div>

$$- \frac{2h^5}{\mu^3}\int_0^\eta \frac{dx}{(1+\cos x+\sin x)^3}$$

Again applying formulae 2.558 of Gradshteyn and Ryzhik to the integral on the right hand side, this becomes

$$\int_0^\eta \lambda_{u'c}(x)\,dx = \big[C_1(\eta)-C_1(0)\big]\sin\eta - \big[C_2(\eta)-C_2(0)\big]\cos\eta$$

$$- \frac{2h^5}{\mu^3}\Bigg(\frac{(\beta\cos\eta-\alpha\sin\eta)\big[3(1+\alpha\cos\eta+\beta\sin\eta) + (1-\alpha^2-\beta^2)\big]}{2(1-\alpha^2-\beta^2)^2(1+\alpha\cos\eta+\beta\sin\eta)^2}$$

<div style="text-align: right">A.43</div>

$$- \frac{\beta\big[3(1+\alpha) + (1-\alpha^2-\beta^2)\big]}{2(1-\alpha^2-\beta^2)^2(1+\alpha)^2} + \frac{3-(1-\alpha^2-\beta^2)}{2(1-\alpha^2-\beta^2)^2}\int_0^\eta \frac{dx}{(1+\cos x+\sin x)}\Bigg),$$

where, again, the final integral is Eq. A.13.

APPENDIX B: THE DOMAIN OF ψ

There are two constraints which restrict the domain of physically valid values of ψ. First, if, from Eq. 7.2.7, a particular value of ψ causes $h_n^2 < 0$, then h_n would be complex, which is not permitted. Also, $h_n = 0$ is not permitted with Schumacher coordinates. Therefore, $h_n^2 > 0$ gives a limit for ψ. That is,

$$\frac{\mu(1 - \cos\eta_f)}{u_n(\eta_f) - u_n(0)\cos\eta_f - \psi\sin\eta_f} > 0. \qquad \text{B.1}$$

Since the numerator is never less than zero, it is therefore required that

$$u_n(\eta_f) - u_n(0)\cos\eta_f - \psi\sin\eta_f > 0, \qquad \text{B.2}$$

or,

$$\psi\sin\eta_f < u_n(\eta_f) - u_n(0)\cos\eta_f. \qquad \text{B.3}$$

If $\sin\eta_f > 0$ (e.g., $\eta_f \in (0,\pi)$), then

$$\psi < \frac{u_n(\eta_f) - u_n(0)\cos\eta_f}{\sin\eta_f} \qquad \text{B.4}$$

creates an upper limit on ψ. On the other hand, if $\sin\eta_f < 0$ (e.g., $\eta_f \in (\pi,2\pi)$), then

$$\psi > \frac{u_n(\eta_f) - u_n(0)\cos\eta_f}{\sin\eta_f} \qquad \text{B.5}$$

creates a lower limit on ψ. Finally, it can be seen from Eq. B.1 that if $\sin\eta_f = 0$ (e.g., $\eta_f = \pi$), then all values of ψ are valid.

The other limit on ψ comes from a more subtle requirement. Suppose, for the sake of discussion, the coasting angle η_f is some arbitrary value less than 2π. Then for some appropriate value of ψ, the coasting arc between the two given positions, $u_n(0)$ and $u_n(\eta_f)$, will be an ellipse. When ψ is decreased from this value, the trajectory between these positions will become increasingly lofted. (Since $\psi = u'_n(0) = \dfrac{\dot{r}(0)}{h}$, decreasing ψ corresponds to increasing the radial component of velocity, $\dot{r}(0)$.) There is a lower limit on ψ, $\tilde{\psi}$, such that the lofted height between these positions goes to infinity; that is, $u_n(\eta)$ goes to zero at one point on this trajectory as η traverses between 0 and η_f. This trajectory is really the open end of a parabolic trajectory. As ψ is decreased even further, the resulting trajectories become hyperbolas (i.e, they pass through the open end of the hyperbola), while $u_n(\eta)$ actually takes on negative values as η traverses between 0 and η_f. Clearly, therefore, $\tilde{\psi}$ is a lower limit on physically meaningful trajectories.

This phenomenon can best be appreciated by selecting an example problem and calculating various $u(\eta)$ values for representative ψ values. Bate, et. al[1] also give a clear description of this phenomenon using the semi-latus rectum, p, as the parameter of choice instead of ψ. Probably the easiest way to obtain an analytical expression for $\tilde{\psi}$ is to borrow the results of Bate, et. al., Eqs. (5.4-14) and (5.4-15) along with (5.4-4), and recast them in terms of Schumacher variables. Taking note of the fact that $p = \dfrac{h^2}{\mu}$, and denoting the critical value of h by $\tilde{h}$ (corresponding to $\tilde{\psi}$), Eq. (5.4-14) of Bate, et. al. becomes for $\sin\eta_f > 0$ (with $u = \frac{1}{r}$, $\eta = \Delta\nu$, and letting $u_0 \triangleq u_n(0)$, and $u_f \triangleq u_n(\eta_f)$)

$$\frac{\tilde{h}^2}{\mu} = \frac{1 - \cos\eta_f}{u_0 + u_f + \sqrt{2u_0 u_f(1 + \cos\eta_f)}}. \qquad \text{B.6}$$

Since this is an upper limit on h^2, Eq. 7.2.7 can be used to substitute for $\frac{\tilde{h}^2}{\mu}$ to obtain an inequality in terms of ψ. That is,

$$\frac{1}{u_f - u_0\cos\eta_f - \psi\sin\eta_f} \geq \frac{\tilde{h}^2}{\mu(1 - \cos\eta_f)} = \frac{1}{u_0 + u_f + \sqrt{2u_0u_f(1 + \cos\eta_f)}}.$$ B.7

Both sides of the inequality are positive, so

$$u_f - u_0\cos\eta_f - \psi\sin\eta_f \leq u_0 + u_f + \sqrt{2u_0u_f(1 + \cos\eta_f)}.$$ B.8

Since it was stipulated that $\sin\eta_f > 0$, this previous inequality leads to the result,

$$\psi \geq \frac{-u_0(1 + \cos\eta_f) - \sqrt{2u_0u_f(1 + \cos\eta_f)}}{\sin\eta_f}.$$ B.9

Using the same approach starting with Eq. (5.4-15) of Bate, et. al., for the case when $\sin\eta_f < 0$,

$$\psi \geq \frac{-u_0(1 + \cos\eta_f) + \sqrt{2u_0u_f(1 + \cos\eta_f)}}{\sin\eta_f}.$$ B.10

Taking $\sin\eta_f = \sqrt{\sin^2\eta_f}$ when $\sin\eta_f > 0$, and $\sin\eta_f = -\sqrt{\sin^2\eta_f}$ when $\sin\eta_f < 0$, both inequalities B.9 and B.10 can be written in the common form,

$$\psi \geq -u_0\frac{1 + \cos\eta_f}{\sin\eta_f} - \sqrt{\frac{2u_0u_f(1 + \cos\eta_f)}{\sin^2\eta_f}}.$$ B.11

Using the trigonometric identity

$$\frac{1 + \cos\eta_f}{\sin\eta_f} = \frac{\sin\eta_f}{1 - \cos\eta_f} \qquad \text{B.12}$$

in this inequality, the common lower limit for all $\eta_f \in (0, 2\pi)$ is

$$\boxed{\tilde{\psi} = -u_0\frac{\sin\eta}{1 - \cos\eta_f} - \sqrt{\frac{2u_0u_f}{1 - \cos\eta_f}}.} \qquad \text{B.13}$$

This equation is valid at $\eta_f = (2n - 1)\pi$ (for integer n), even though this value of η_f was avoided in the derivation, because the limit from the left and the limit from the right exist and are equal.

Putting all of the information together, for $\sin\eta_f > 0$ there is a lower bound (Eq. B.13) and an upper bound (Ineq. B.4), while for $\sin\eta_f < 0$ there are two lower bounds. The question remains, which lower bound is the correct one? Hypothesizing that $\tilde{\psi}$ is at least as large as the lower limit keeping h^2 from going negative, the following is conjectured:

$$\frac{-u_0(1 + \cos\eta_f) + \sqrt{2u_0u_f(1 + \cos\eta_f)}}{\sin\eta_f} \overset{?}{\geq} \frac{u_f - u_0\cos\eta_f}{\sin\eta_f}. \qquad \text{B.14}$$

Since $\sin\eta_f < 0$, multiplying through by $\sin\eta_f$ gives

$$-u_0(1 + \cos\eta_f) + \sqrt{2u_0u_f(1 + \cos\eta_f)} \overset{?}{\leq} u_f - u_0\cos\eta_f. \qquad \text{B.15}$$

Adding $u_0(1 + \cos\eta_f)$ to both sides,

$$\sqrt{2u_0 u_f(1 + \cos\eta_f)} \quad \overset{?}{\leq} \quad u_f + u_0. \qquad\qquad \text{B.16}$$

Since both sides are positive, squaring both sides maintains the direction of the inequality, so

$$2u_0 u_f(1 + \cos\eta_f) \quad \overset{?}{\leq} \quad u_f^2 + u_0^2 + 2u_f u_0. \qquad\qquad \text{A.17}$$

Or,

$$2u_0 u_f \cos\eta_f \quad \overset{?}{\leq} \quad u_f^2 + u_0^2. \qquad\qquad \text{B.18}$$

The left hand side is largest when $\cos\eta_f = 1$, so the inequality is certainly true if

$$u_f^2 + u_0^2 - 2u_0 u_f \quad \overset{?}{\geq} \quad 0. \qquad\qquad \text{B.19}$$

The left hand side is a perfect square, so this and the original conjectured inequalities are indeed true. Therefore, the correct lower bound is $\tilde{\psi}$, Eq. B.13, when $\sin\eta_f < 0$.

In summary, when $\sin\eta_f > 0$, ψ has a lower bound, Eq. B.13, and an upper bound, Ineq. B.4. On the other hand, when $\sin\eta_f \leq 0$, the lower bound on ψ is Eq. B.13, but there is no upper bound.

<u>VITA</u>

John Arthur Lawton was born on March 4, 1960, in San Diego, California. He received his B.S. in Aerospace Engineering from the University of Virginia in May, 1983, at which time he commenced work in space flight analysis for the Space Flight Sciences Branch at the Naval Surface Weapons Center, Dahlgren, Virginia. In May, 1988, he received his Master of Science in Aerospace Engineering from Virginia Polytechnic Institute and State University through the off-campus program offered at Dahlgren. Work was begun immediately thereafter on coursework and research heading toward a Doctor of Philosophy in Aerospace Engineering, for which this dissertation is a requirement.

John A. Lawton